Experimental techniques in high-energy nuclear and particle physics

"Dottorato di Ricerca in Ingegneria dell'Informazione"

LECTURE 10.

Prof. Rino Castaldi
INFN-Pisa
rino.castaldi@pi.infn.it

But what research in elementary particles, and its accelerators and detectors have to do with everyday life?

Fundamental research has always been a driving force for innovation

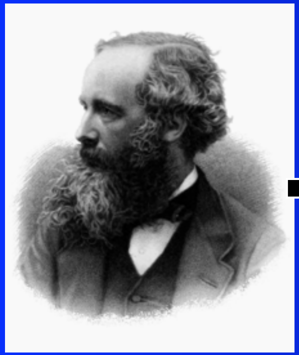

J.C. Maxwell

Electromagnetism

100% SCIENCE

Telephones use electromagnetic waves to communicate

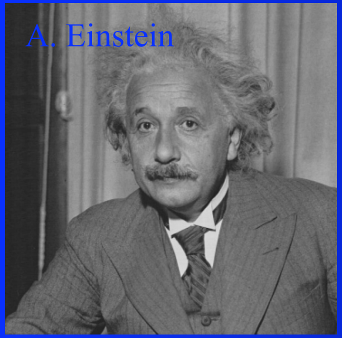

Relativity

100% SCIENCE

For GPS to work, we have to take into account the correction due to time dilation. Otherwise, there would be a position error of around 10m after just 5 minutes of travel-time!

spinoffs include… WWW >20 years old!

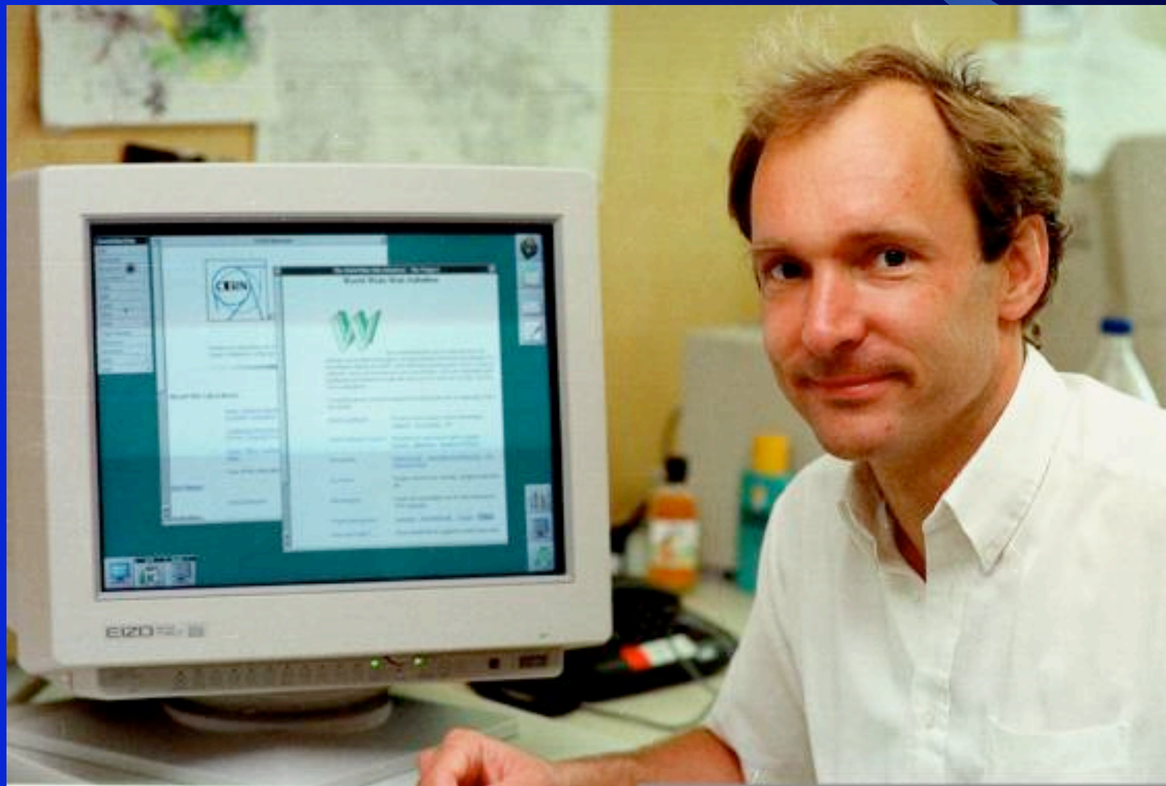

Accelerators: developed in physics labs & used in hospitals

Around 9000 of the 17000 accelerators operating in the World today are used for medicine.

Hadron therapy is a growing method of treating tumours

Detectors: developed in physics labs & used for medical imaging

PET (Positron Emission Tomography) uses antimatter (positrons).

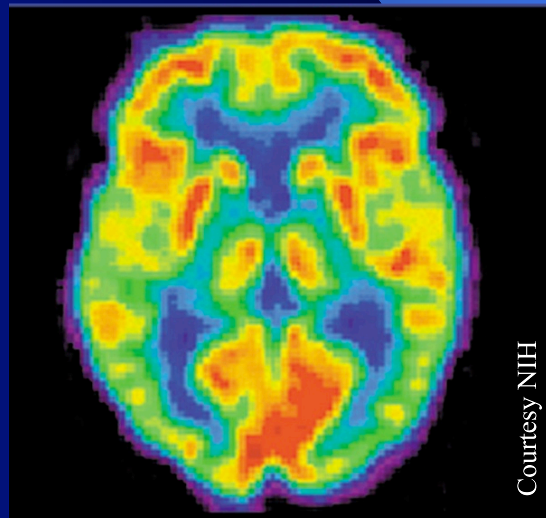

The beginnings of modern physics and of medical physics

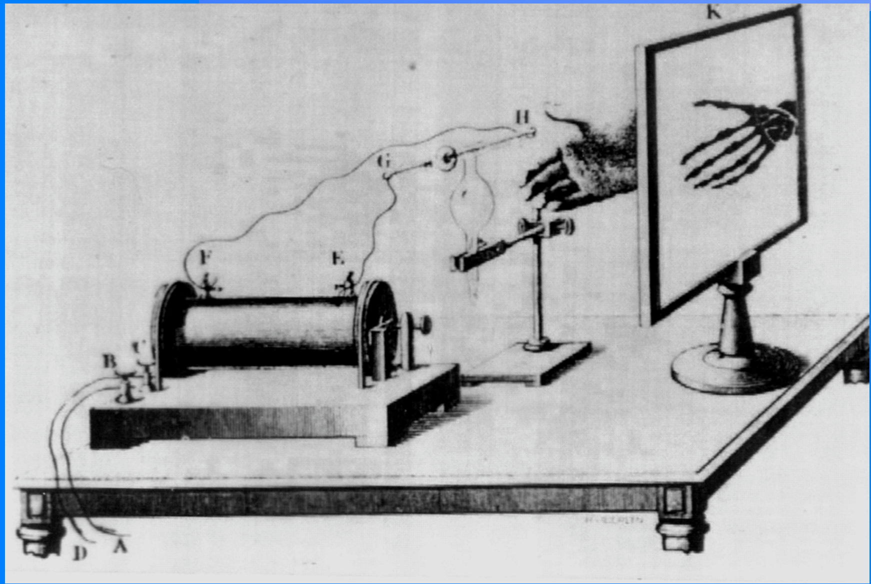

1895

discovery of X rays

Wilhelm Conrad Röntgen

J.J. Thompson

1897

“discovery” of the electron

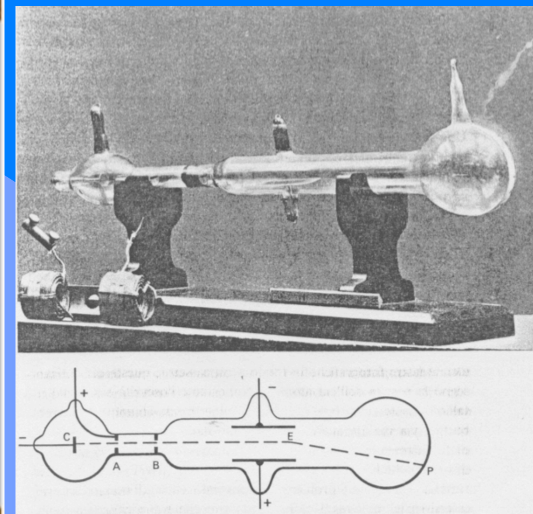

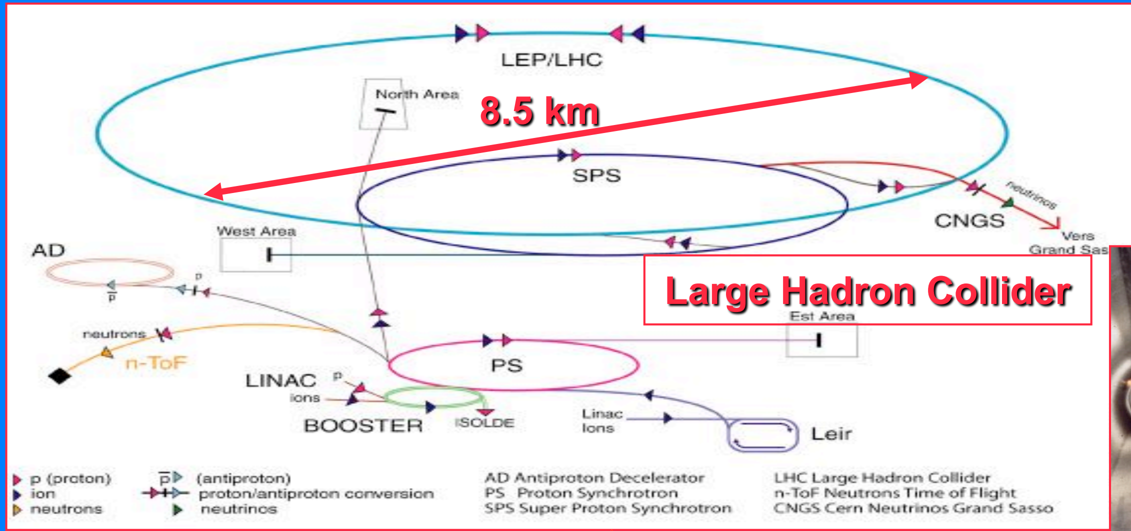

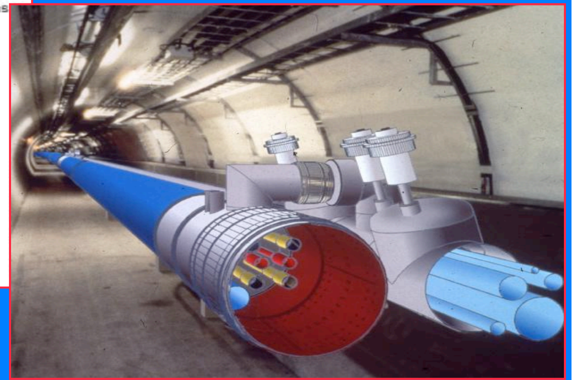

Research in fundamental physics

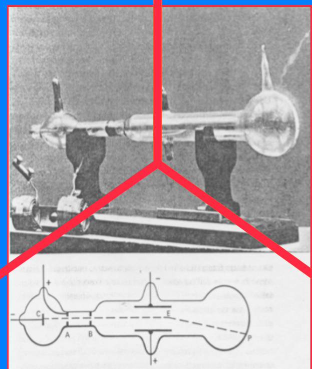

1897

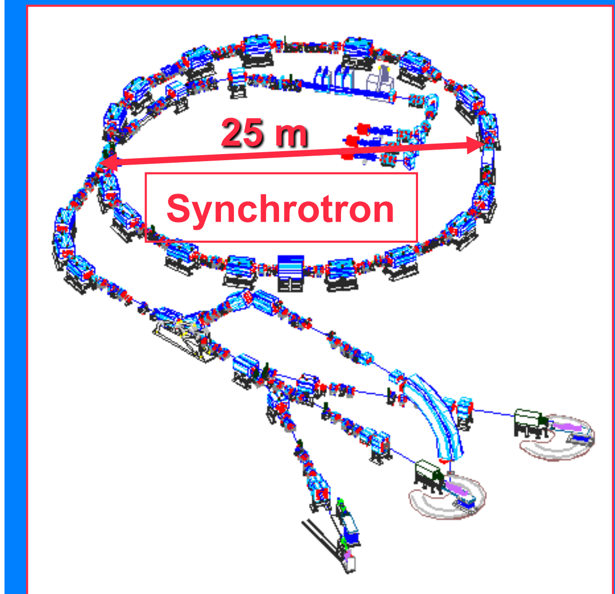

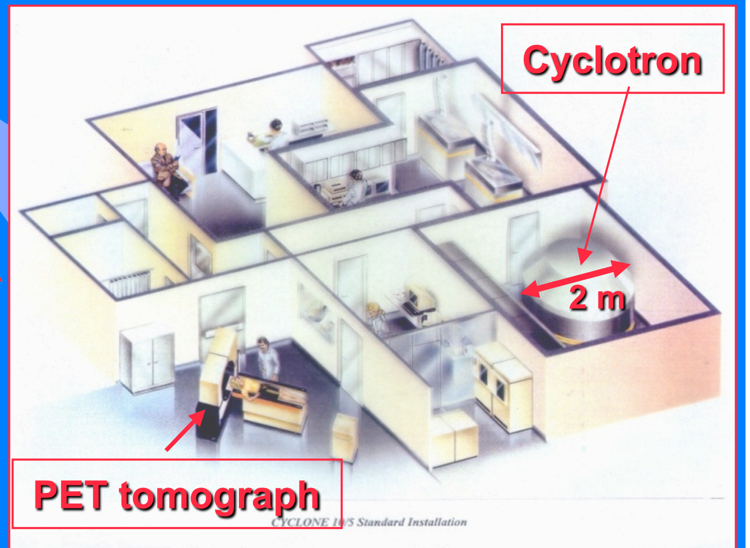

Today:

Therapy

Diagnostics

The beginning of medical imaging

- 1895 Prof. Wilhelm Conrad Roentgen discovers X-rays
- Phosphor screens introduced early 20th century
- In the ‘70 years routine use of fluoroscopy with image intensifiers coupled to TV cameras
- In the ‘80 years 'the radiography becomes digital (imaging plates, CCDs, flat-panels, semiconductor detectors both amorphous and crystalline) M. Hoheisel, NIM A563 (2006) 215–224

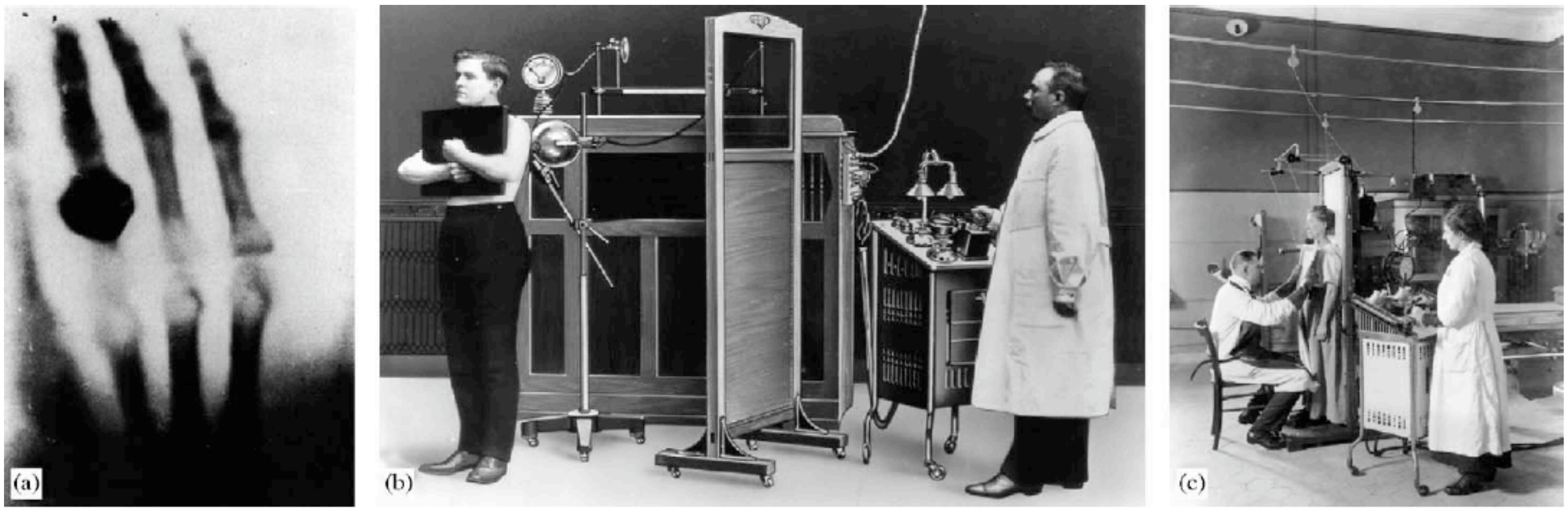

X-ray image versus CT scan

A conventional X-ray image is basically a shadow: you shine a “light” on one side of the body, and a piece of film on the other side registers the silhouette of the bones (to be more precise, organs and tissues of different densities show up differently on the radiographic film).

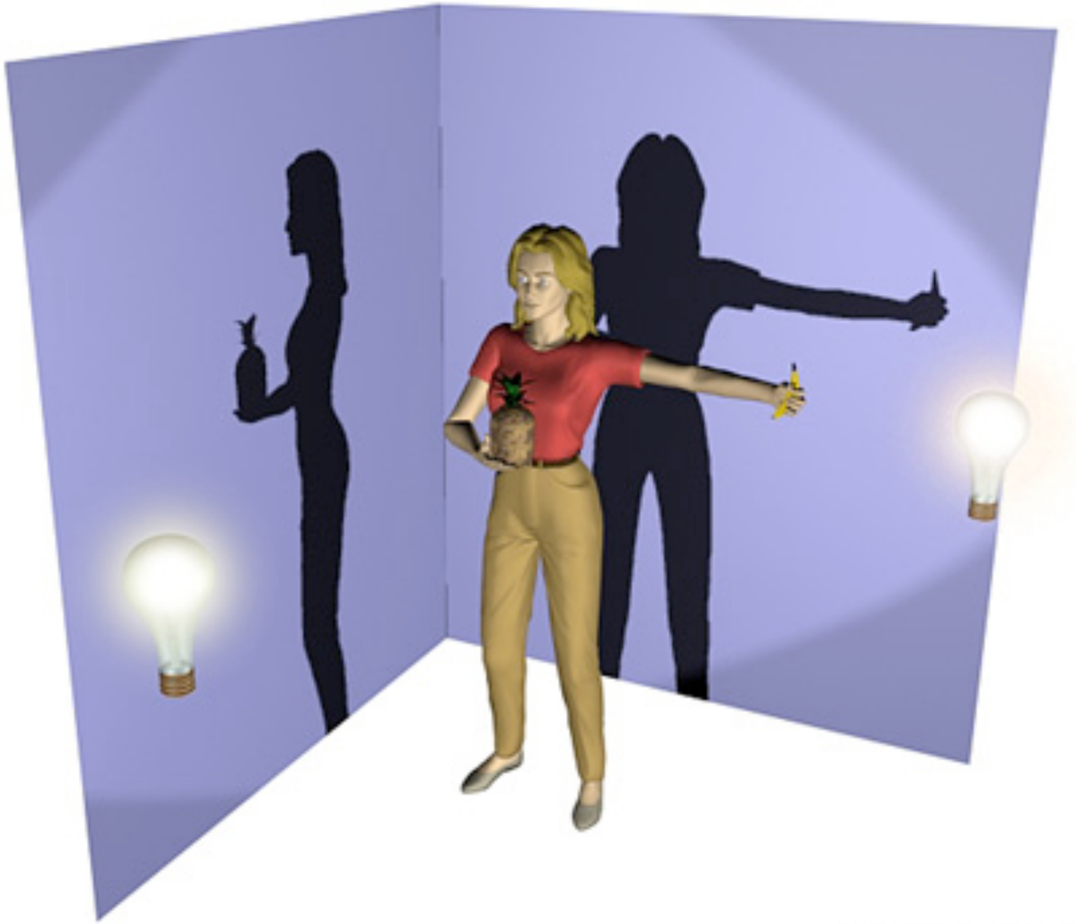

© 2002 HowStuffWorks

Shadows give an incomplete picture of an object's shape.

Look at the wall, not at the person. If there's a lamp in front of the person, you see the silhouette holding the banana, but not the pineapple as the shadow of the torso blocks the pineapple. If the lamp is to the left, you see the outline of the pineapple, but not the banana.

X RAYS COMPUTERIZED TOMOGRAPHY (CT)

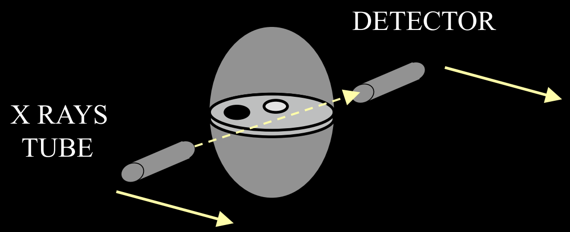

A – LINEAR SAMPLING

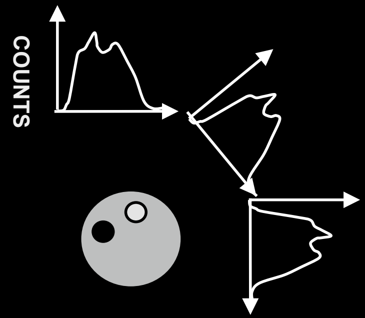

B – ANGULAR SAMPLING

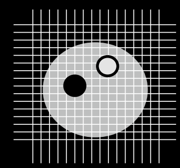

C - RECONSTRUCTION

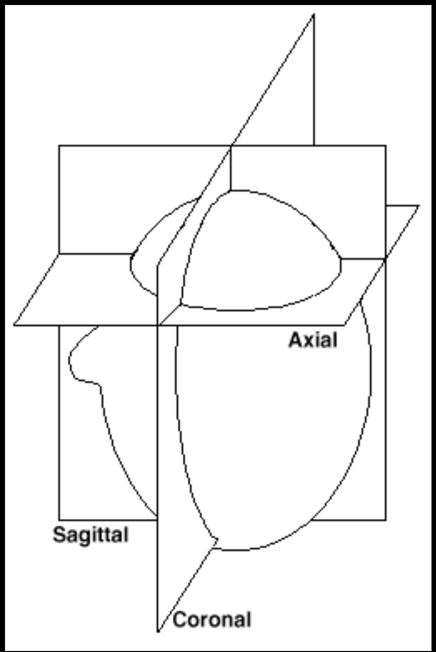

This is the basic idea of computer aided tomography. In a CAT scan machine, the X-ray beam moves all around the patient, scanning from hundreds of different angles. The computer takes all this information and puts together a **3-D image** of the body.

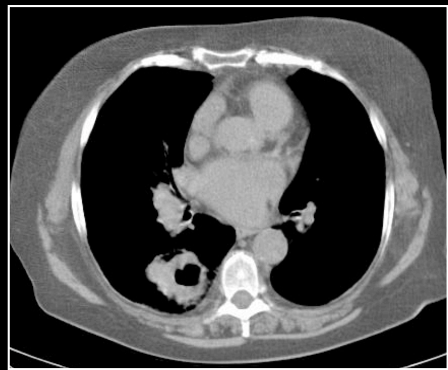

X RAYS
COMPUTERIZED TOMOGRAPHY

CT SCANNERS

GENERATION	I 1972	II 1974	III 1976	IV 1977
	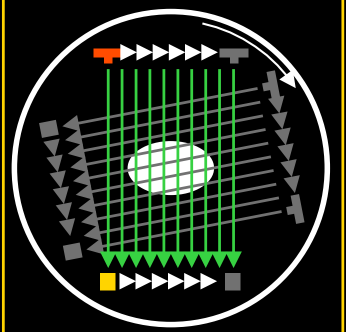	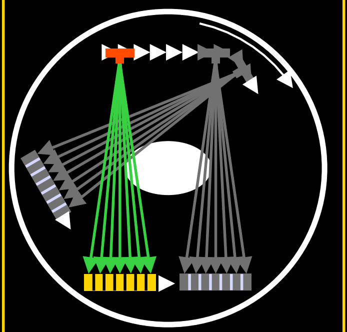	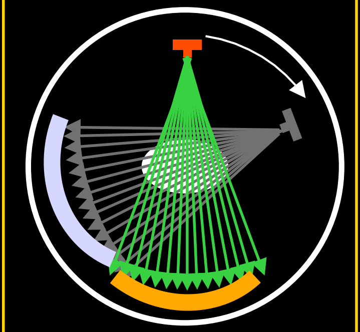	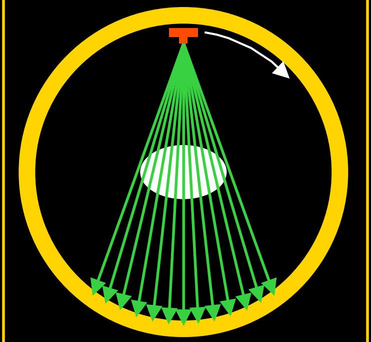
SOURCE-DETECTOR MOTION	TRANSLATION ROTATION	TRANSLATION ROTATION	ROTATION	ROTATION
DETECTORS NUMBER	1	~ 3-30	~ 400-500	~ 600-4800
SCAN (ROTATION) TIME	5 min	~ 10-60 sec	~ sec	~ sec
SLICE Number Thickness Pixel size	1 13 mm ~ 5 x 5 mm	1	1 1 mm 0,5 x 0,5 mm	1 1 mm 0,5 x 0,5 mm
	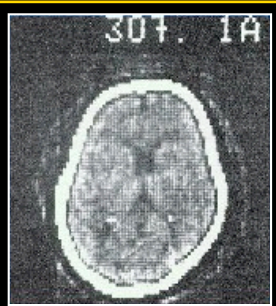		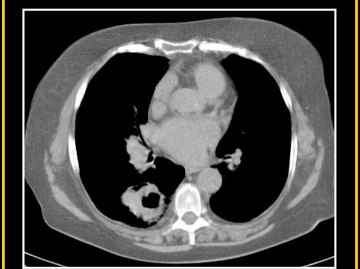	STEP AND SHOOT 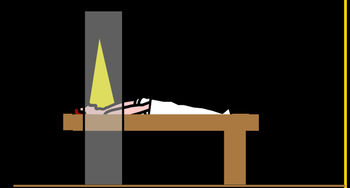

CT SCANNERS

GENERATION	I 1972	II 1974	III 1976	IV 1977
	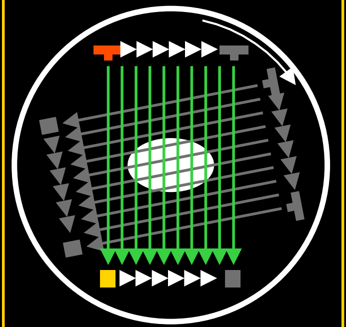	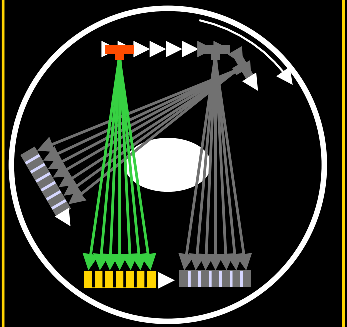	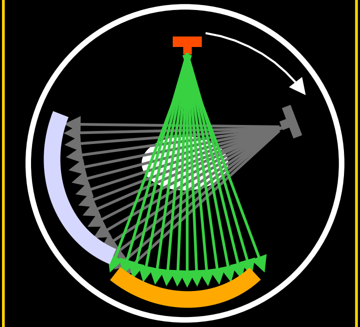	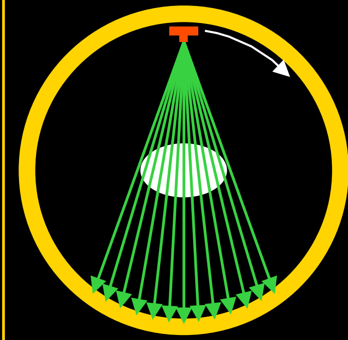
SOURCE-DETECTOR MOTION	TRANSLATION ROTATION	TRANSLATION ROTATION	ROTATION	ROTATION
DETECTORS NUMBER	1	~ 3-30	~ 400-500	~ 600-4800
SCAN (ROTATION) TIME	5 min	~ 10-60 sec	~ sec	~ sec
SLICE Number Thickness Pixel size	1 13 mm ~ 5 x 5 mm	1	1 1 mm 0,5 x 0,5 mm	1 1 mm 0,5 x 0,5 mm
	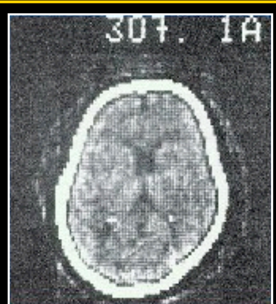			STEP AND SHOOT 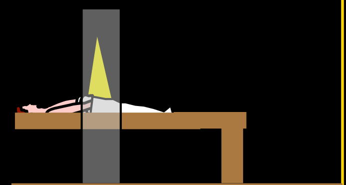

CT SCANNERS

GENERATION	SPIRAL CT 1989	1994	MULTI SLICE SPIRAL CT 1998	2002	2004
	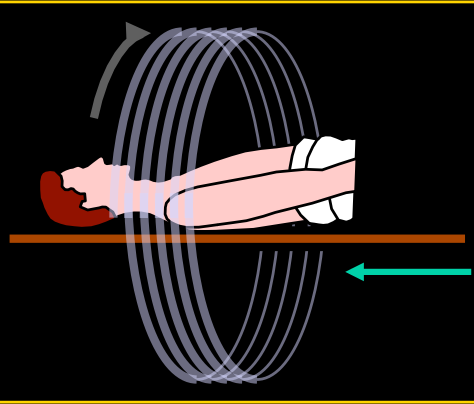		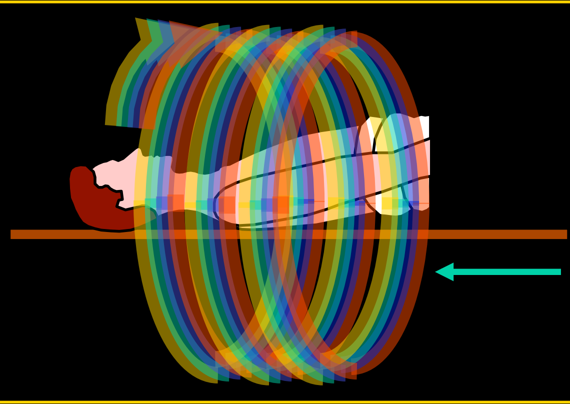		
DETECTOR MOTION	Continuous volume acquisition		Continuous volume acquisition		
ROTATION TIME	1 sec	0,75 sec	0,5 sec	0,4 sec	< 0,4 sec
SPEED	24 sec / 24 cm PITCH=1	100 sec / 130 cm PITCH=1			
SLICES Number min Thickness	1 2 mm	1 1 mm	4 1 mm	16 0,6 mm	64 < 0,4 mm
	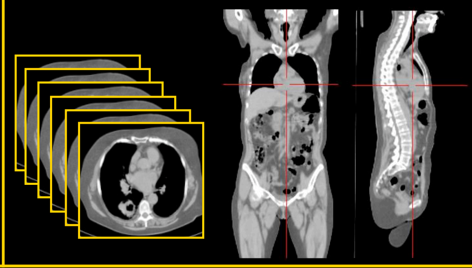				

PITCH = TABLE FEED PER ROTATION/COLLIMATION

Emission vs. transmission tomography

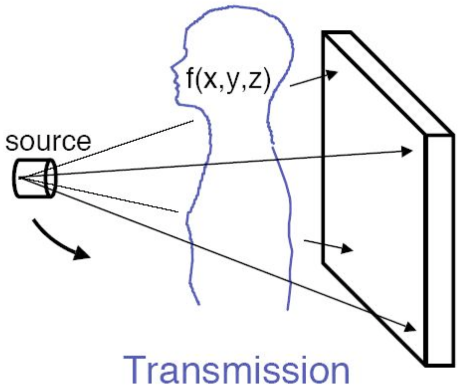

Transmission

- external radiation source
  (X-ray : 10 keV - 100 keV)
- anatomical structure
- Computed Tomography (CT), radiography
- spatial resolution: 1-2 mm, fraction of mm

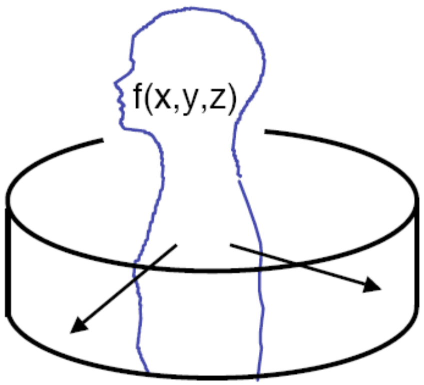

Emission

- radioactively labeled substance administered within the body (injected or inhalated)
- functional imaging
- SPECT: Single Photon Emission CT,
  PET: Positron Emission Tomography
- spatial resolution: 4 - 6 mm PET
  10 - 12 mm SPECT

Nuclear medicine tomographic techniques

γ emitting isotope

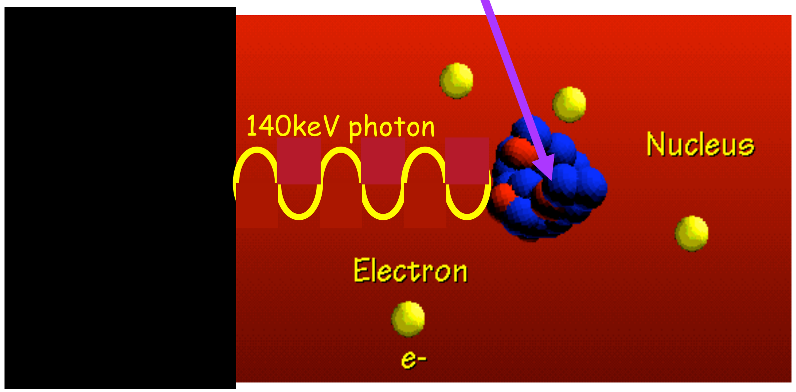

SPECT
Single Photon Emission
(Computed) Tomography

Single photon detection

(β+) emitting isotope

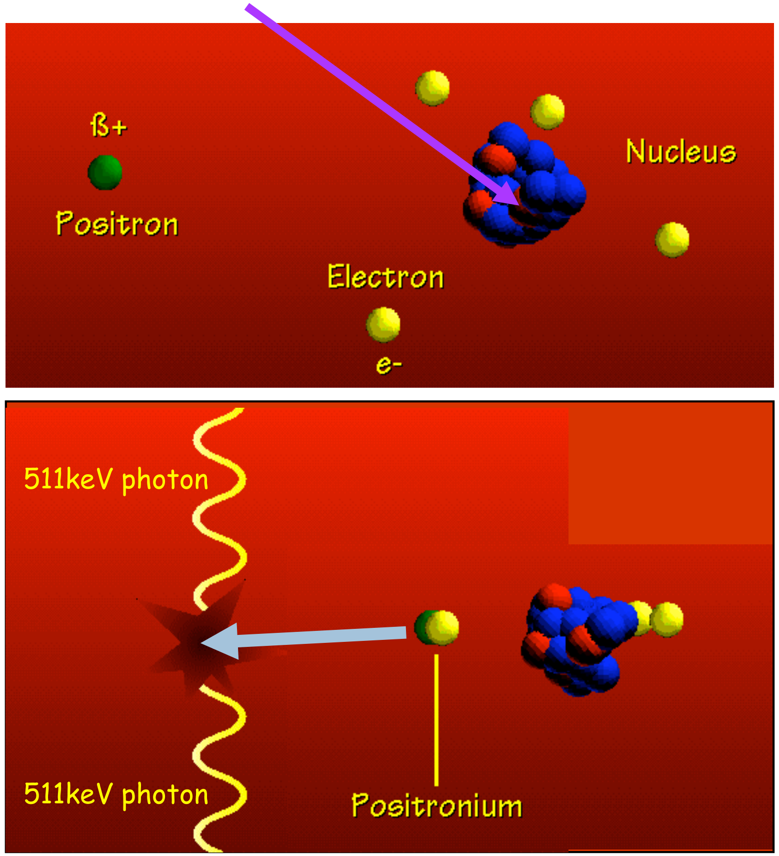

PET Positron (β+) Emission
Tomography

SPECT = Single Photon Emission Computer Tomography

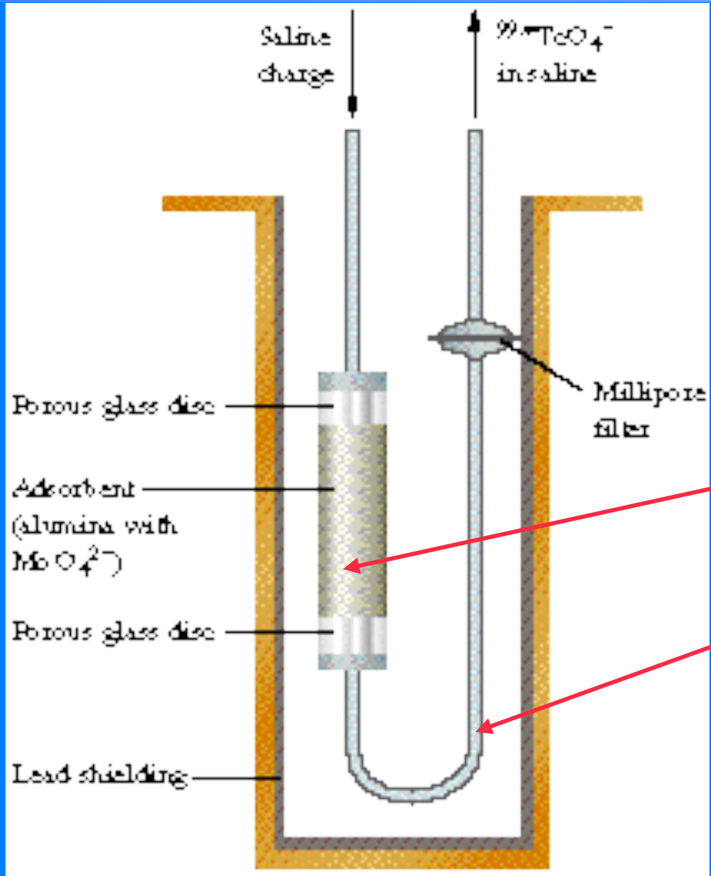

In reactors **slow neutrons** produce

$^{98}Mo + n = {}^{99}Mo + \gamma$

$^{99}Mo\ (66\ h) = {}^{99m}Tc\ (6\ h) + e^{-} + \bar{\nu}$

gamma of 0.14 MeV

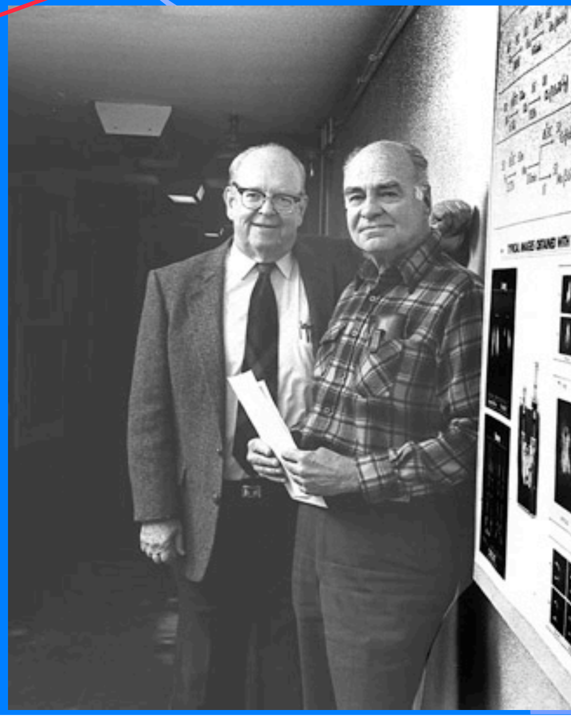

Molibdenum 'generator'

BNL - 1960

Powel Richards

and Walter Tucker

SPECT scanner

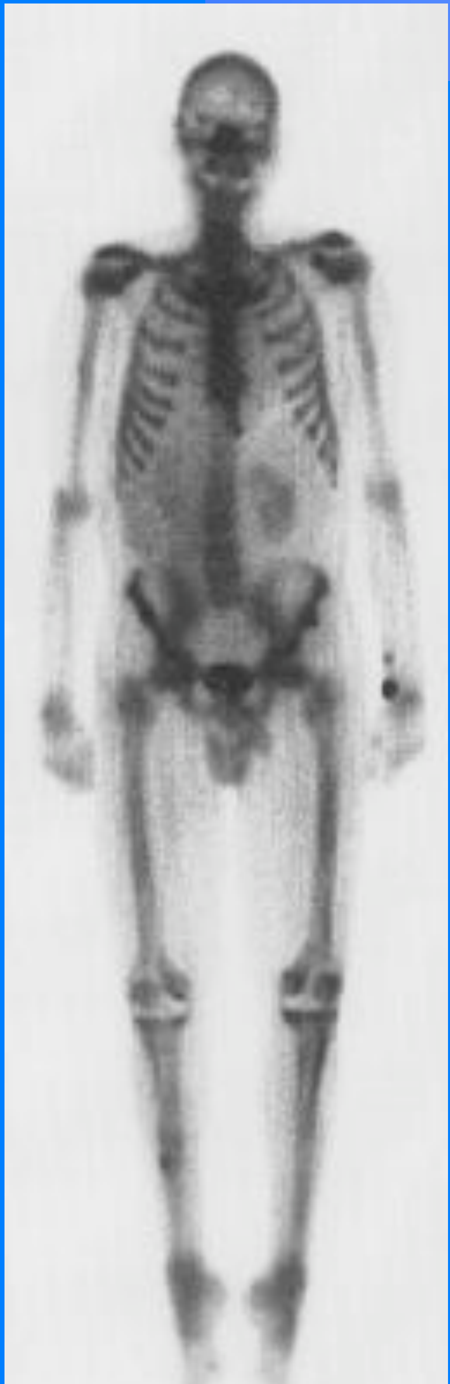

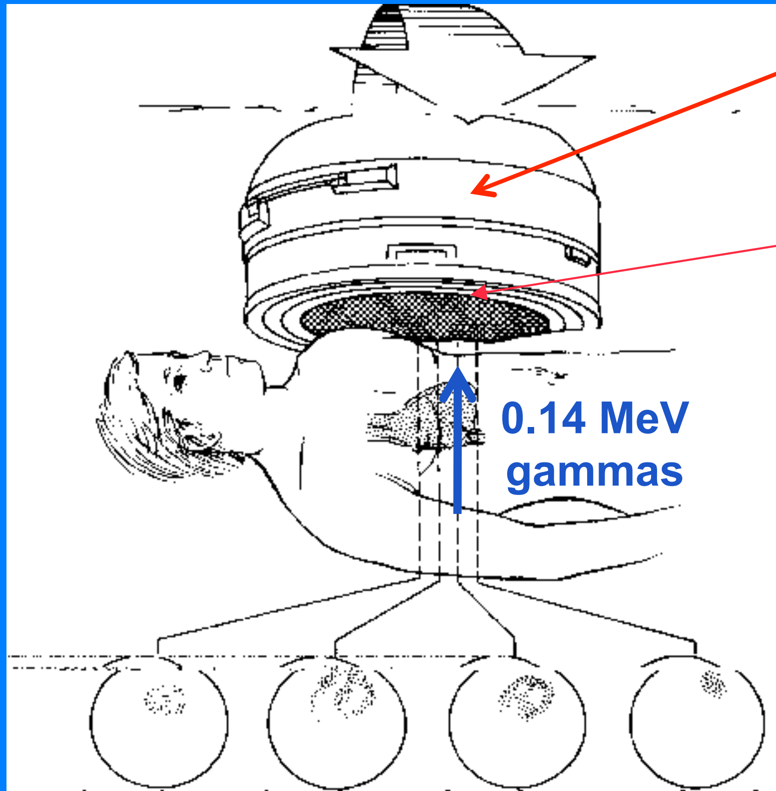

Rotating head with detectors

Collimators of the 0.14 MeV gammas

85% of all nuclear medicine examinations use ^{99m}Tc

Generators for diagnostics of liver, lungs, bones ……

SPECT: single γ -ray detection

γ -rays (Typically:140 keV from ^{99m}Tc) are emitted in all the directions

Hence, necessity of collimators to determine the line of response.

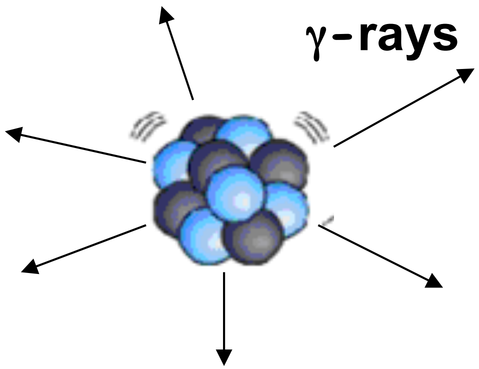

γ-emitting radionuclide

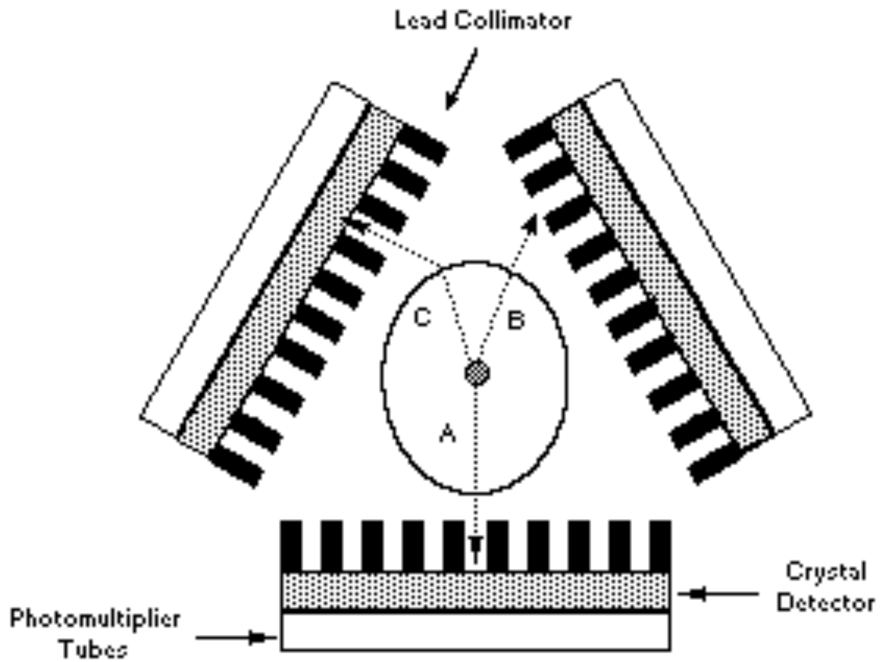

Gamma Camera

Principle:
many photomultiplier tubes "see" the same large scintillation crystal; an electronic circuit decodes the coordinates of each event

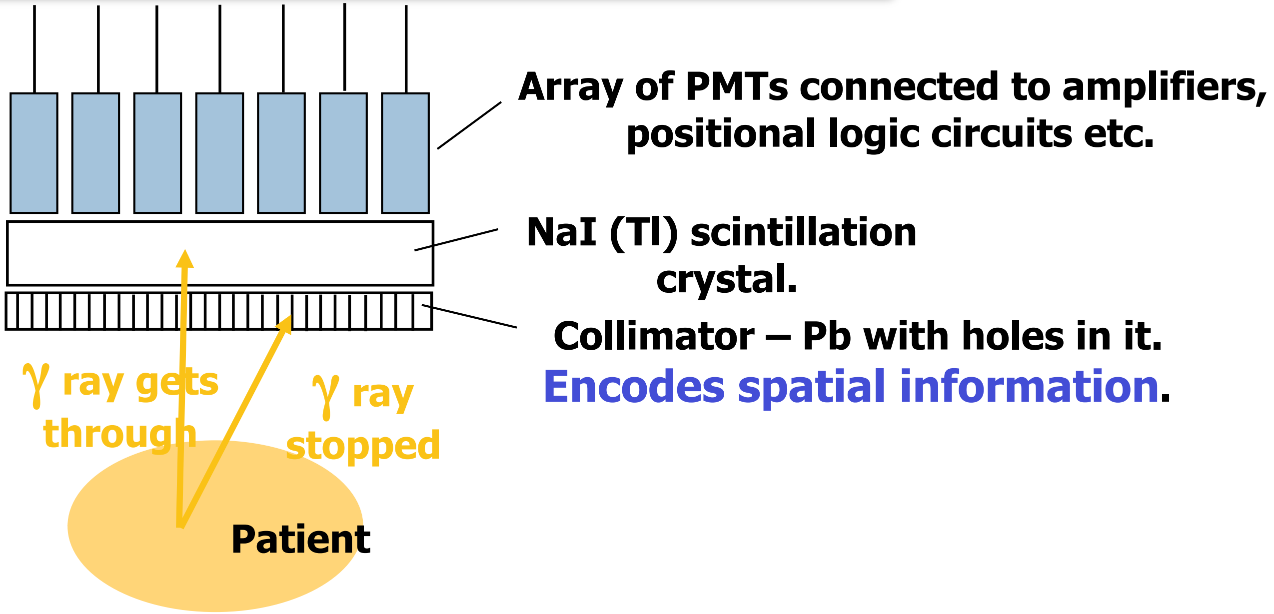

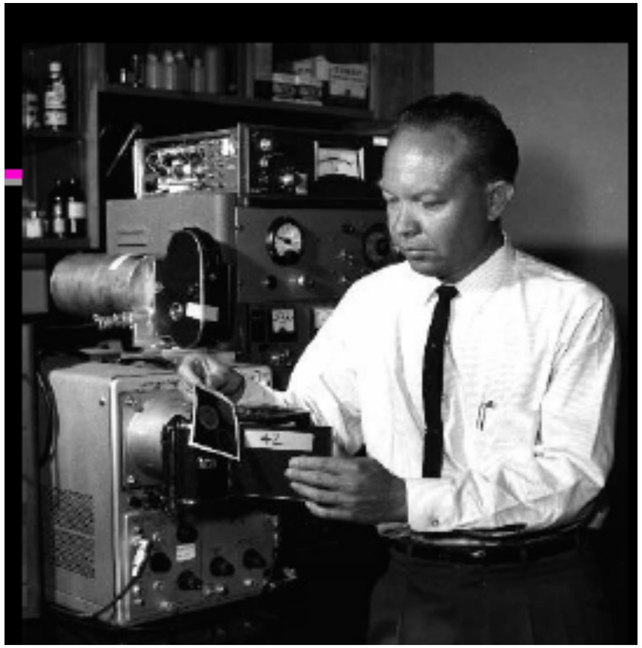

1957 H. Anger with his positron camera (Berkeley)

Some clinical SPECT applications

Oncology

^{99m}Tc
Whole body scan

^{131}I
thyroid study

Cardiology

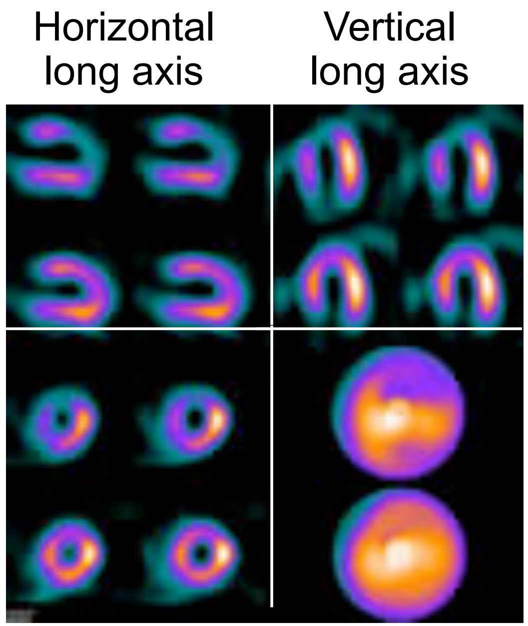

^{99m}Tc-MIBI
myocardium perfusion

Nuclear medicine tomographic techniques

γ emitting isotope

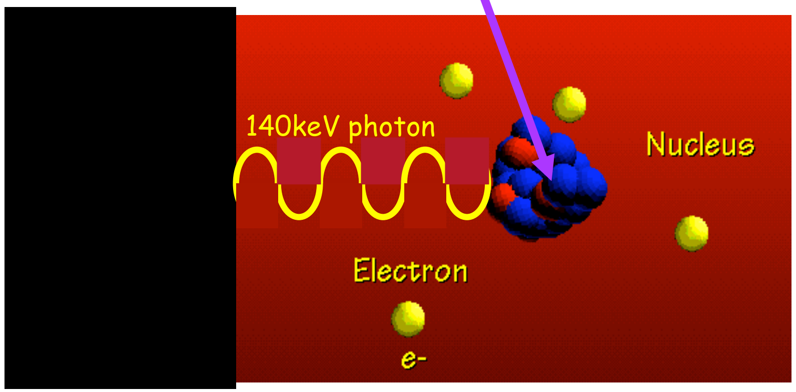

SPECT
Single Photon Emission (Computed) Tomography

Single photon detection

(β+) emitting isotope

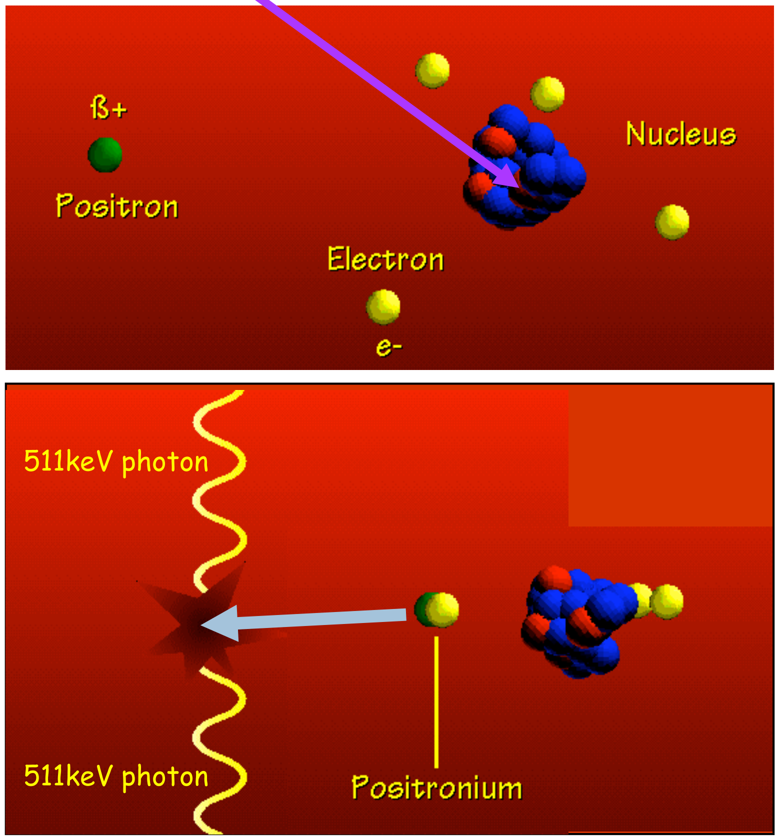

PET Positron (β+) Emission Tomography

Positron Emission Tomography (PET)

Cyclotron

ISOTOPES	Half-Life	
11-C	20.4 min,	"natural"
13-N	10.0 min	"natural"
15-O	2.0 min	"natural"
18-F	109.8 min	"pseudo-natural"

Radiochemistry

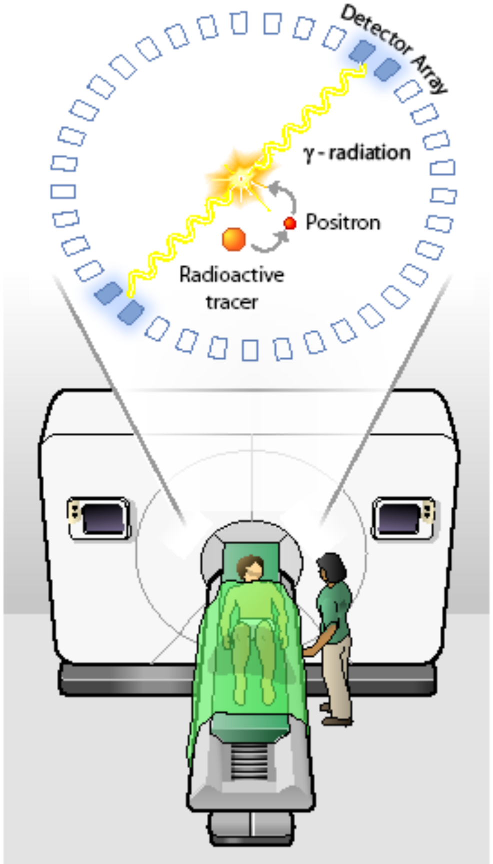

J. Long, "The Science Creative Quarterly",scq.ubc.ca

Centre for Nuclear Medicine

For PET the most used compound

FDG = sugar

F = ^{18}F

with half-life 1.6 h

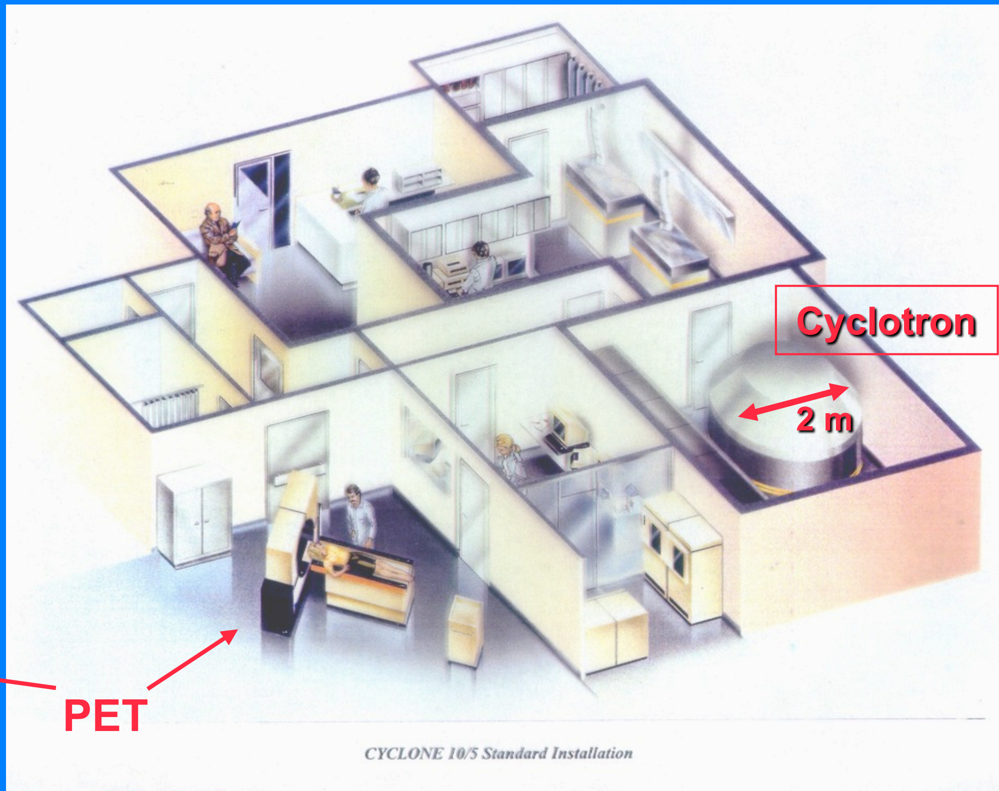

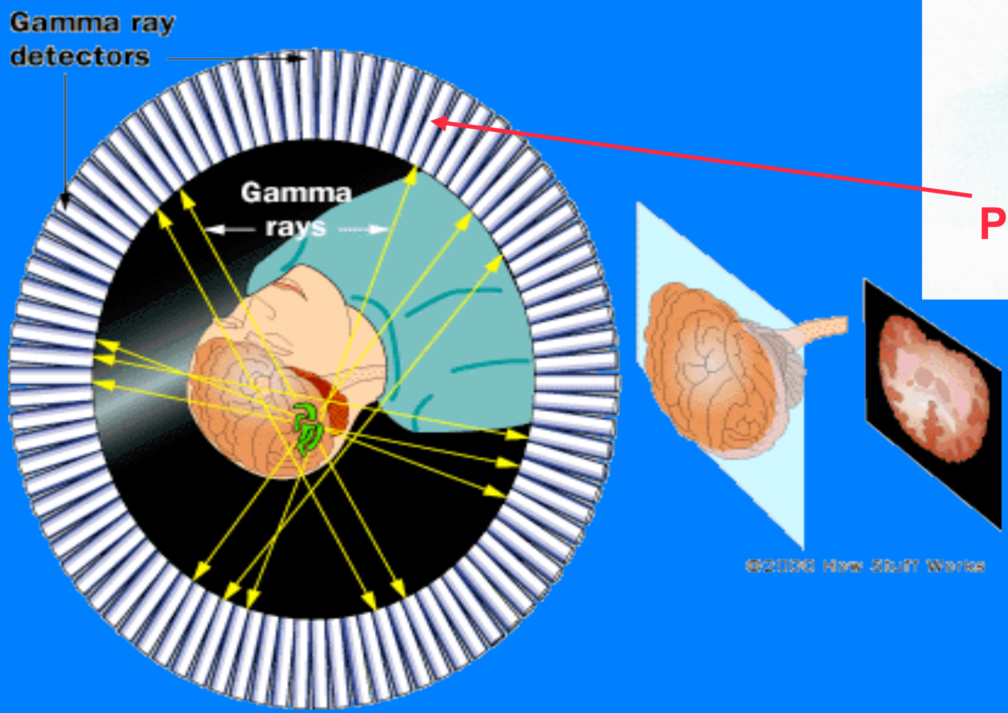

PET geometries

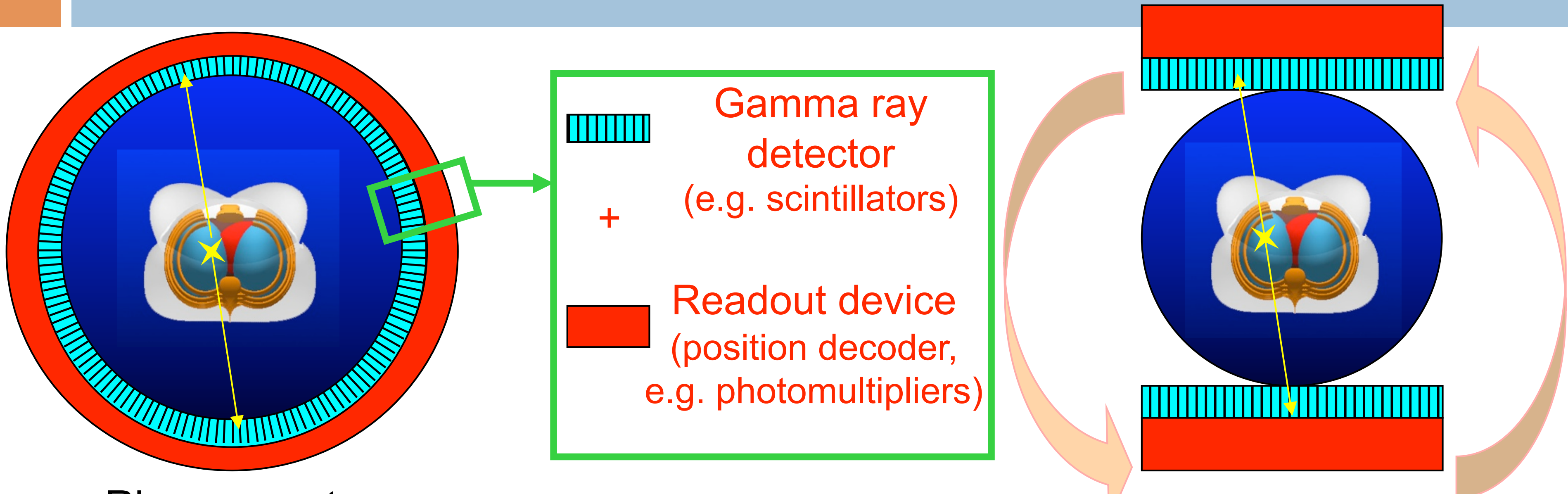

Ring geometry

Parallel plane geometry

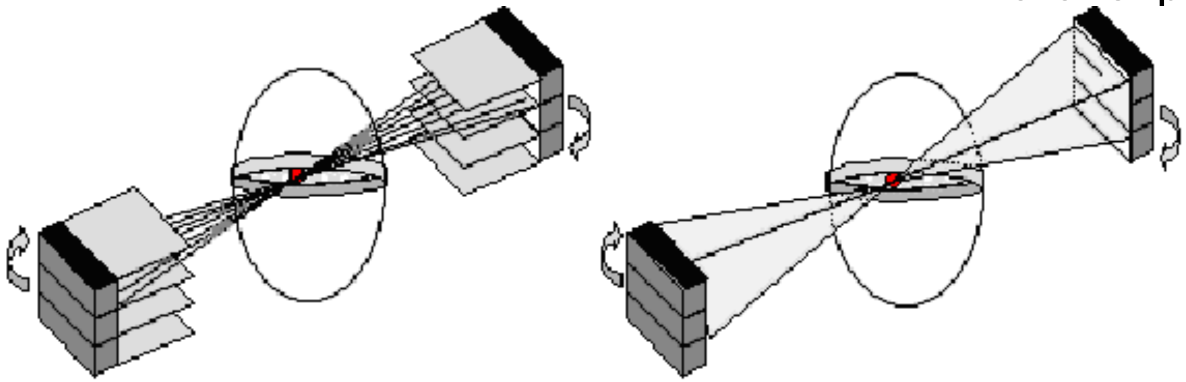

2D acquisition
with lead (or "software") septa

3D acquisition
without septa

The Block Detector

1984-1985

Burnham, Brownell and colleagues at MGH developed a technique where scintillators were placed on a circular lightguide with photomultipliers placed on the opposite side of the lightguide. Charlie Burnham demonstrated that by taking the ratio of two adjacent photomultiplier signals, the scintillator that detected the gamma ray could be identified.

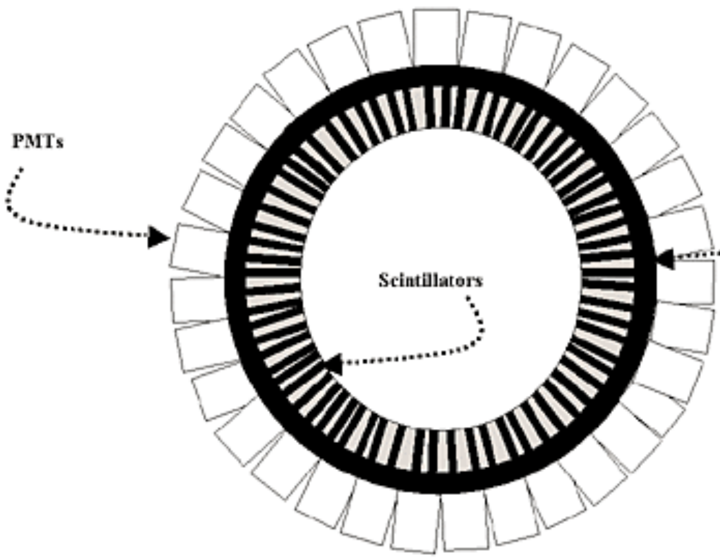

Scintillators placed on a circular light guide with photomultipliers on opposite side of light guide.

The block detector

Mike Casey and Ronald Nutt, from CTI, introduce the "Block“ detector that was conceived as a means to simplify the Burnham detector and to make it easier to manufacture. Almost all dedicated tomographs built since 1985 have used some forms of the Block detector. This invention has made possible high-resolution PET tomographs at a much-reduced cost.

Principle of Operation

In a block detector, a 2D array of crystals are attached to 4 PMTs.
Usually the array will be cut from a single crystal and the cuts filled with light-reflecting material. When a photon is incident on one of the crystals, the resultant light is shared by all 4 PMTs. Information on the position of the detecting crystal may be obtained from the PMT outputs by calculating the following ratios and comparing them to pre-set values:

$$R_x = \frac{A+B}{A+B+C+D}$$

$$R_y = \frac{A+C}{A+B+C+D}$$

where A, B, C and D are the fractional amounts of light detected by each PMT

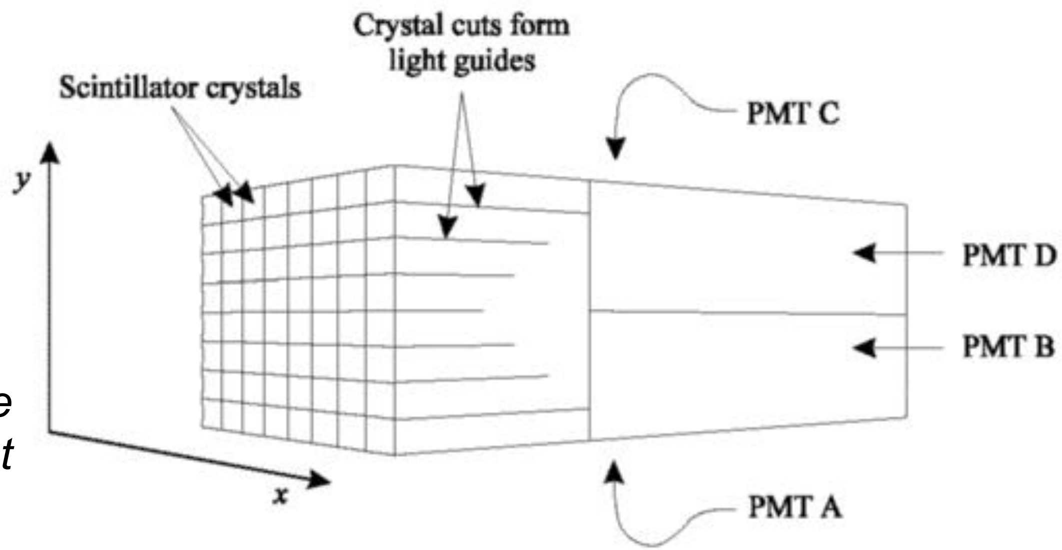

From the block detector to PSPMT's

"Block detector"

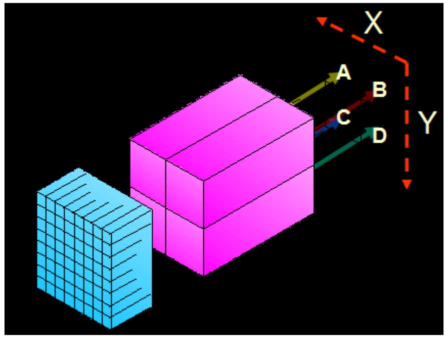

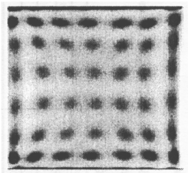

•Large "b"
•Limitations on minimum "d"

"*1st generation*" PSPMT

Hamamatsu
PS-PMT R2486.
•50 mm Ø active area
• 16 x + 16 y anodes

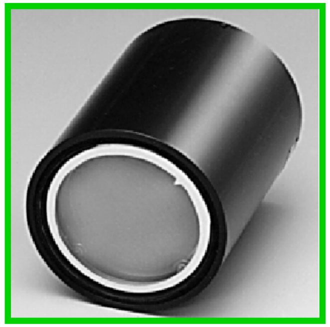

Small crystals can be used
(down to d = 1mm)

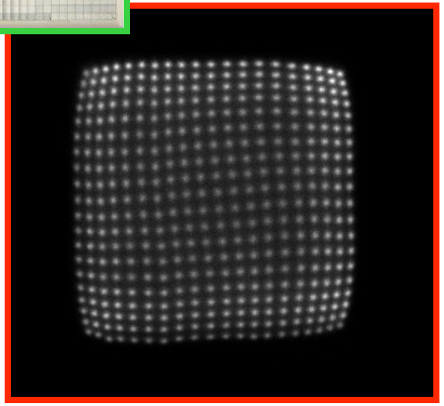

Used in the
YAP-(S)PET
(Univ of Ferrara
Italy,1993)

Flood field irradiation (511 keV)
of a matrix of scintillator YAP:Ce,
read by a Hamamatsu R2486
(resistive readout)

Still PMTs?

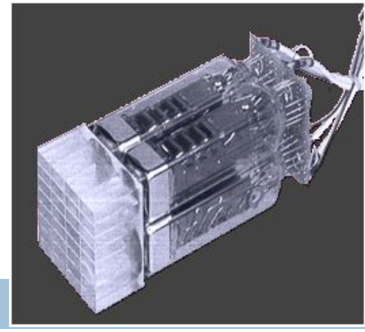

Since more than 80 years, the PMT is the photodetector of choice to convert scintillation photons into electrical signals in most of the applications related to the radiation detection. This is due to its high gain, low noise and fast response

Research is now moving to solid state photodetectors that show the following advantages with respect to PMTs:

- Compactness
- High quantum efficiency (to provide an energy resolution comparable to PMTs)
- Insensitivity to magnetic fields(PET/MRI)

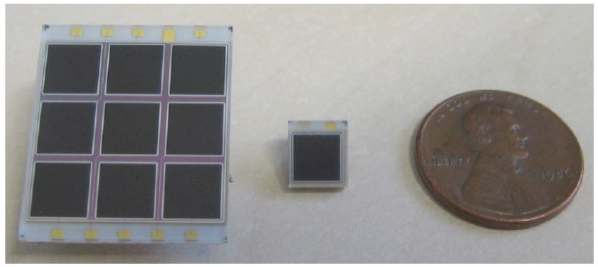

Avalanche Photodiodes (APDs)

Silicon Photomultipliers(SiPMs) o Geiger-mode APD

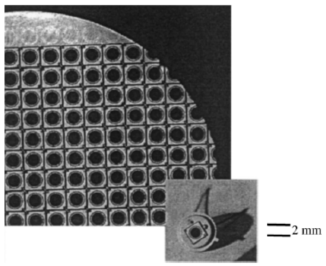

Coding problem: “Individual coupling” with APD’s or light sharing with PSPMT’s

APD

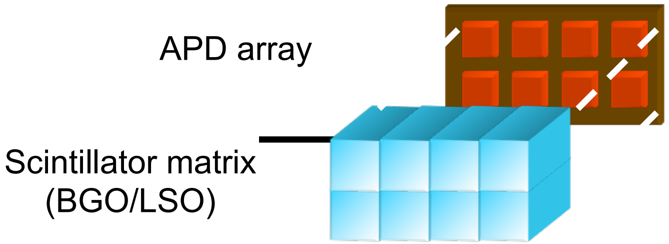

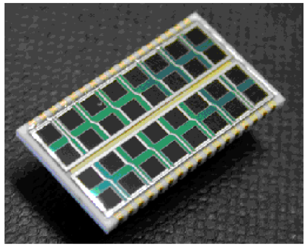

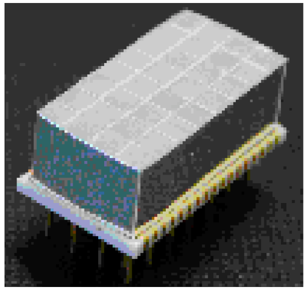

+ High spatial resolution (b=0)

+ No Pile-up

+ No scattering in the crystals

- Expensive

- Many channels

- Difficult tuning

The detector module is composed by a matrix of 8×4 LSO crystals readout by a Hamamatsu S8550 (*Pichler B., IEEE TNS 45 (1998) 1298-1302)*

2nd generation PSPMT

Hamamatsu
PS-PMTR8520-C12

- Active area 22 mm × 22mm
- 6 x + 6 y anodes

+ Few channels to readout (resistive chain)

+ High gain and stability

- Non negligible coding error

- Pile-up increases with area

-

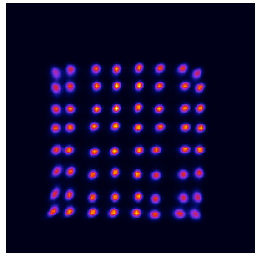

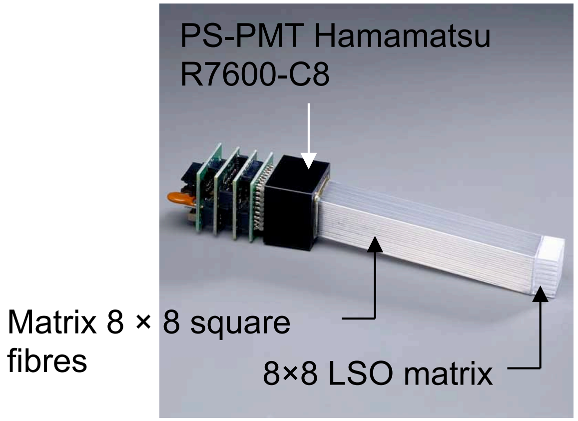

PET scintillators

Material	Density [g/cm^3]	Atomic numbers	Light yield [%NaI(Tl)]	Decay time [ns]	Peak wavelength [nm]	Time resolution [ns]	Index of refraction	Comments
NaI(Tl)	3.76	11,53	100	230	410	1.5	1.85	Hygroscopic Low density
BGO	7.13	83,32,8	15	300	480	7	2.15	Low light yield Slow
LSO	7.4	71,32,8	75	40	480	1.4	1.82	Intr. background 400 cps/cm^3
GSO	6.71	64,32,8	26	600	430	-	1.85	Low light yield Slow
CsI(Tl)	4.51	55,53	45	1000	565	-	1.80	Slow
YAP:Ce	5.37	39,13,8	55	27	370	1.1	1.95	Medium Z

Detectors are usually scintillators:
the most often used is BGO (Bismuth germanate, $Bi_4Ge_3O_{12}$) and more recently LSO (Lutetium Oxi-orto Silicate (LuSiO).

FUTURE DEVELOPMENTS IN PET

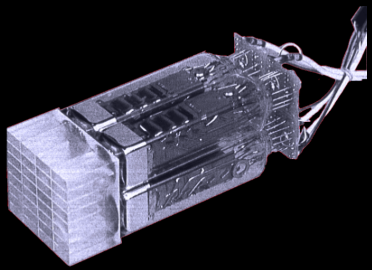

CURRENT DETECTORS: BGO, GSO, LSO

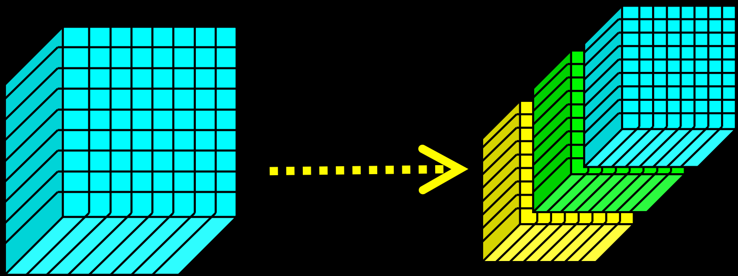

SANDWICH OF DETECTORS

NEW DETECTORS with:

- SMALLER SIZE (2-3 mm)
- GOOD ENERGY RESOLUTION
- DEPTH OF INTERACTION INFORMATION

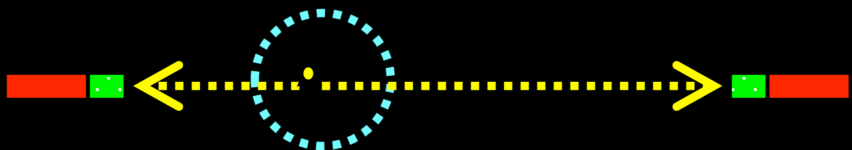

FASTER DETECTORS for

- HIGH COUNT RATE CAPABILITY
- TIME OF FLIGHT INFORMATION

TOF systems: principle of operation

- TOF-PET systems exploit the time difference between the two emitted photons to better locate the annihilation position.

- The limit in the annihilation point location is mainly due to the error in the time difference measurement , namely the time resolution **Δt** of the coincidence system

- Time resolution is used by the reconstruction algorithm to locate the annihilation point **Δx** (**Δx** $= c\ \Delta t/2$)

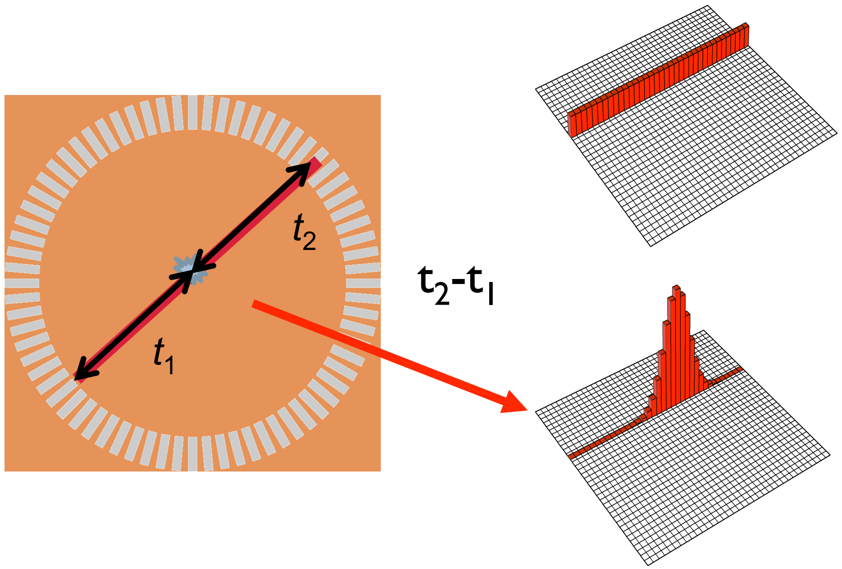

PET traditional

The probability for the event to be located along the LOR is uniform

PET Time-of-Flight

The most likelihood position is in the center of the error distribution

Time Of Flight (TOF) systems

a "renaissance"

1) Development of new scintillators that combine fast decay time with high light yield and stopping power
2) Improvement of the performance and reliability of the PMTs and electronics
3) Progress in the image reconstruction algorithms

…made the coming back of time of flight systems possible, though already proposed in the '80s

Gemini TF (Philips)

Biograph mCT (Siemens)

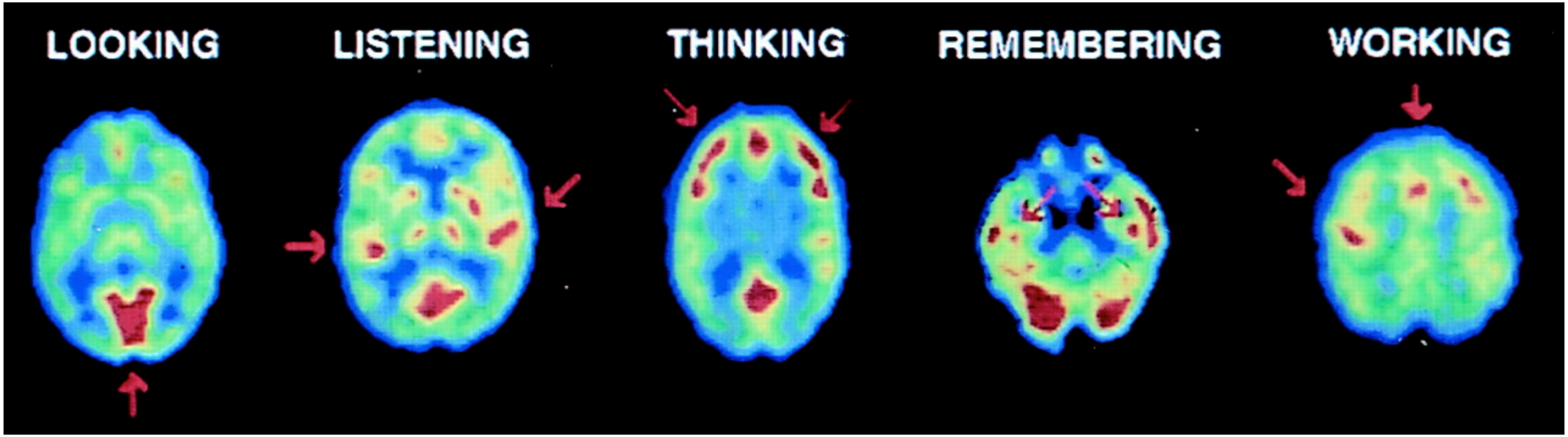

PET studies of glucose metabolism to map human brain's response in performing different tasks. Subjects looking at a visual scene activated visual cortex (arrow), listening to a mystery story with language and music activated left and right auditory cortices (arrows), counting backwards from 100 by sevens activated frontal cortex (arrows), recalling previously learned objects activated hippocampus bilaterally (arrows), and touching thumb to fingers of right hand activated left motor cortex and supplementary motor system (arrows). Images are cross-sections with front of brain at top. Highest metabolic rates are in red, with lower values from yellow to blue.

Clinical PET applications

Oncology

^{18}F-FDG
Total body

Neurology

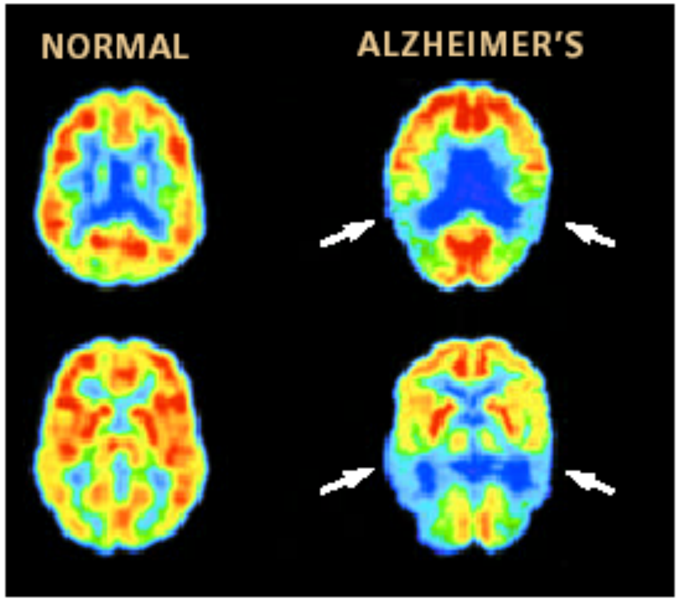

^{18}F-FDG
Brain study for
Alzhemeir's disease

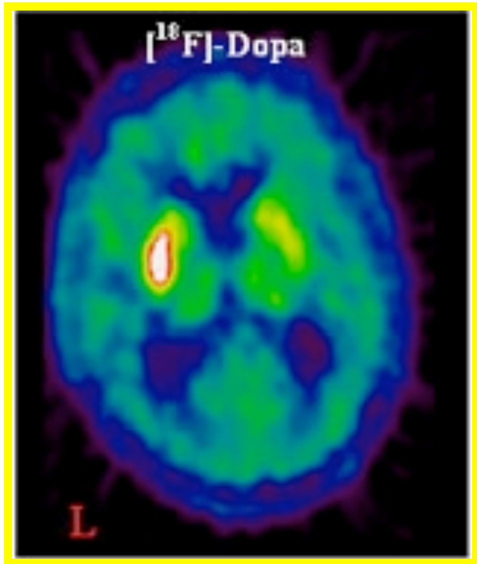

^{18}F-DOPA
Brain study for
Parkinsons's disease

CLINICAL PET IN ITALY

TOTAL EXAMS/YEAR

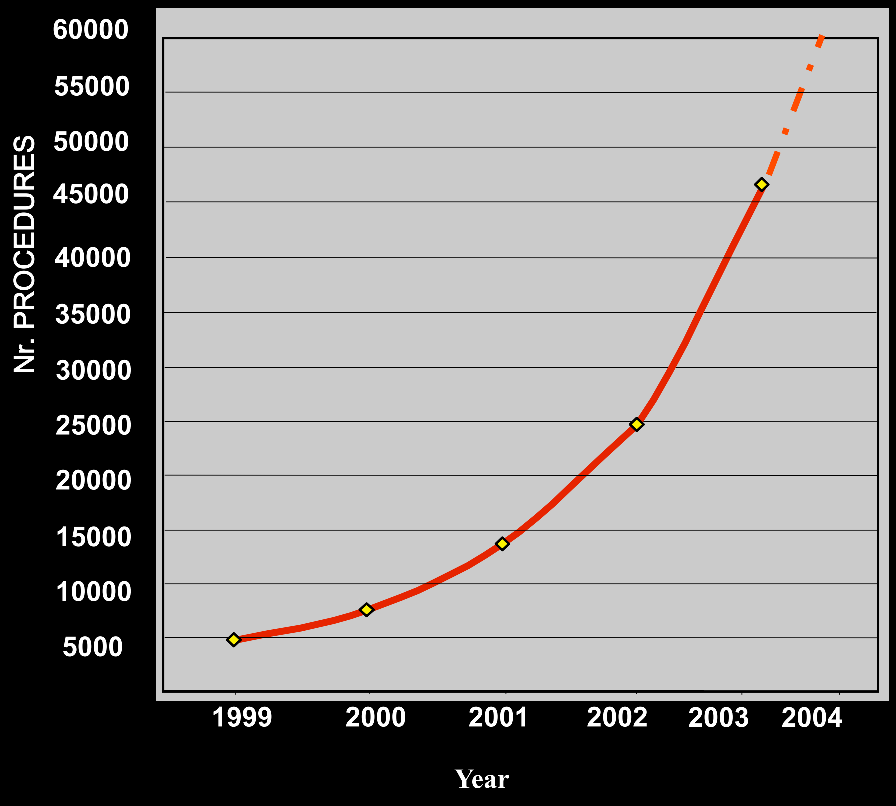

ESTIMATED PET - PET/CT SCANNER UNITS WW

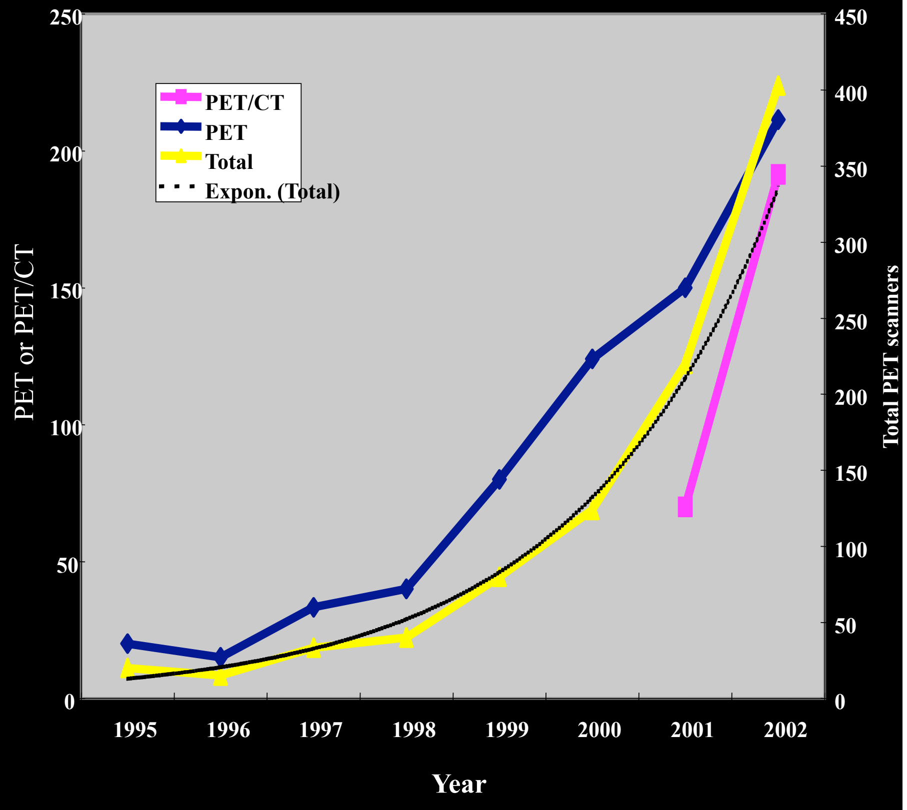

PET – [^{18}F]FDG

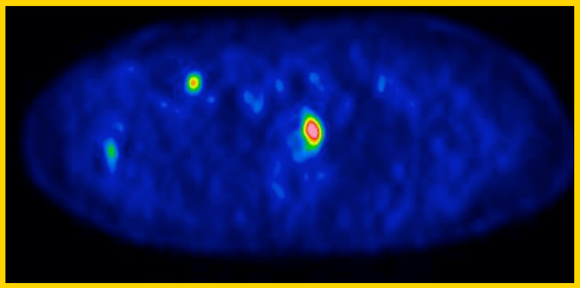

PET

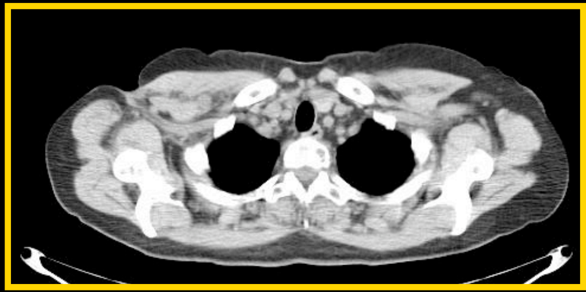

CT

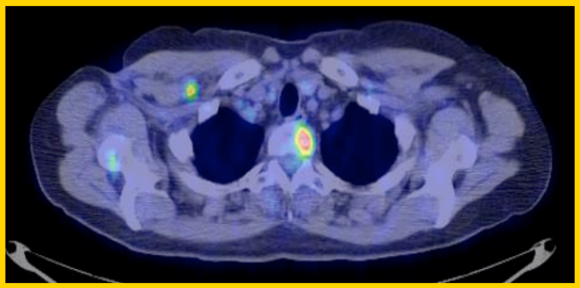

PET/CT

LACK OF ANATOMICAL INFORMATION

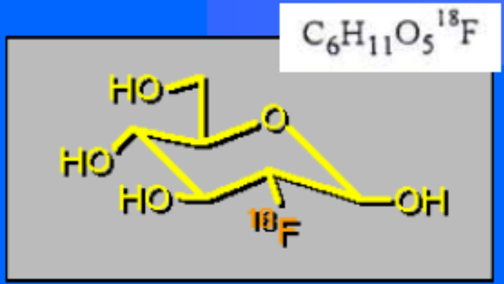

^{18}F production : $^{18}O(p, n)^{18}F$

2-[^{18}F]fluoro-2-deoxy-D-glucose = FDG for PET exams

in oncology, cardiology, neuro-receptor imaging

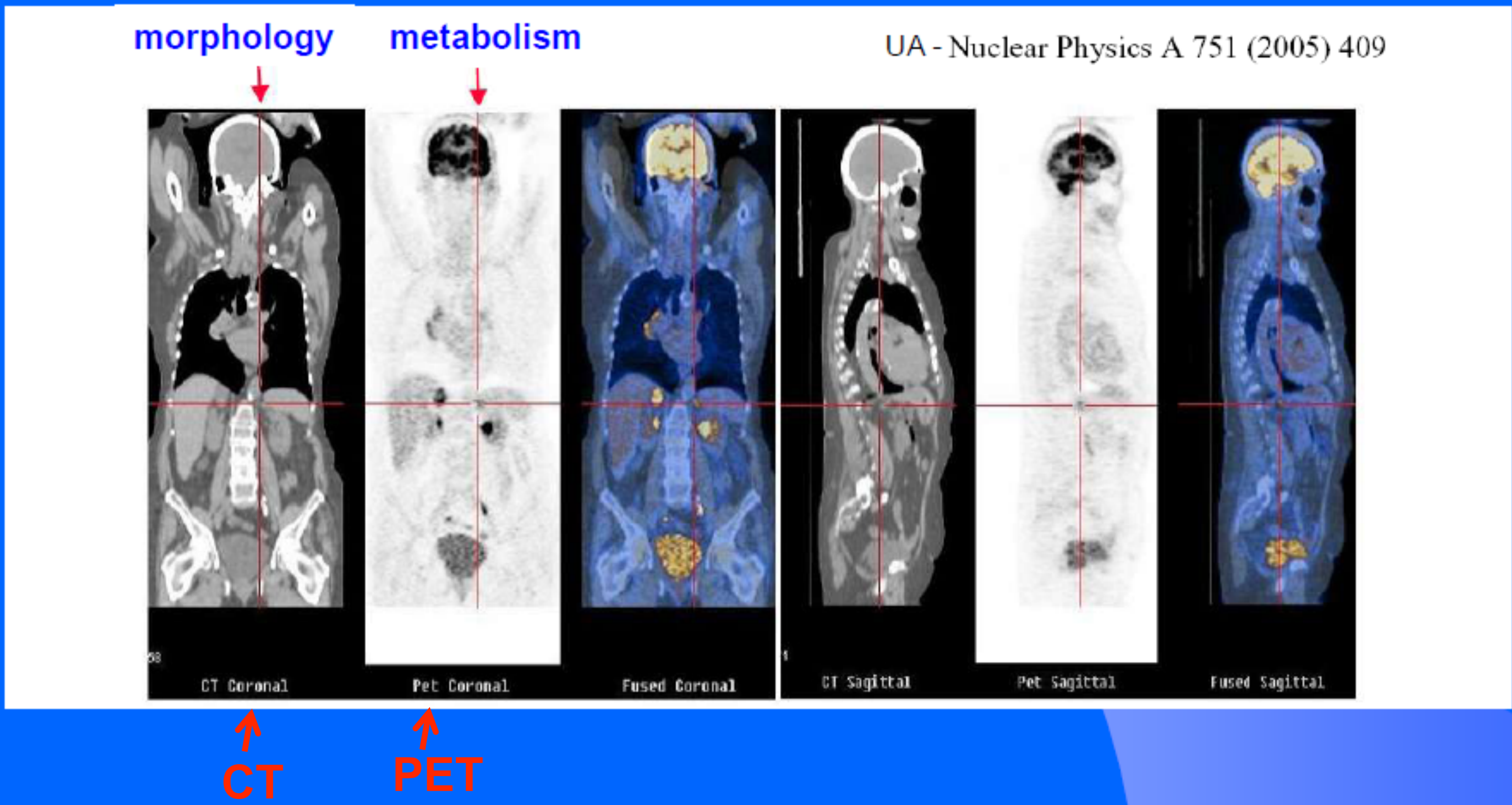

PET-CT: a new revolution

"PET-CT is a technical *evolution* that has led to a medical *revolution*"

J.Czernin, UCLA

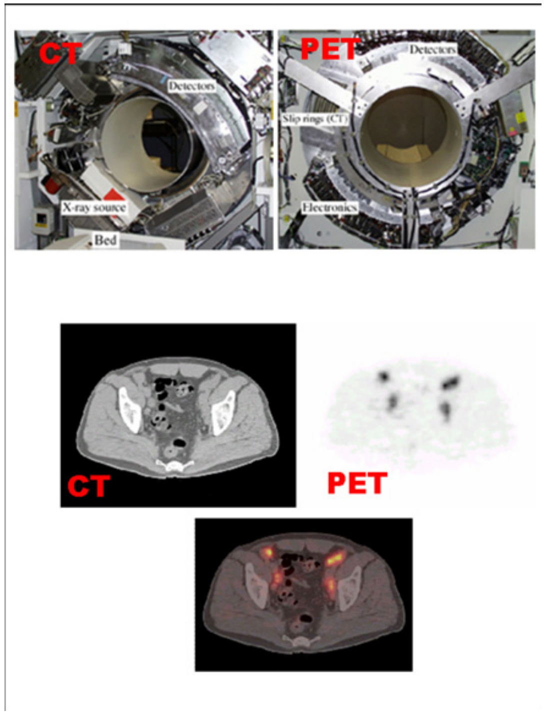

First PET/CT (1998)
CTI PET Systems (now Siemens)

- New detectors (materials, geometries)
- 3D Acquisitions
- Faster electronics
- New reconstruction algorithms
- High performance CT systems

PET intrinsic limitations

Positron range | Angular deviation

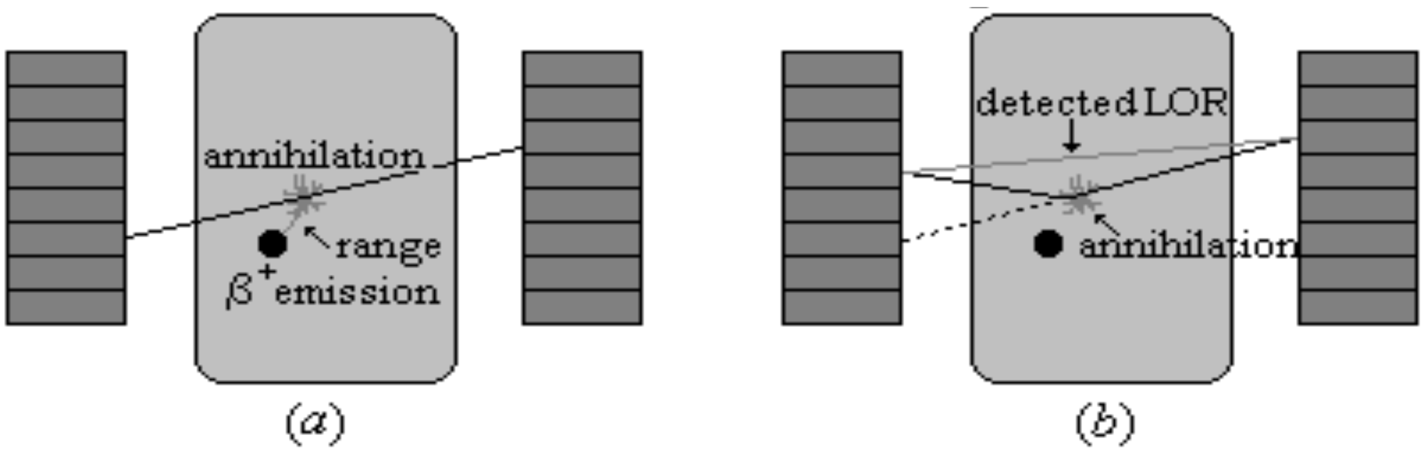

» **Depends on the radioisotope**

	<E_c > (MeV)	*<Range> in water*	*FWHM (mm)*
^{18}F	0.242	1.4 mm	0.22
^{11}C	0.385	1.7 mm	0.28
^{68}Ga	0.740	3.0 mm	1.35

» **Depends on the ring radius**
(1.8 mm for a 400 mm radius)

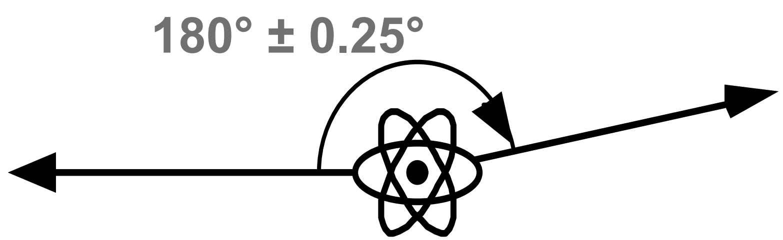

PET/CT

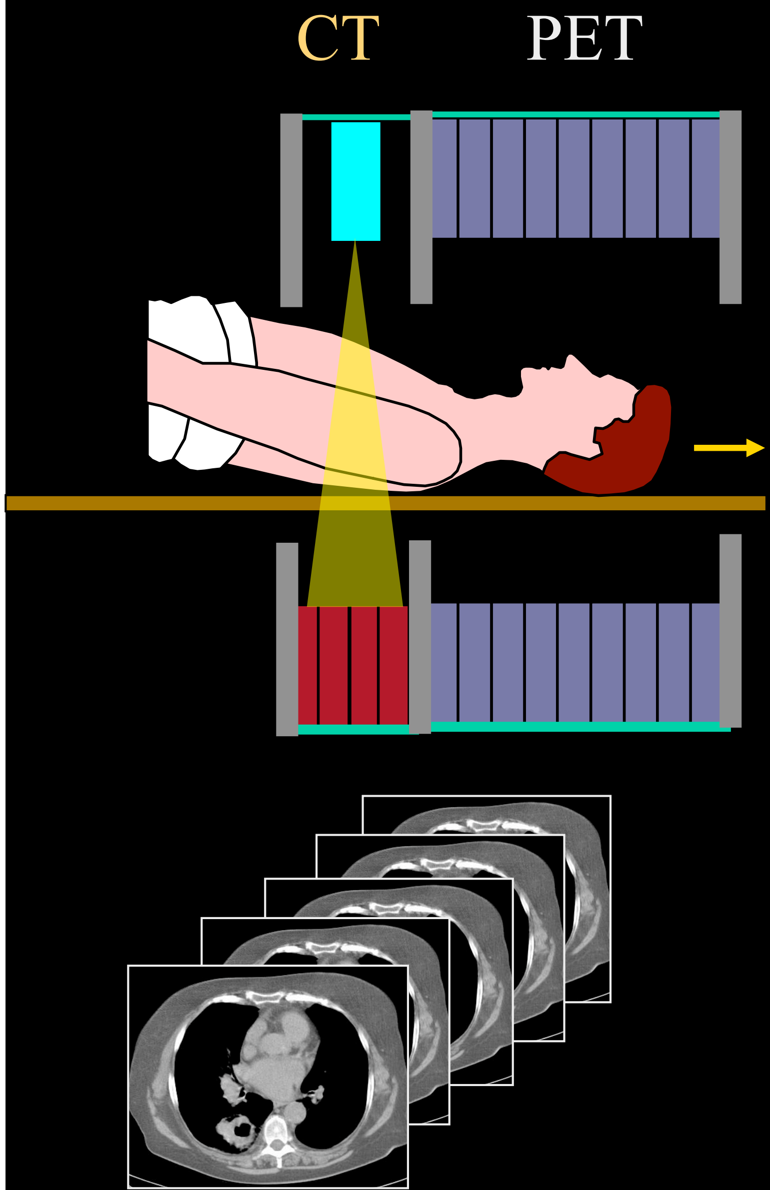

PET/CT

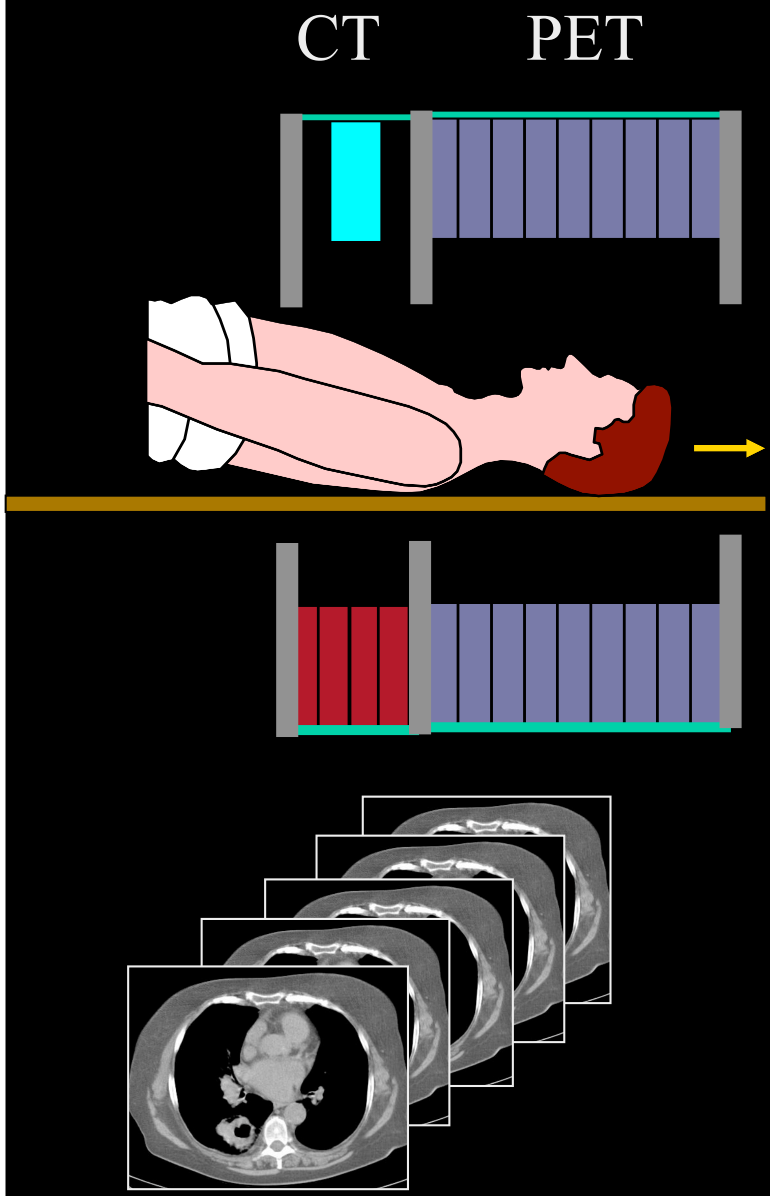

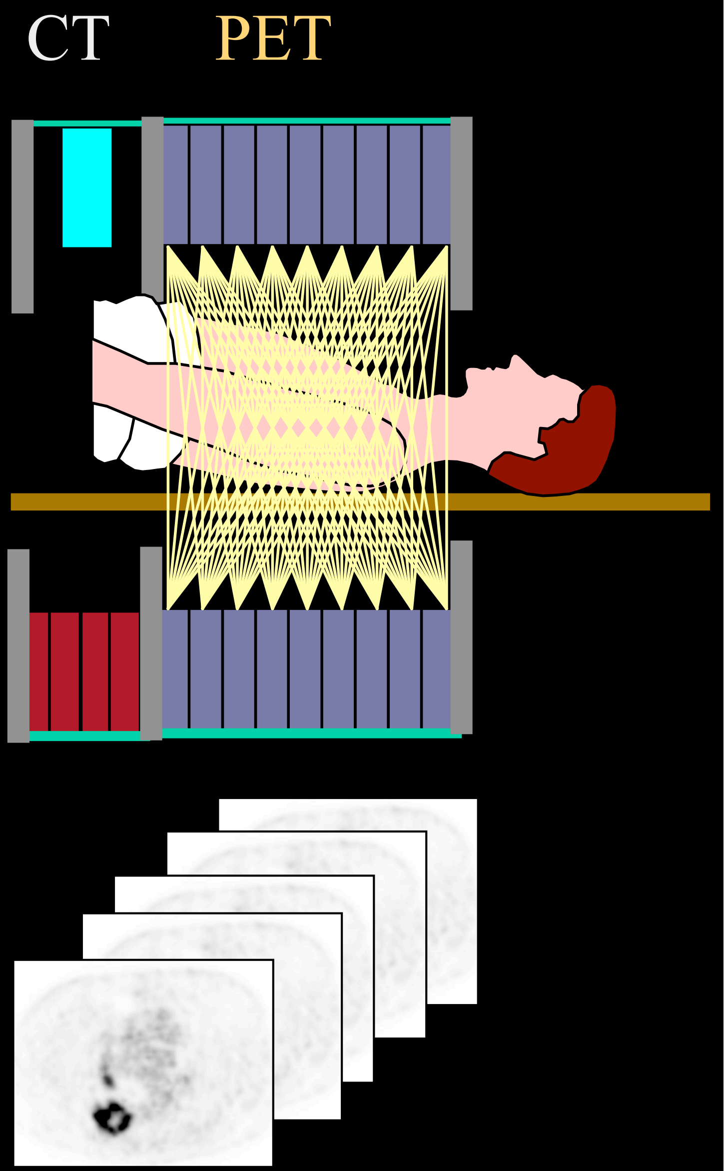

HSR MILANO

Commercial PET-CT systems

Gemini GXL, TF

LYSO: 4x4x22 mm^3
GSO: 4x4x30 mm^3
3D only
6, 10, 16, 64 slice CT
71,7 cm bore,
18 cm axial FOV
6 ns coincidence

Biograph 6,16, 40, 64, mCT

LSO: 4x4x20 mm^3
3D only
6,16,40,64,128 slice CT
70 cm bore
16.2 – 21.6 cm axial FOV
4.3 ns coincidence

Discovery HD platform
Discovery 600 platform

BGO, LYSO(only non commercial systems):
4.7x6.3x30 mm^3 (BGO)
4.2x6.2x30 mm^3 (LYSO)
2D/3D
8,16,64 slice CT
70 cm bore,
15.7 cm axial FOV
11.7 ns coincidence

4D PET/CT

Respiration control during PET/CT

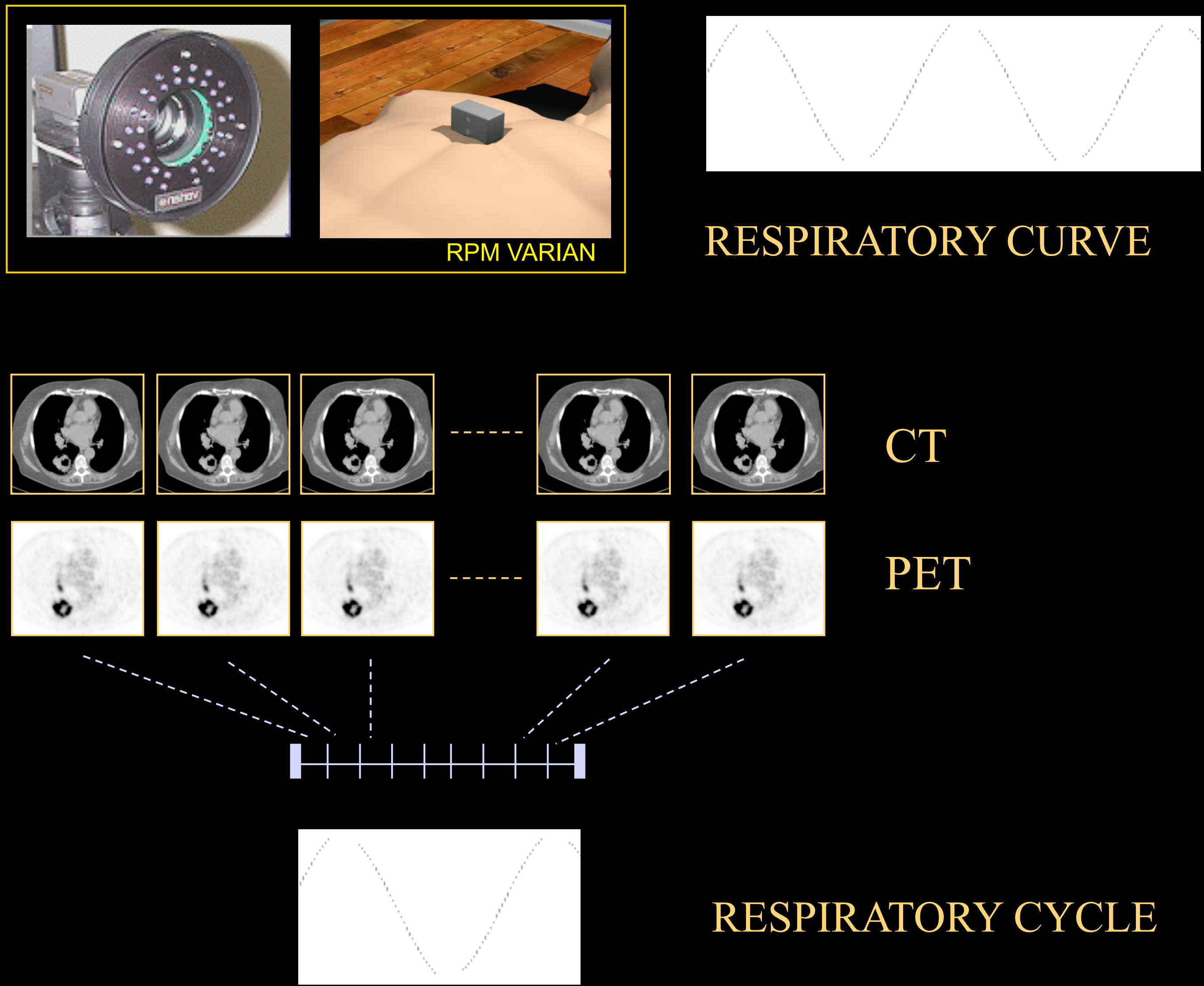

PET-MR

"PET/MR is a medical evolution based on a technical revolution"

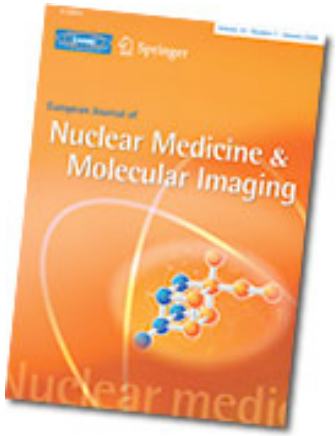

Volume 36, Supplement 1 / March, 2009
Multi-modality imaging: PET/MR

"We believe that both PET/CT and PET/MR are here to stay, because both platforms incorporate the diagnostic power of PET.
In fact, with PET/CT being a "dual-modality imaging" platform by virtue of combining functional (PET) and anatomical (CT) imaging, PET/MR offers true "multimodality imaging" by virtue of combining function (PET) and anatomy and function (both MR). This will open, without a doubt, new avenues in non-invasive imaging as part of clinical patient management and clinical research".

(T. Beyer and B. Pichler)

Nuclear Magnetic Resonance

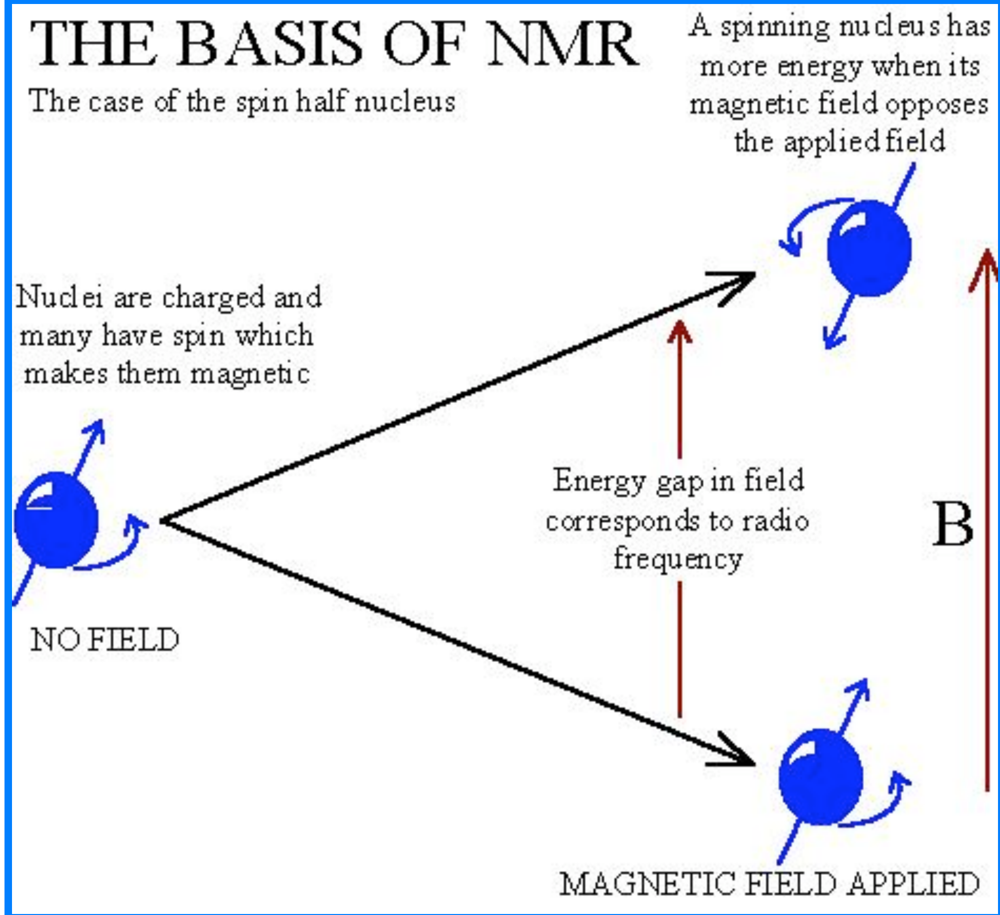

1938-1945

Felix Bloch and Edward Purcell discover and study NMR

1952: Nobel prize in physics

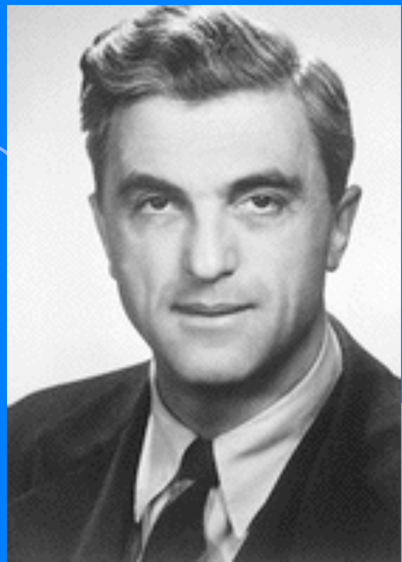

Felix Bloch
In 1954 became the first CERN Director General

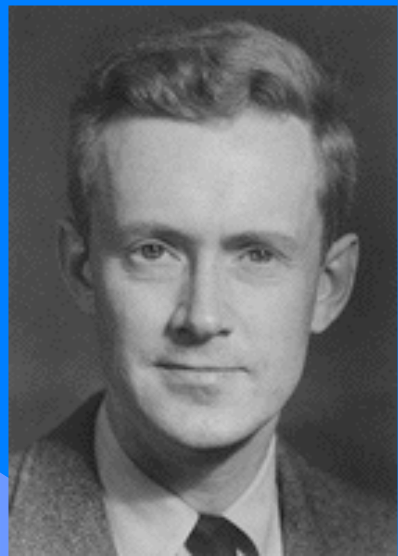

Edward Purcell

MAGNETIC RESONANCE IMAGING (MRI)

MAGNETIC FIELD: 1.5 – 7Tesla

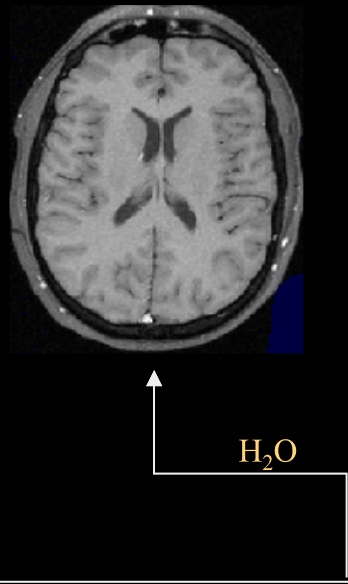

LARMOUR FREQUENCY

$$\nu_0 = [\,\gamma / 2\pi\,]\, B_0$$

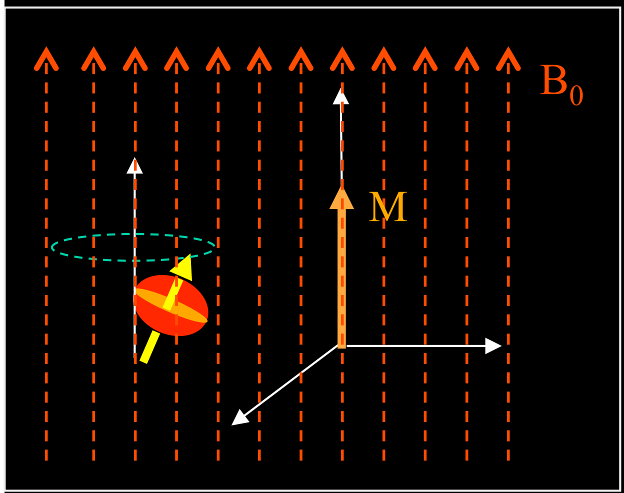

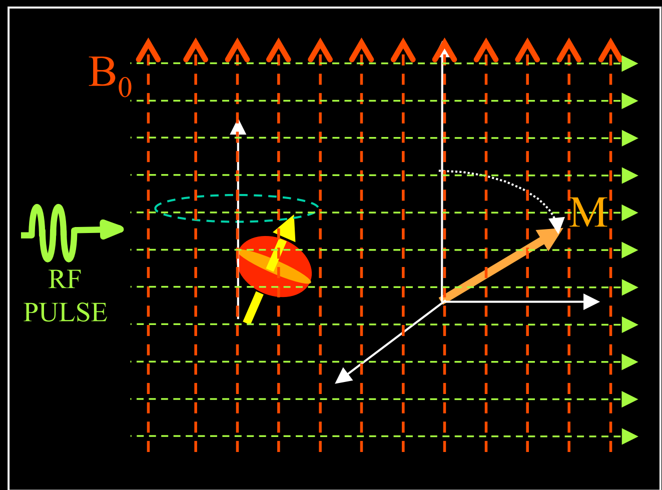

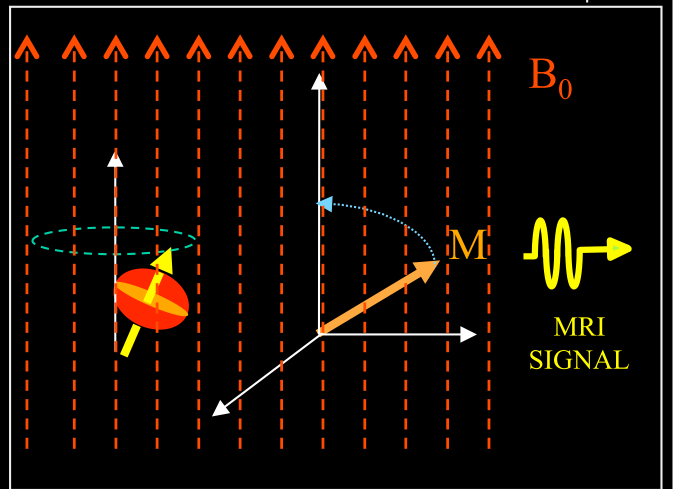

EXCITATION

RELAXATION

Equipment

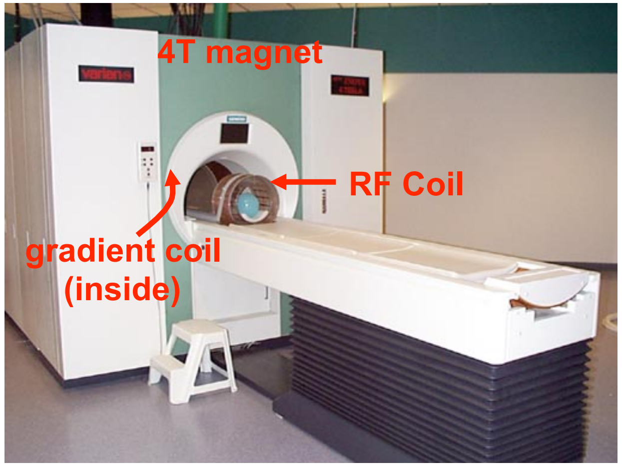

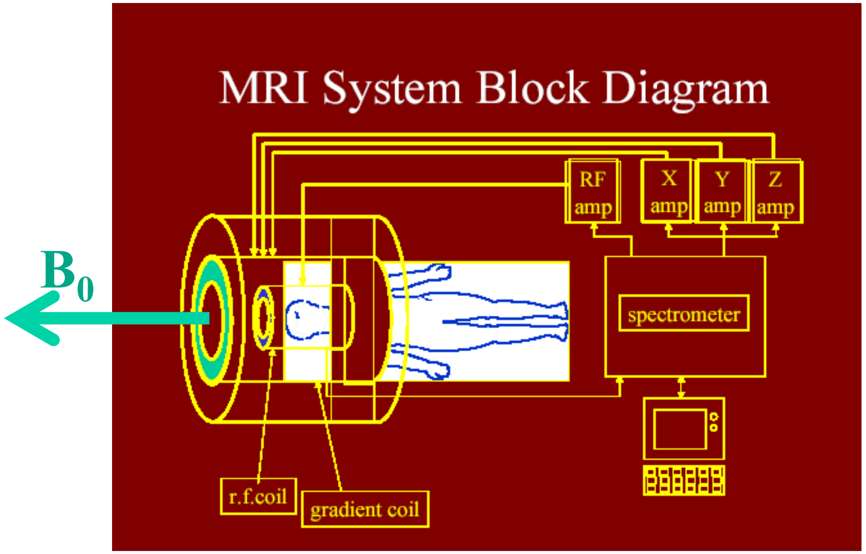

Magnet

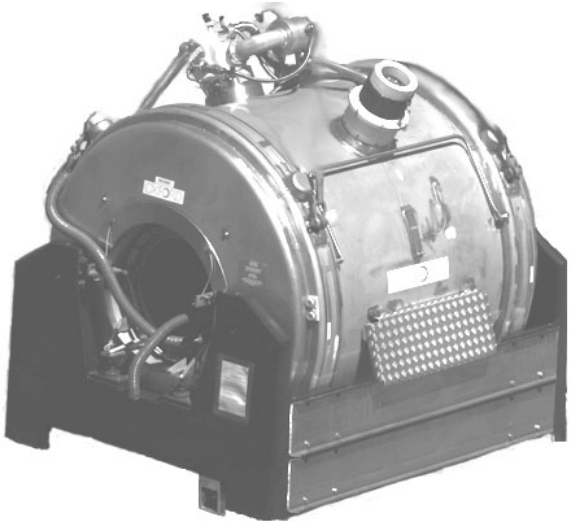

Gradient Coil

RF Coil

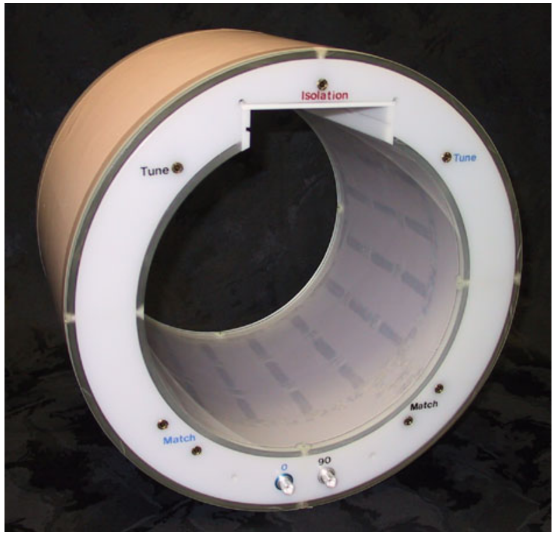

Schematic illustration of motion in a magnetic field B_0 of protons

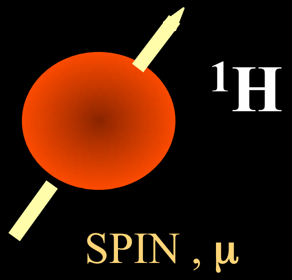

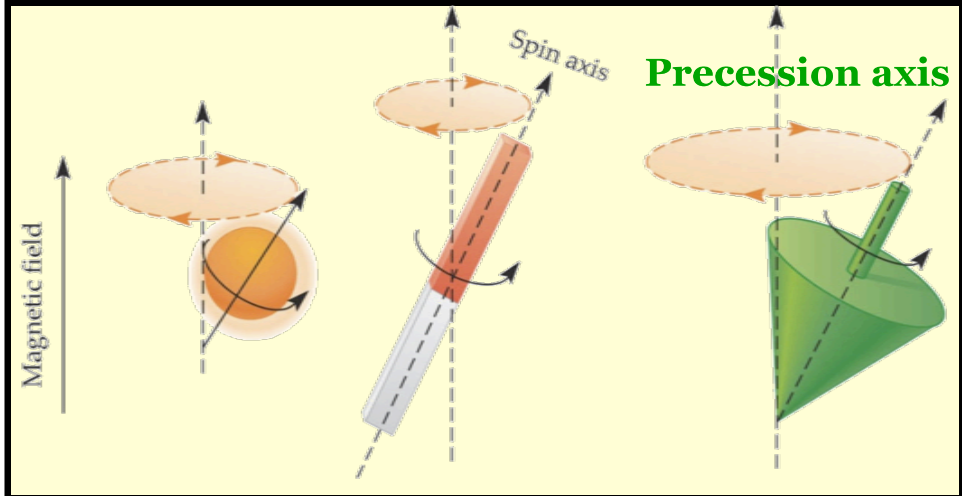

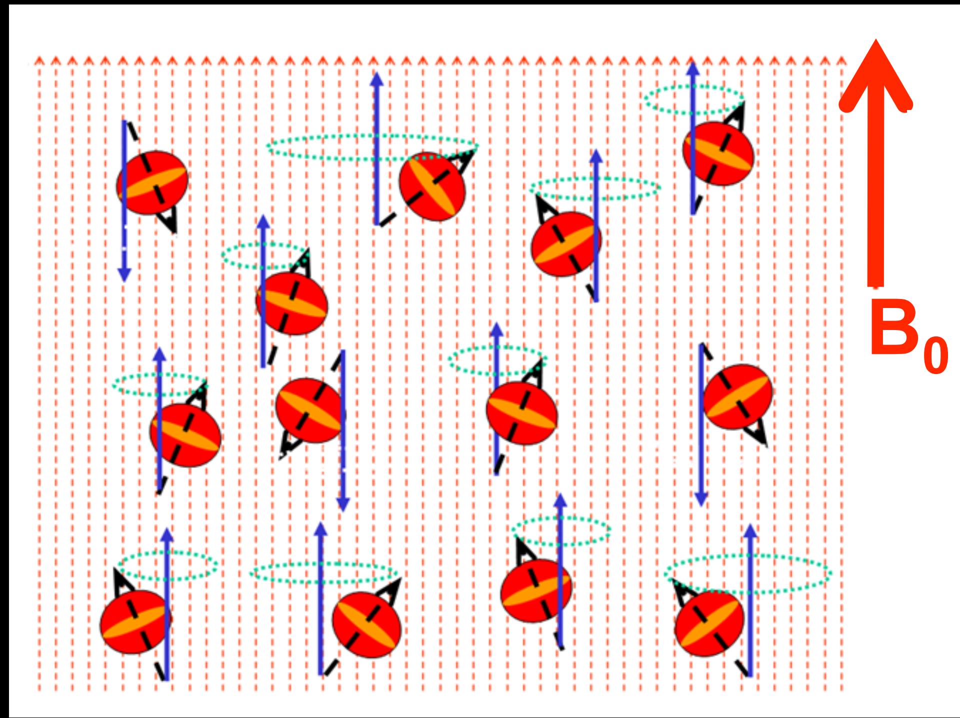

Larmor Frequency $\omega = \gamma B_o$

For hydrogen:

γ = 42.58 MHz/Tesla = 42.58×10^6 Hz/Tesla

at 3 Tesla:

ω = (42.58 MHz / Tesla)(3 Tesla)

ω = 127.74 MHz

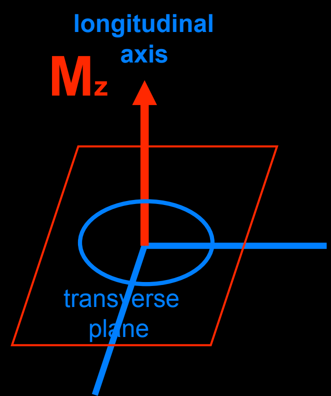

Longitudinal magnetization

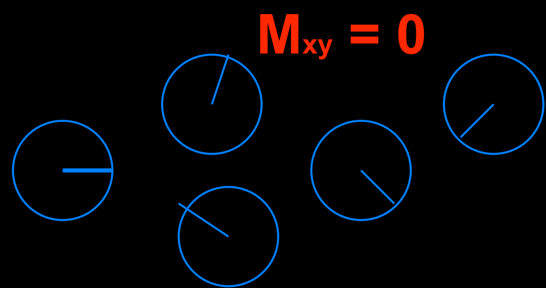

Transverse magnetization

Energy states: Magnetic field effects

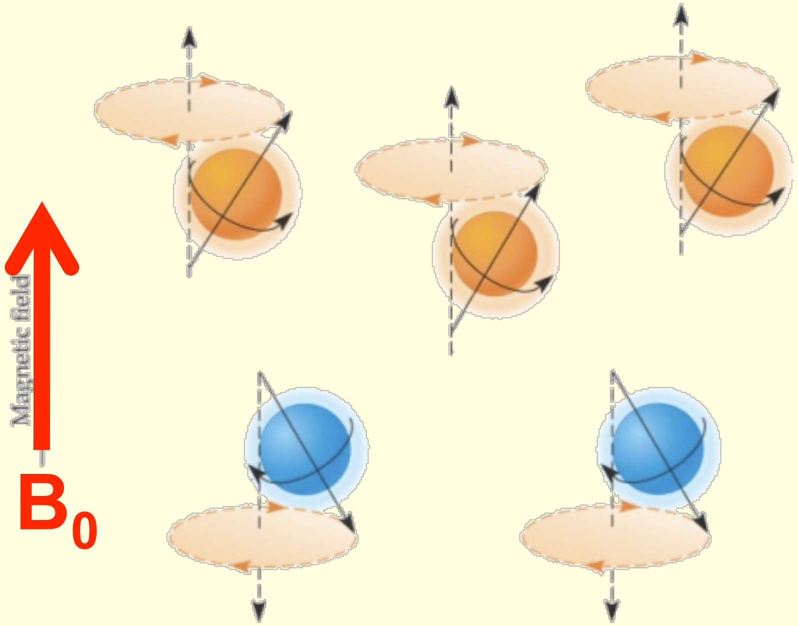

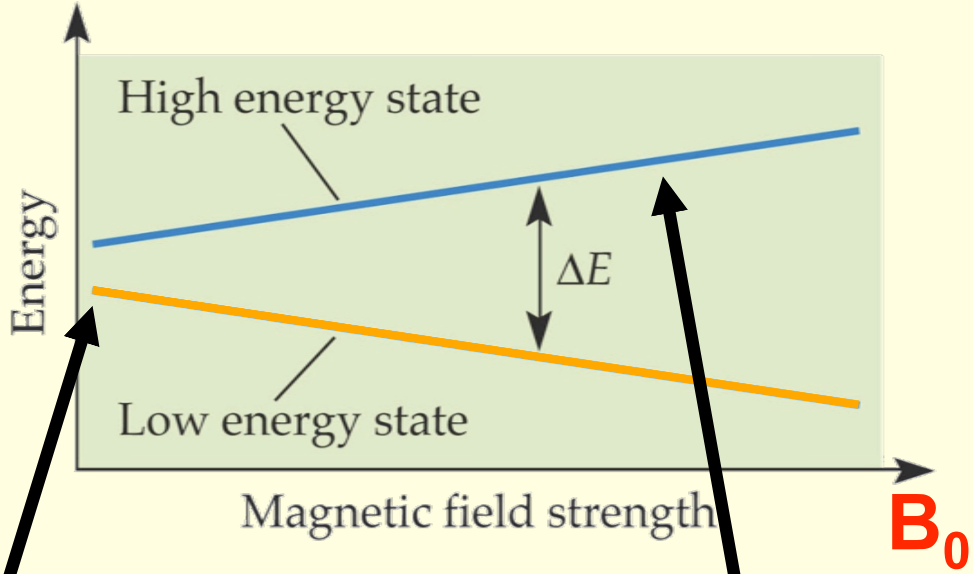

When the magnetic field is weak, little energy is required for a proton to change between high and low states (ΔE is small).

But, when the magnetic field is strong, much more energy is required (ΔE is large).

Thus, protons in the lower-energy state tend to stay in that state

Energy states: Temperature effects

Protons move back and forth between states because of thermal energy.

The Boltzman equation describes the population ratio of the two energy states:

$$N^-/N^+ = e^{-E/kT}$$

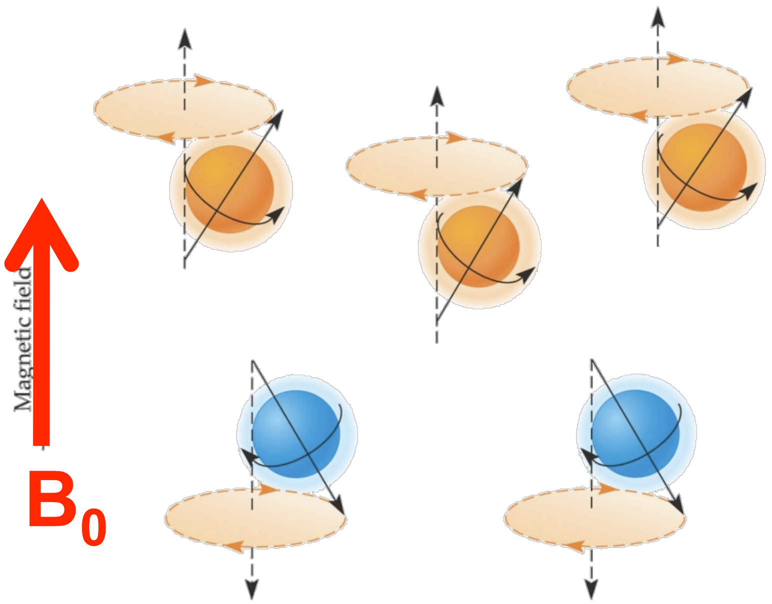

FUNCTIONAL MAGNETIC RESONANCE IMAGING, Figure 3.5 © 2004 Sinauer Associates, Inc.

Low-energy protons at room temperature in Earth's B:

~50.000000001%

High-energy protons at room temperature in Earth's B:

~49.999999999%

- Larger B_0 produces larger net magnetization M, lined up with B_0
- Thermal motions try to randomize alignment of proton magnets
- At room temperature, the population ratio is roughly 100,000 to 100,006 per Tesla of B_0

Excite Radio Frequency (RF) field

- apply RF represented here with a magnetic field B_1 (perpendicular to B_0) oscillating at Larmor frequency
- Larmor frequencies in RF range; B_1 is small: ~1/10,000 T
- tips M to transverse plane – spirals down

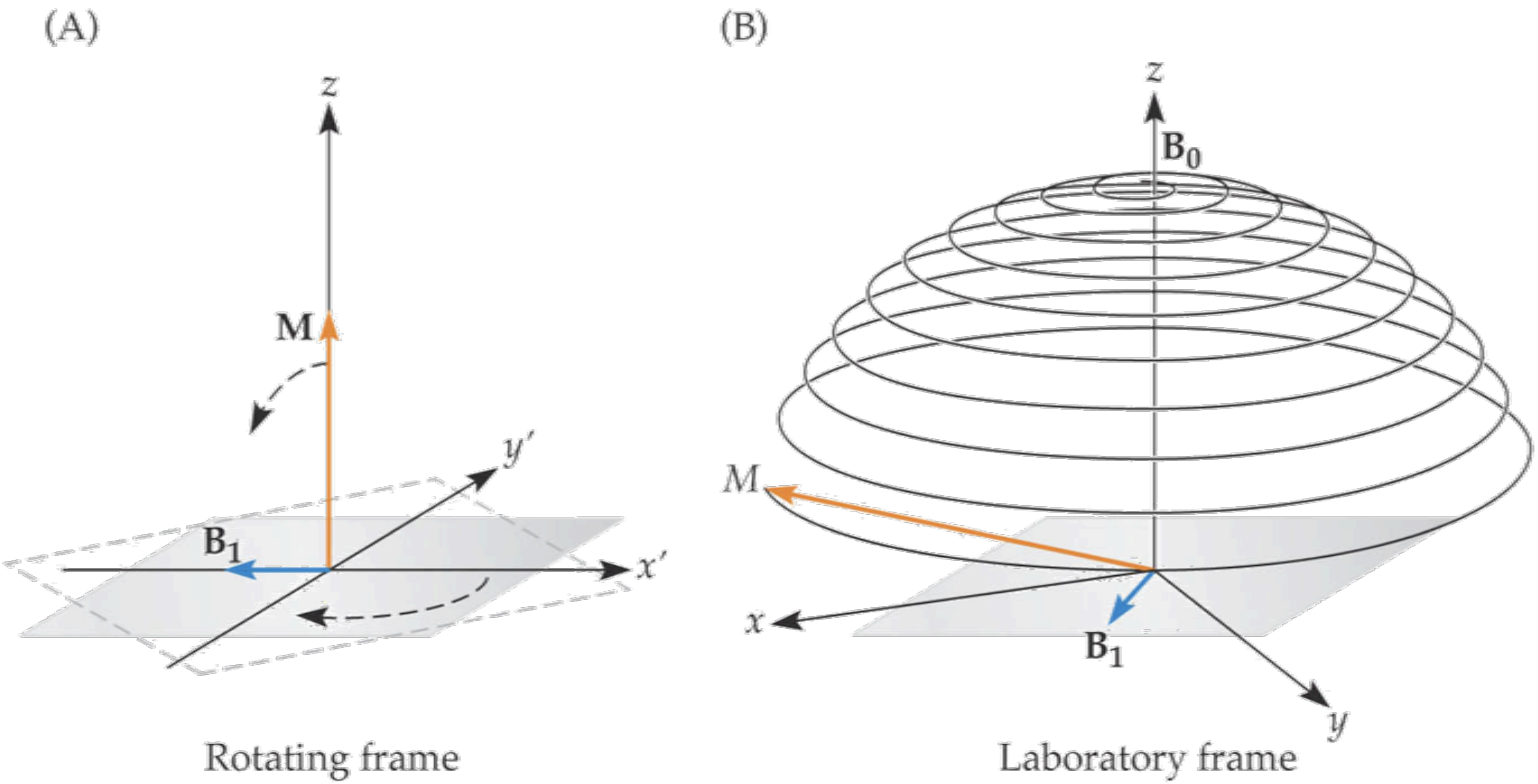

The RF energy is represented here with B_1 as a second magnetic field superimposed to B_0.

Relaxation:

- Once we stop applying energy, M will go back to being aligned with static field B_0
- This process is called <u>relaxation</u>
- The part of M perpendicular to B_0 shrinks [M_{xy}]
  - This part of M is called *transverse magnetization*
  - It provides the detectable RF signal
- Part of M parallel to B_0 grows back [M_z]
  - This part of M is called *longitudinal magnetization*

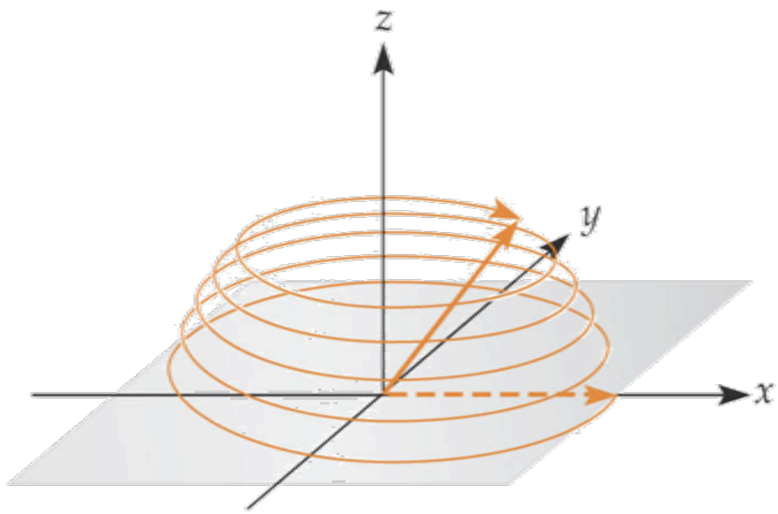

Longitudinal relaxation

T_1

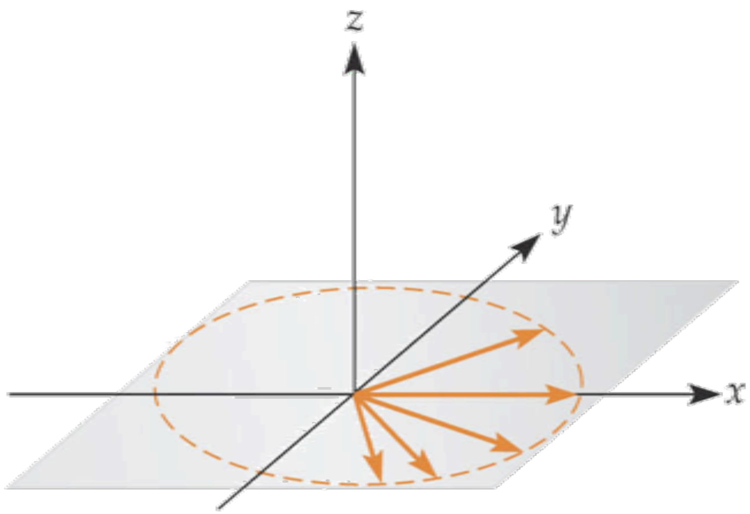

Transverse relaxation

T_2

Tipping the net magnetization provides measurable MR signal!

Before Excitation

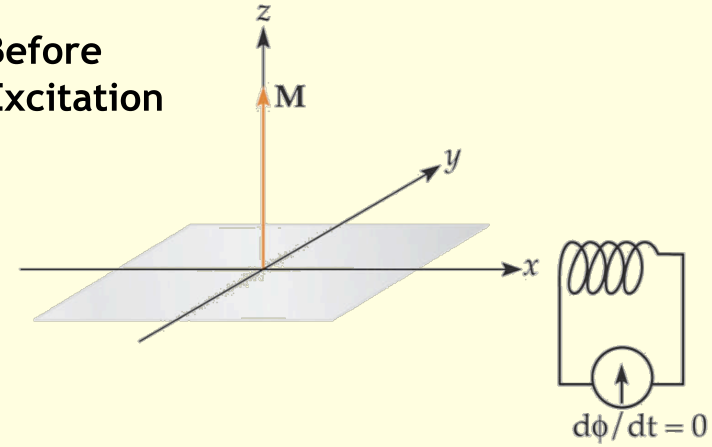

During Excitation (t_o)

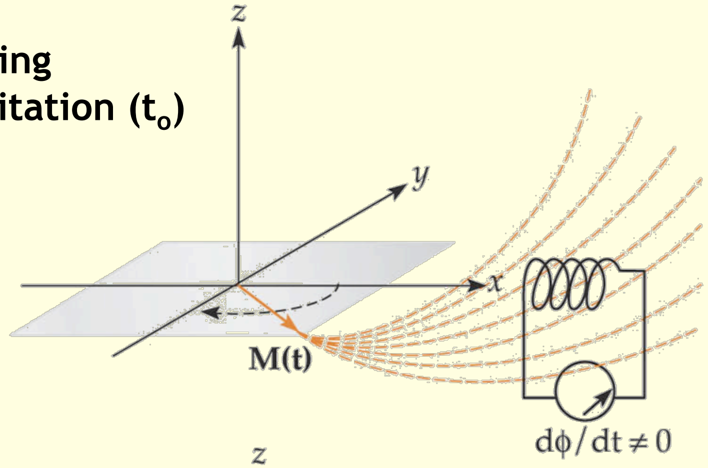

After Excitation

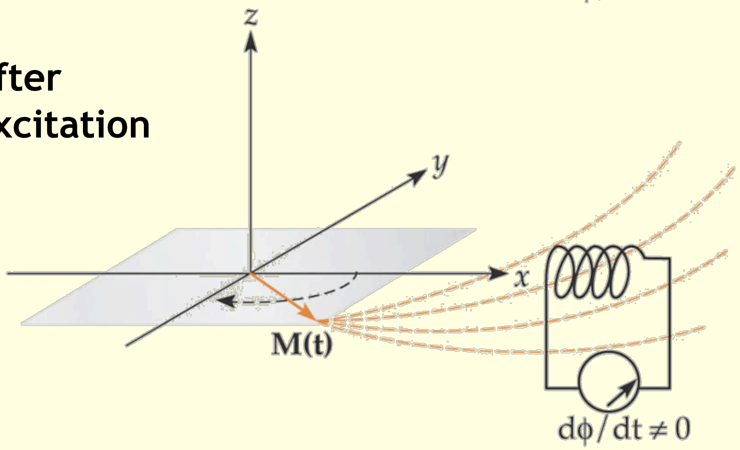

During Excitation (t_1)

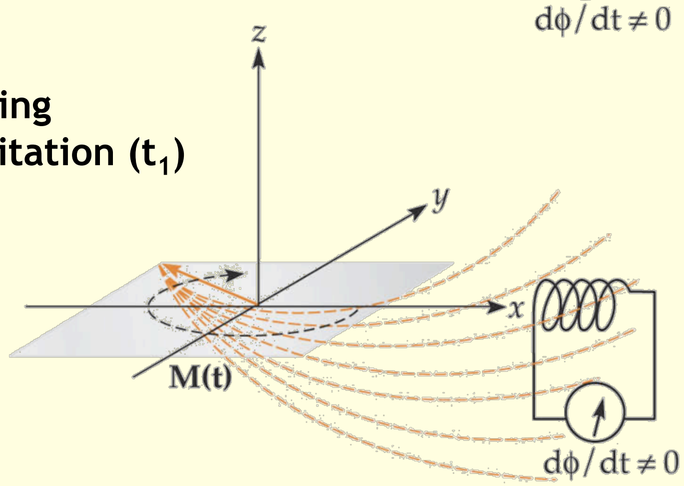

Excitation tips the net magnetization (M) down into the transverse plane, where it can generate current in detector coils (i.e., via induction).

The amount of current oscillates at the (Larmor) frequency of the net magnetization.

Relaxation Times and Rates

- Net magnetization changes in an exponential fashion
  - Constant rate (R) for a given tissue type in a given magnetic field
  - R = 1/T, leading to equations like e^{-Rt}
- T_1 (recovery): Relaxation of **M** back to alignment with $\mathbf{B_0}$
  - Usually 500-1000 ms in the brain (lengthens with bigger $\mathbf{B_0}$)
- T_2 (decay): Loss of transverse magnetization over a microscopic region (≈ 5-10 micron size)
  - Usually 50-100 ms in the brain (shortens with bigger $\mathbf{B_0}$)
- T_2*: Overall decay of the observable RF signal over a macroscopic region (millimeter size)
  - Usually about half of T_2 in the brain (i.e., faster relaxation)

T_1 and T_2 values at 1.5T

Tissue	T_1 (s)	T_2 (ms)
CSF	2 - 6	~200
White matter	~0.6	~80
Gray matter	~0.9	~100
Meninges	0.5 - 2.2	50 - 165
Muscle	0.95 - 1.82	20 - 67

MAGNETIC RESONANCE IMAGING

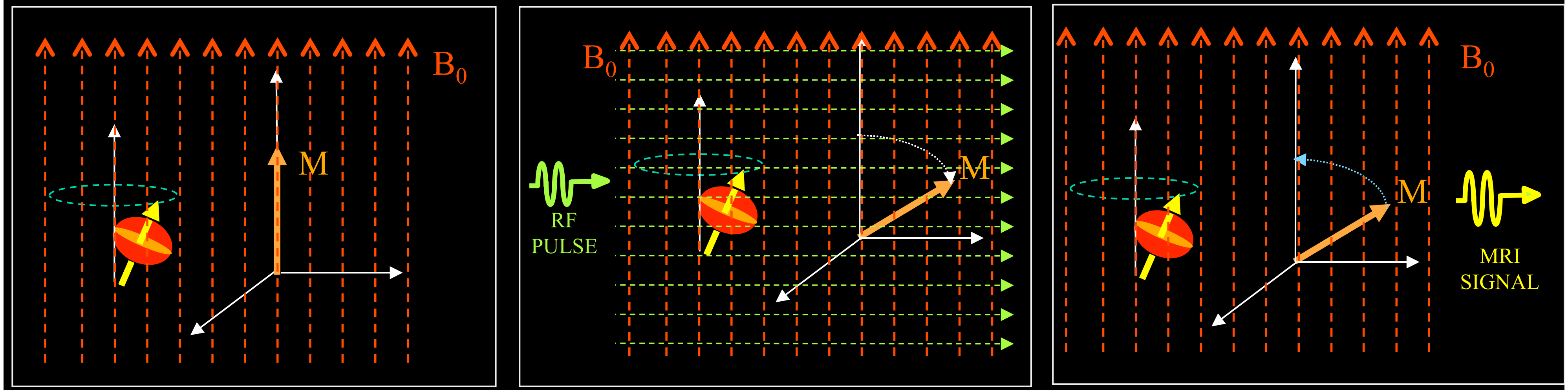

EXCITATION

RELAXATION

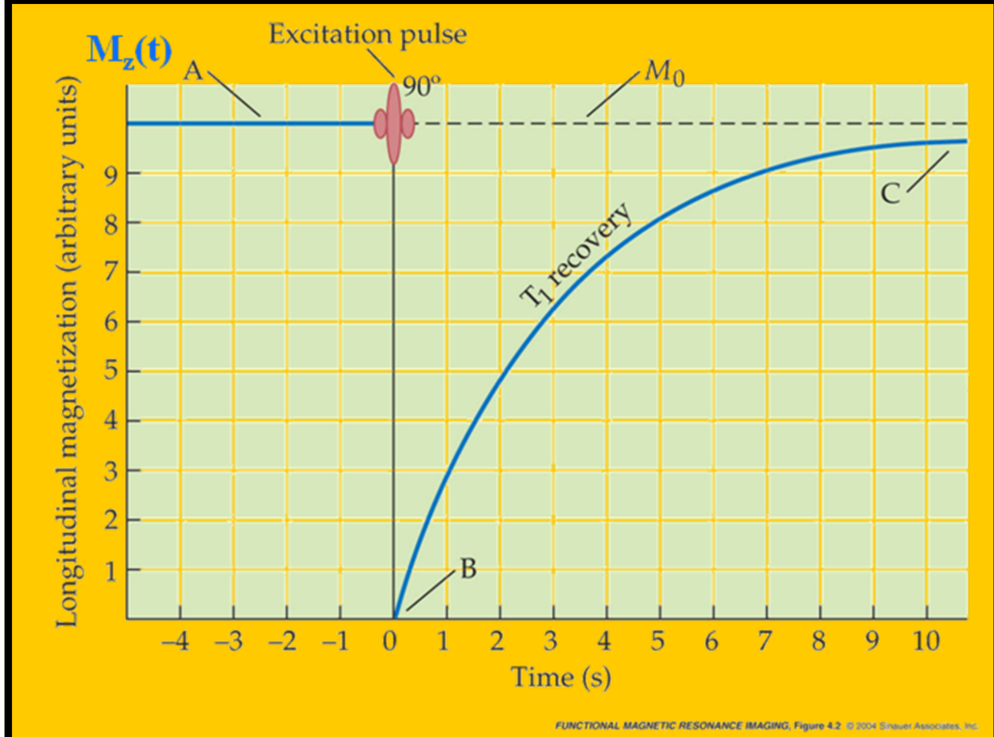

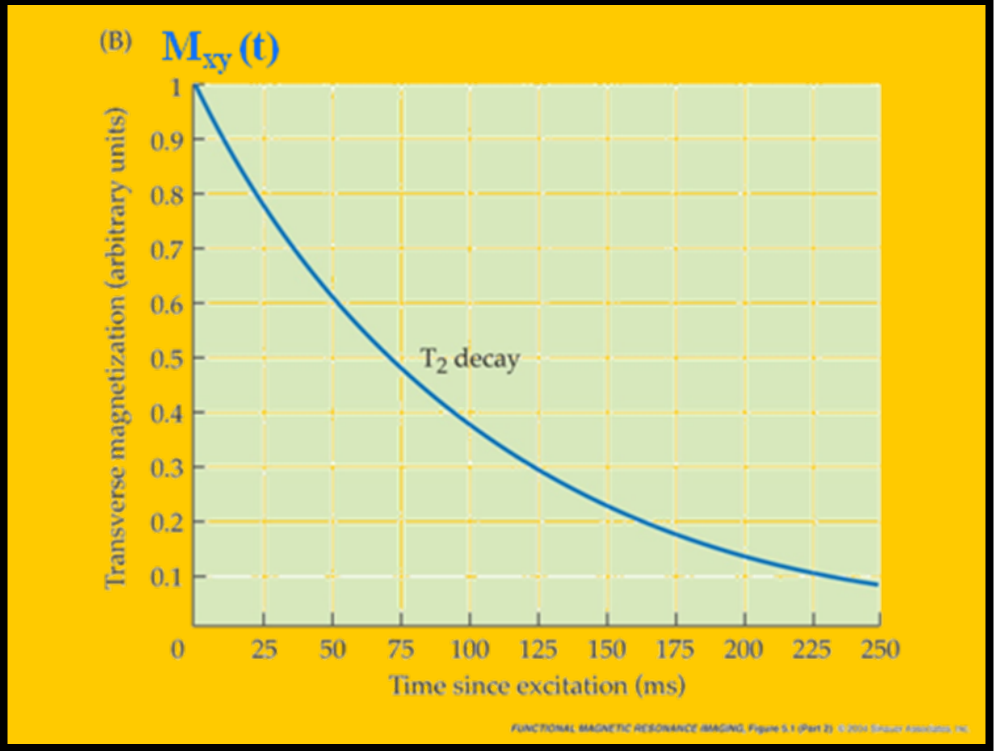

Apply a z-gradient field G_z for slice selection

Gradients change the <u>Strength</u>, not Direction of the Magnetic Field B_0

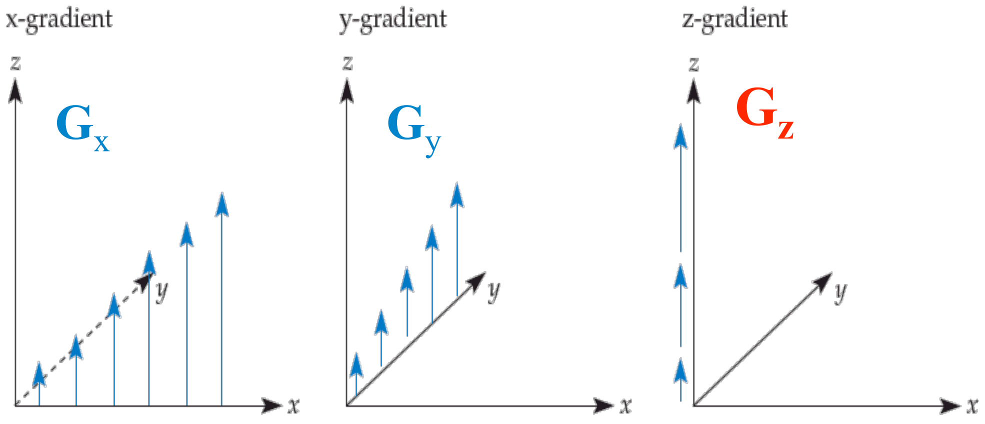

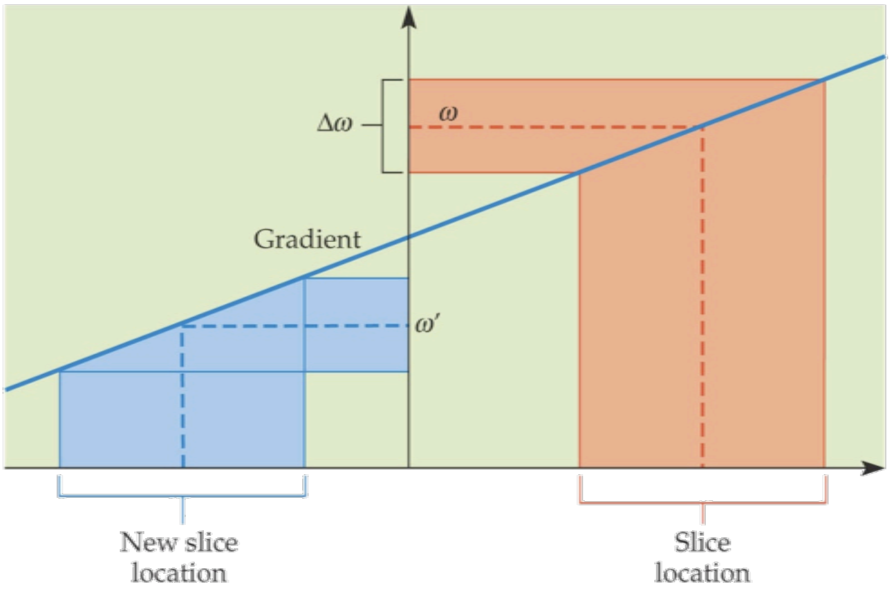

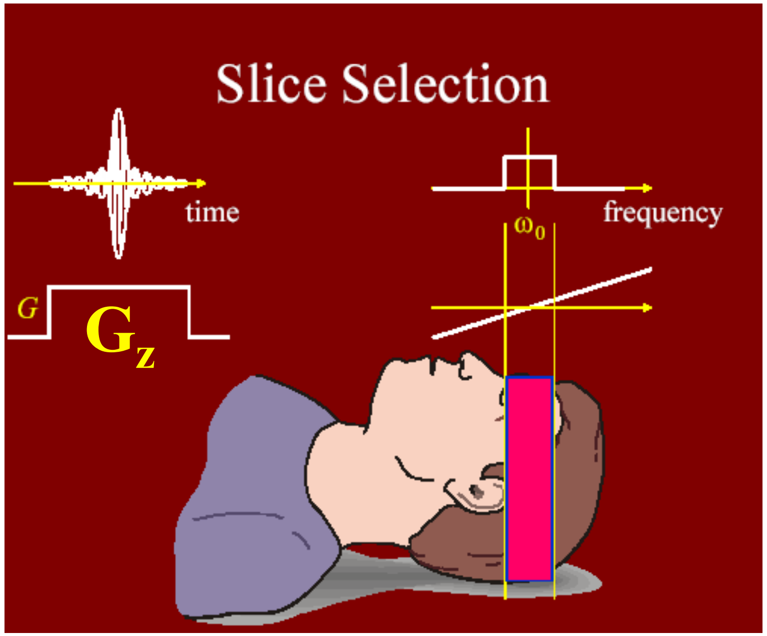

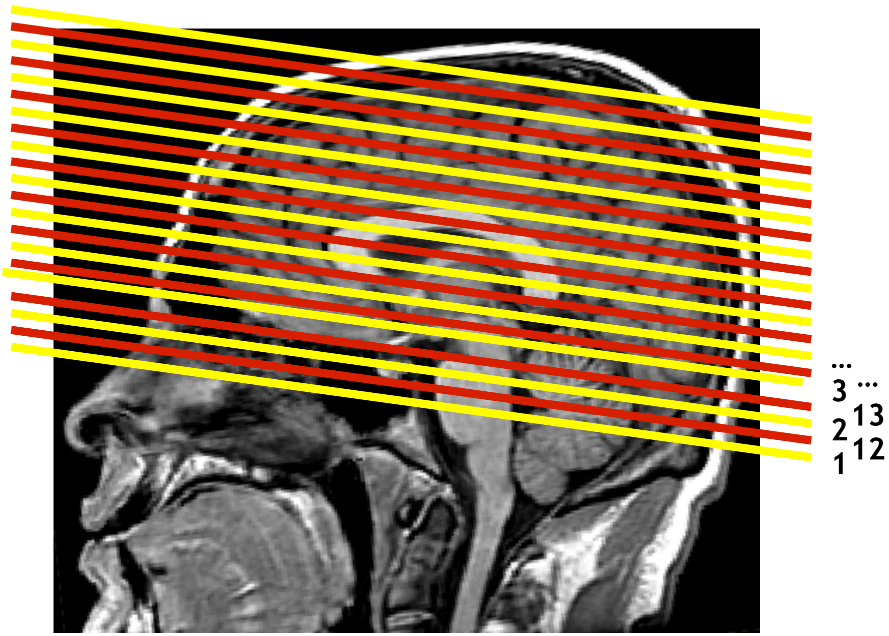

Spatial encoding within the slice

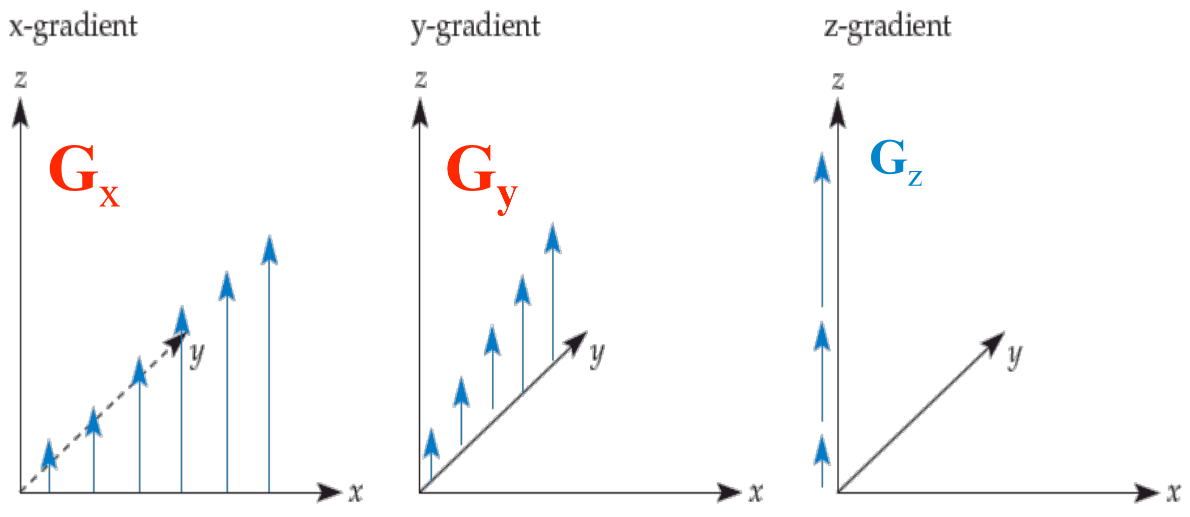

The selected slice is then subdivided in a matrix of voxels along the x,y coordinates applying the gradient fields G_x and G_y with a procedure called Phase and Frequency encoding.

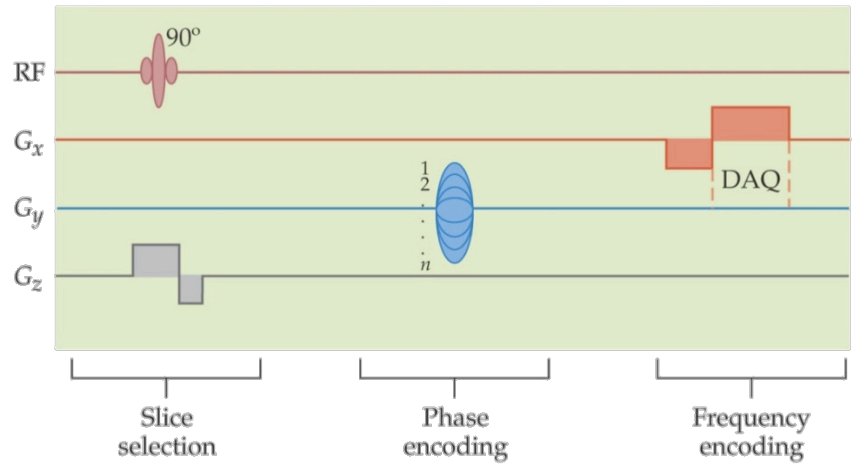

Phase Encoding

When the gradient field G_y (that vary linearly along the y-axis) is applied, all the spins of the voxels of the matrix line at a given y-coordinate start to process at the same Larmor frequency with the same phase, while all the other voxel lines at different y-coordinate process with different Larmor frequencies and therefore, in a given amount of time, accumulate a certain amount of phase offset.

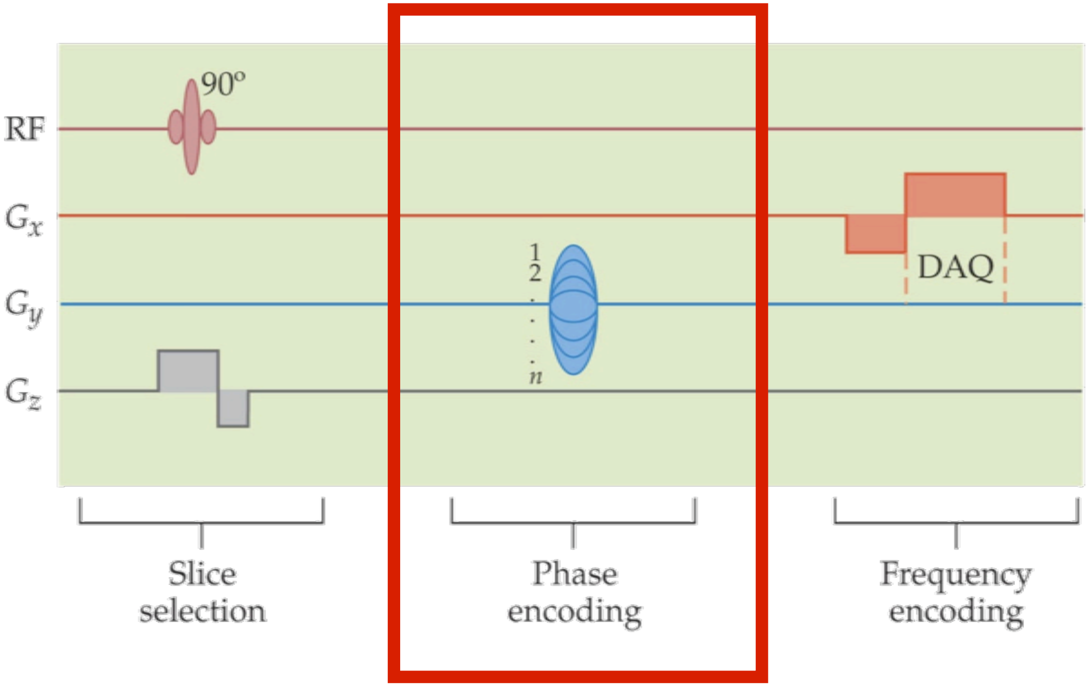

When the phase encoding gradient G_y is turned off all the spins of the voxels of all the lines return to process at the same frequency but now with different phases, determined by the duration and the intensity of G_y (Phase Encoding).

Frequency Encoding

When the phase encoding process have been completed, the gradient field G_x (that vary linearly along the x-axis) is turned on and therefore the spins of the voxels of the matrix columns at different y-coordinate are forced to process at different Larmor frequencies (Frequency Encoding).
At this point each individual voxel is going to have a different combination of phase and frequency and the Data Acquisition (DAQ) of the raw MR signals can be performed.

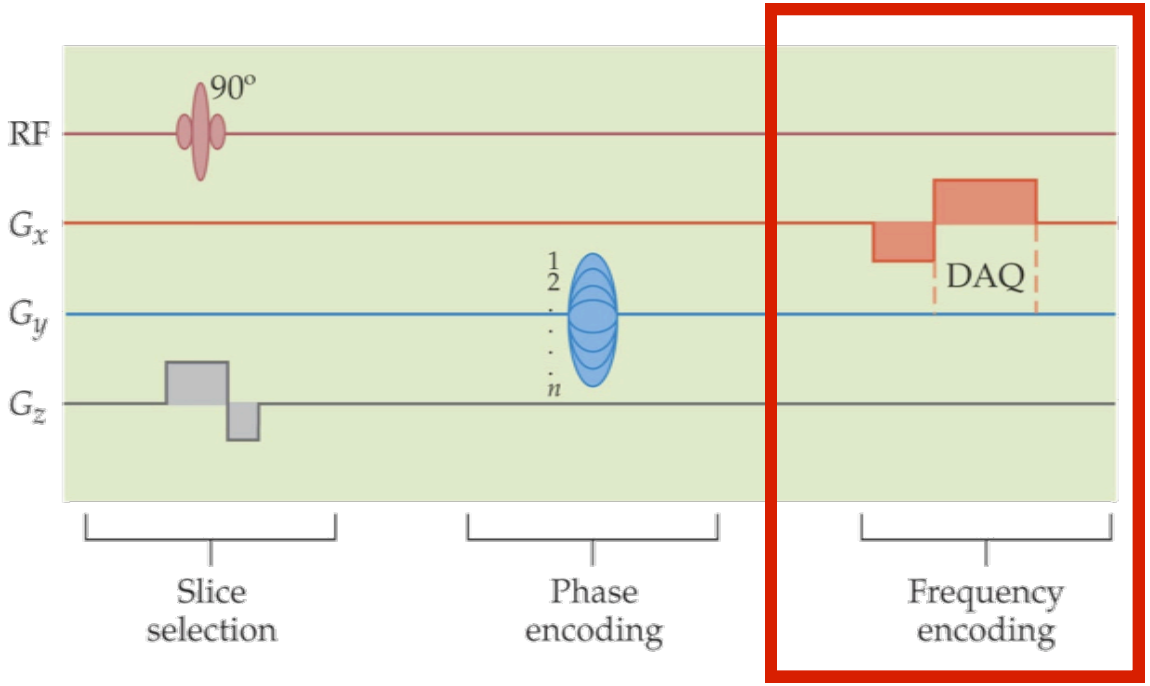

The complete image of the selected slice can then be obtained performing a 2-D inverse Fourier trasform of the raw signal. This is possible because the raw MR signal acquired contains, through the phase and frequency encoding, the information from each individual voxel

T1-weighted and T2-weighted sequeces

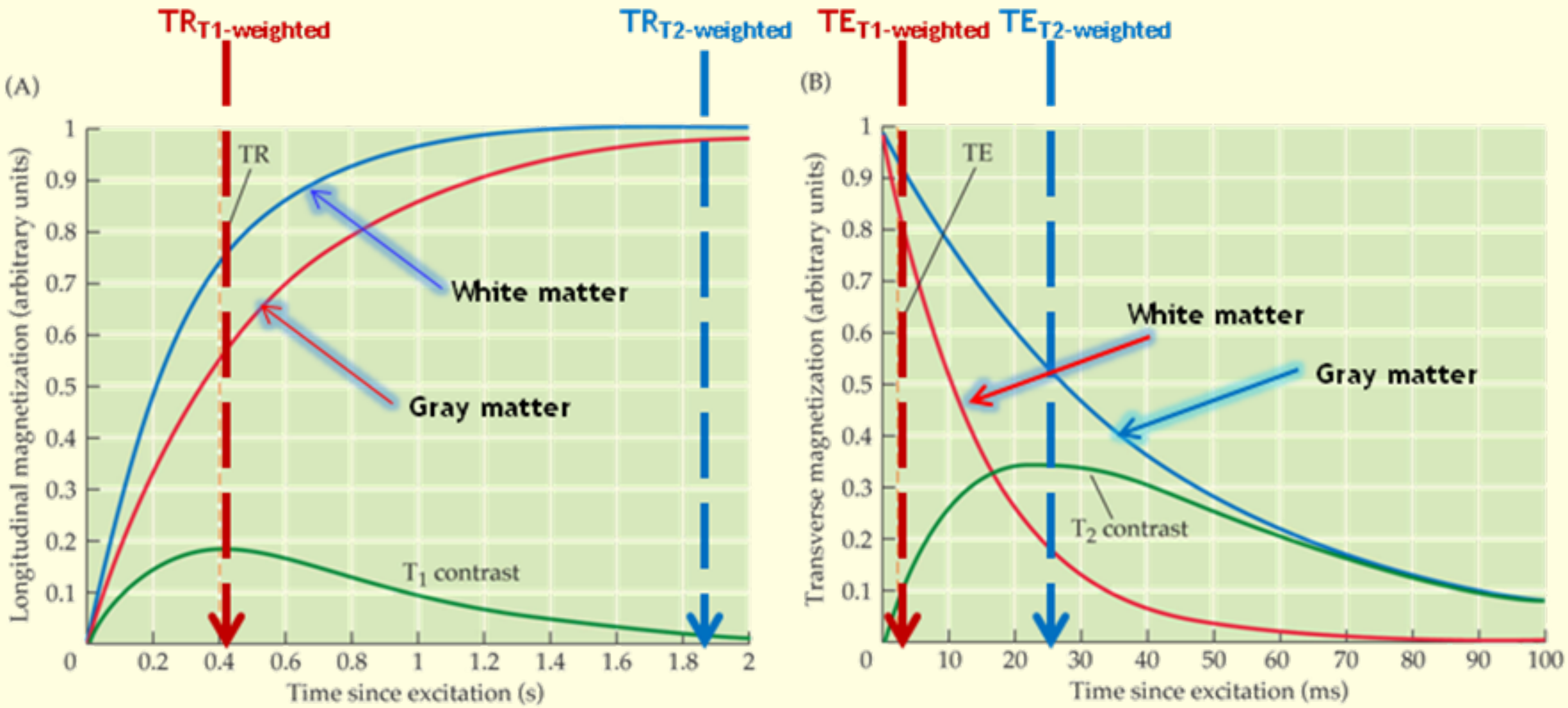

By selecting appropriate pulse sequence parameters, images can be made sensitive to tissue differences in T_1, T_2, or a combination.

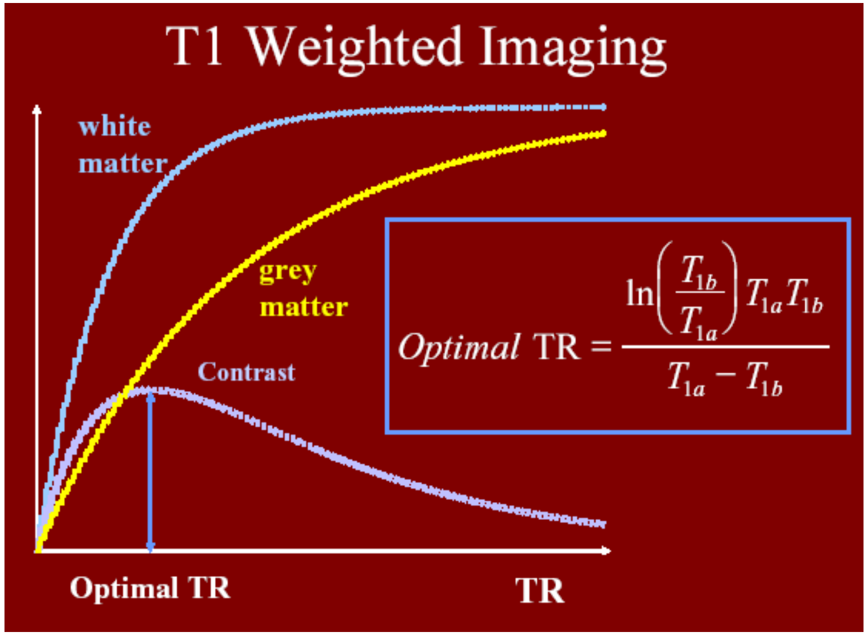

T1 Weighted Imaging
white matter
grey matter
Contrast
$Optimal\ \mathrm{TR} = \dfrac{\ln\left(\dfrac{T_{1b}}{T_{1a}}\right) T_{1a} T_{1b}}{T_{1a} - T_{1b}}$
Optimal TR
TR

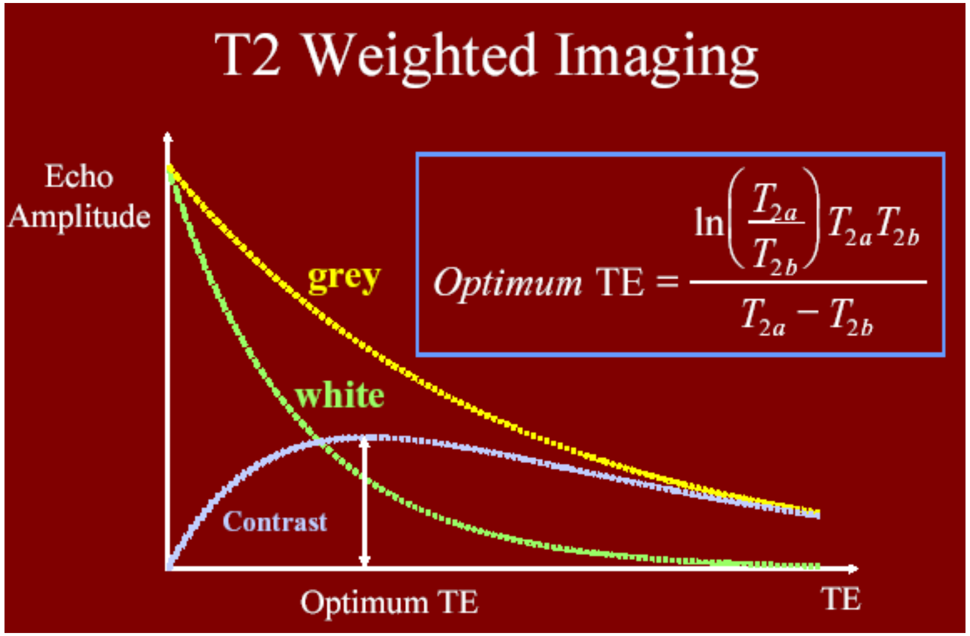

T2 Weighted Imaging
Echo Amplitude
grey
white
Contrast
$Optimum\ \mathrm{TE} = \dfrac{\ln\left(\dfrac{T_{2a}}{T_{2b}}\right) T_{2a} T_{2b}}{T_{2a} - T_{2b}}$
Optimum TE
TE

MAGNETIC RESONANCE IMAGING (MRI)

MORPHOLOGY

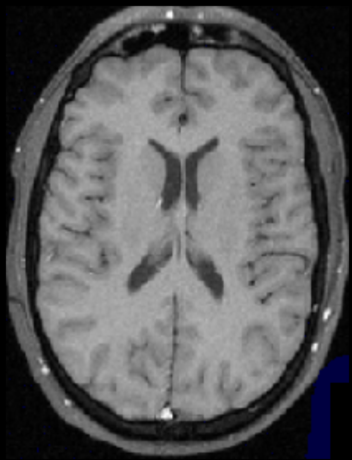	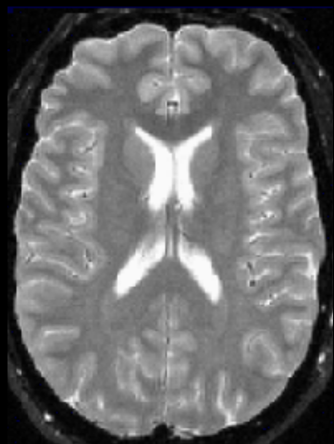	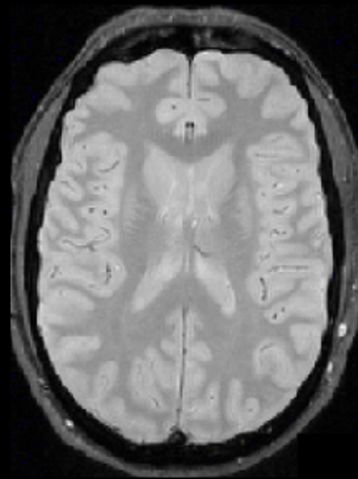
T1	T2	PD

SCAN TIME to cover an entire organ:	~ min
SPATIAL RESOLUTION:	~ mm
CONTRAST RESOLUTION:	very high for soft tissues

fMRI BOLD

Blood

Oxygenation

Level

Dependent

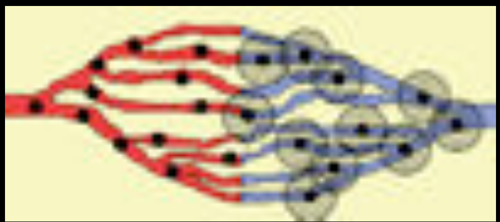

- Oxyhaemoglobin in the arterial blood is diamagnetic
- Deoxyhaemoglobin in the draining veins is strongly PARAMAGNETIC
- Deoxyhaemoglobin can serve as an intrisic paramagnetic contrast agent

Blood Oxygenation Level Dependent

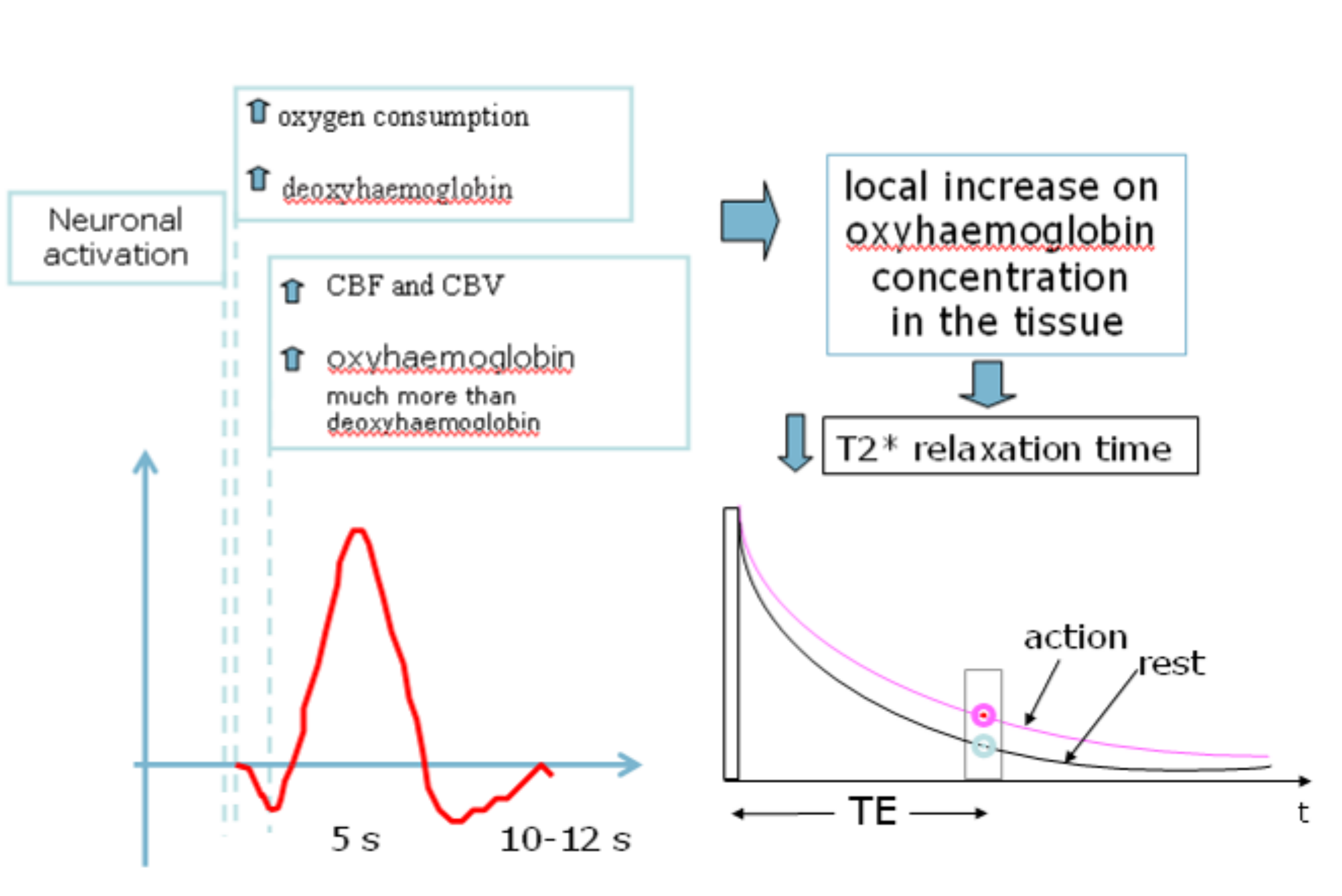

ACTIVATION STUDIES

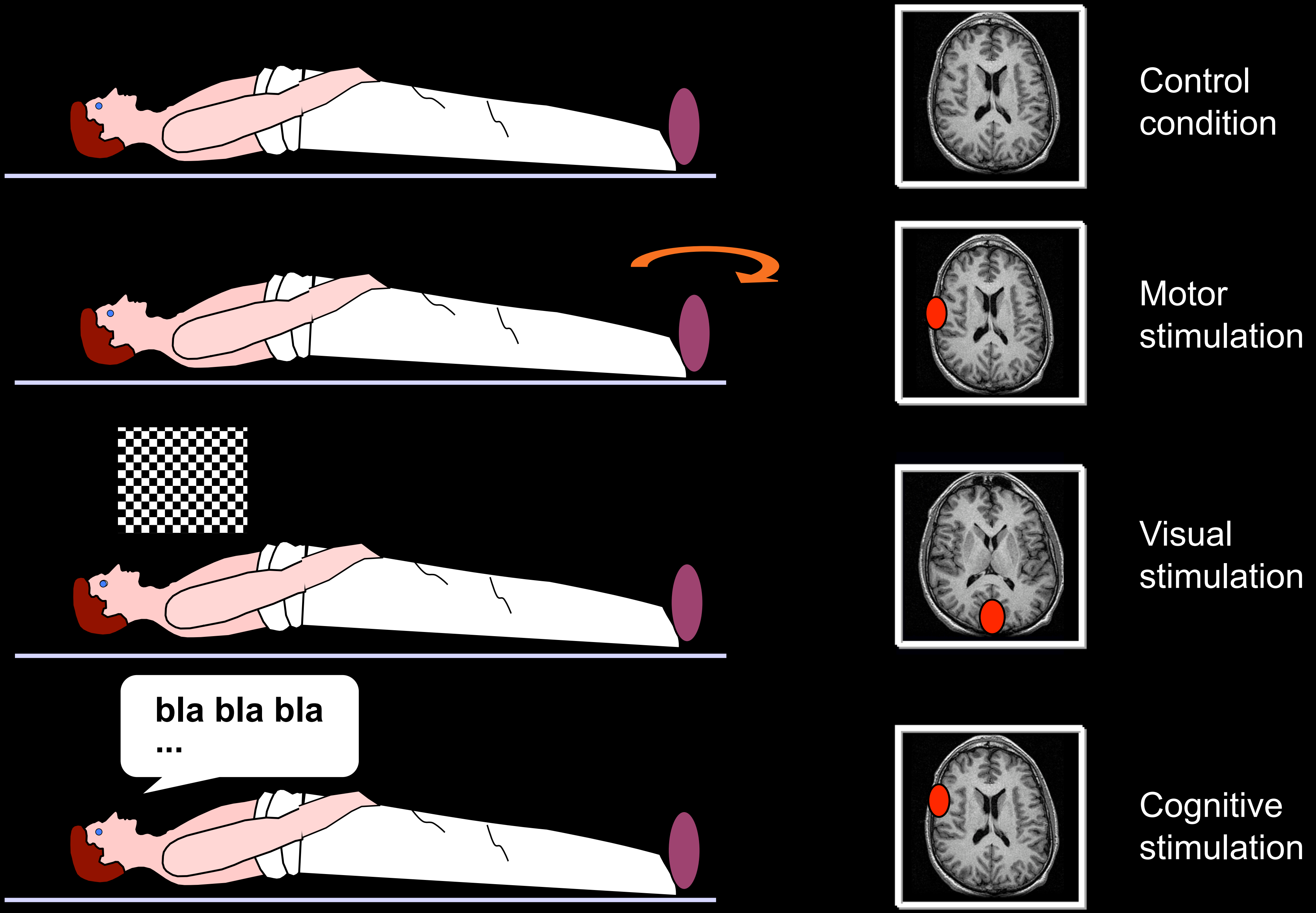

fMRI BOLD ACTIVATION STUDIES

	Brain stimulation
↑↑↑	rCBF
↑	Oxygen extraction
↑↑	oxyHb
↓↓	deoxyHb
↑↑	MR signal

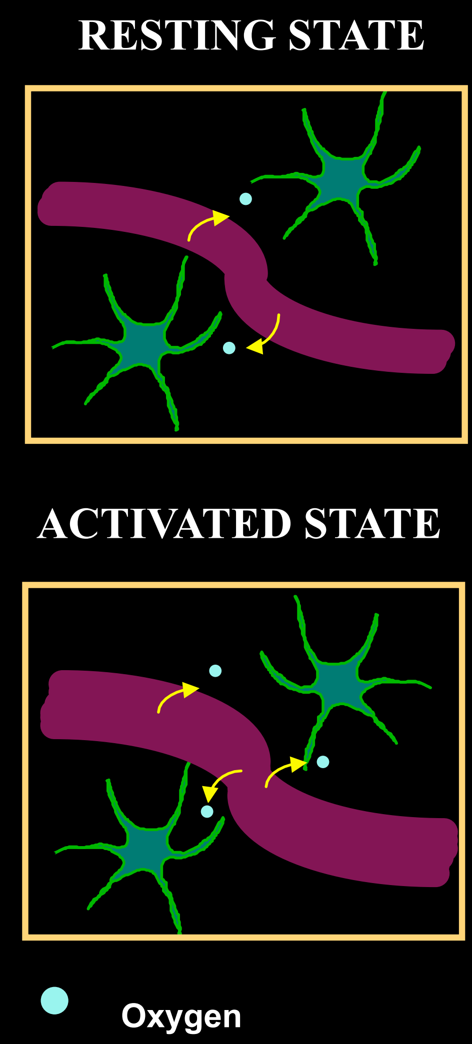

Technical Challenges in PET/MR

- ***Interference on PET (photomultiplier and electronics)***
  - Static magnetic field
  - Electromagnetic interference from RF and gradients
- ***Interference on MR (homogeneity and gradients)***
  - Electromagnetic radiation from PET electronics
  - Maintaining magnetic field homogeneity
  - Susceptibility artifacts
- ***General Challenges***
  - Space
  - Environmental factors (temperature, vibration…)
  - Cost
- ***PET attenuation correction via MR data is a challenge!***

PET + MR: Semantic Dementia

MR

[^{18}F]FDG

Fused

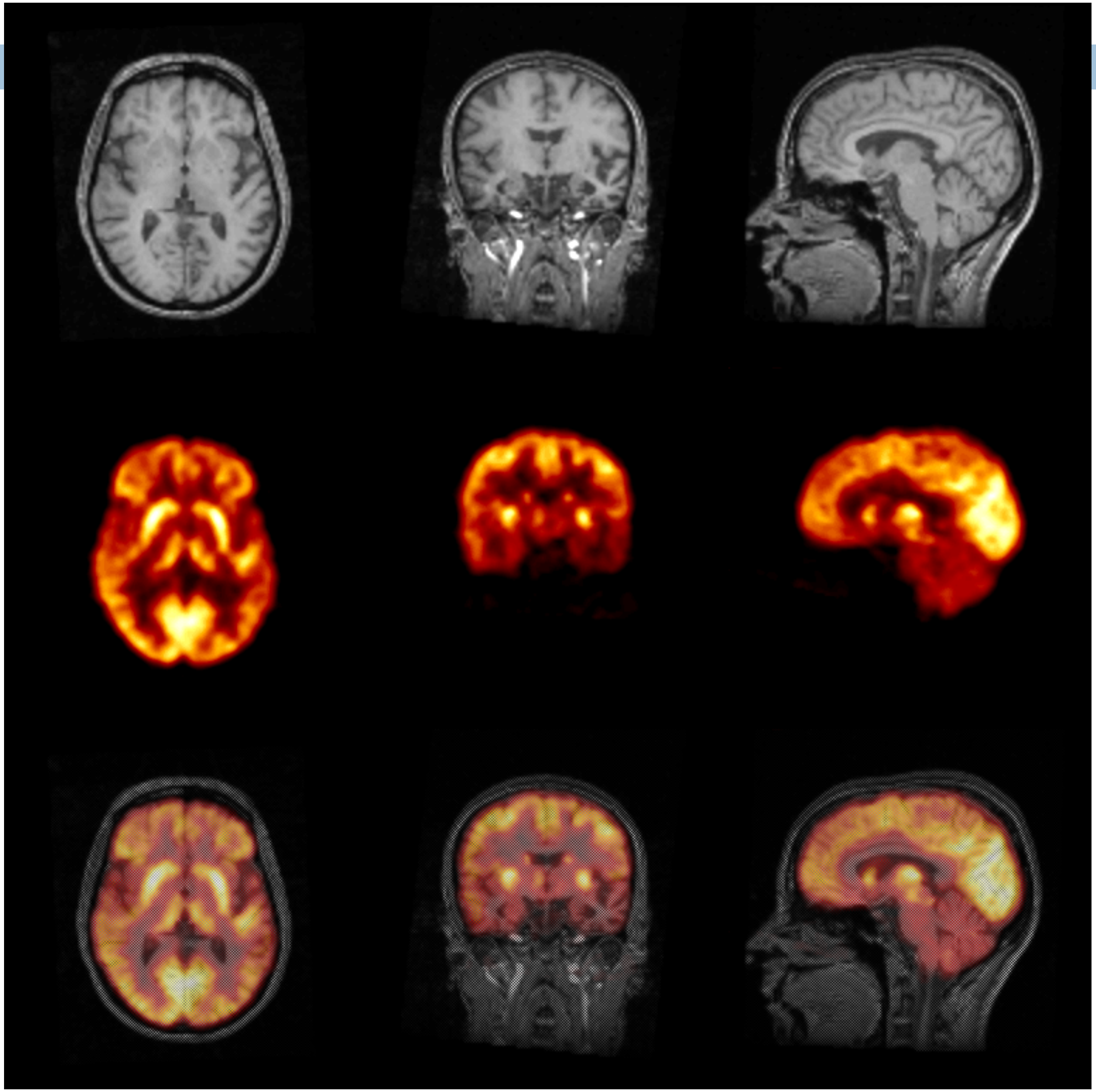

MR/PET:"one-stop-shop"

New whole-body imaging procedures allow comprehensive imaging examinations

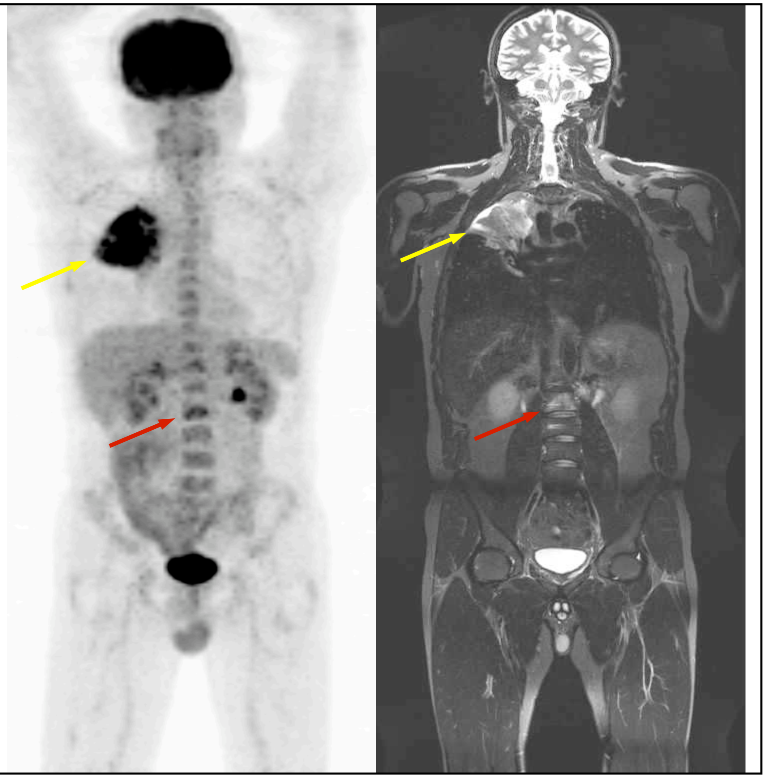

Coronal overview of 18F-FDG PET and MRI (T2- weighted Turbo-STIR)

Fused MRI/PET facilitates accurate registration of morphological and molecular aspects of diseases

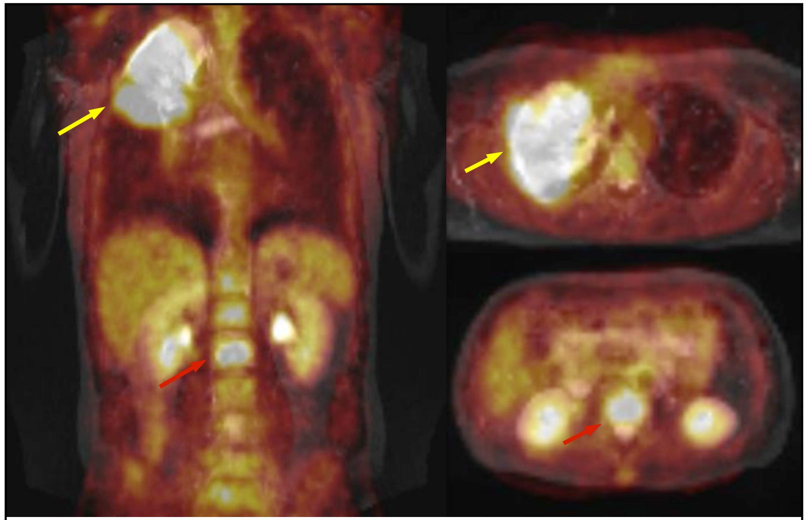

Pulmonary and osseous (arrow, red) metastatic disease of a non-small cell lung cancer (arrow, yellow)

Coronal and transversal MRI/PET fusion images

Courtesy of Dr. Gaa, TU Munich

Technology for MR/PET

- (1) Scintillating crystals plus photomultiplier tubes (PMT)

- (2) Scintillating crystals plus solid state light detectors

Technology for MR/PET (1)

- PMT Approach
  - Well understood, stable electronics, high gain (10^6)
  - However, Position sensitive PMT (PSPMT) operate in 1mT
  - Combination of distance (light guide) and iron shield (1-2mm of soft iron can further reduce 30mT -> 1mT) to operate in 1mT

Technology for MR/PET (1)

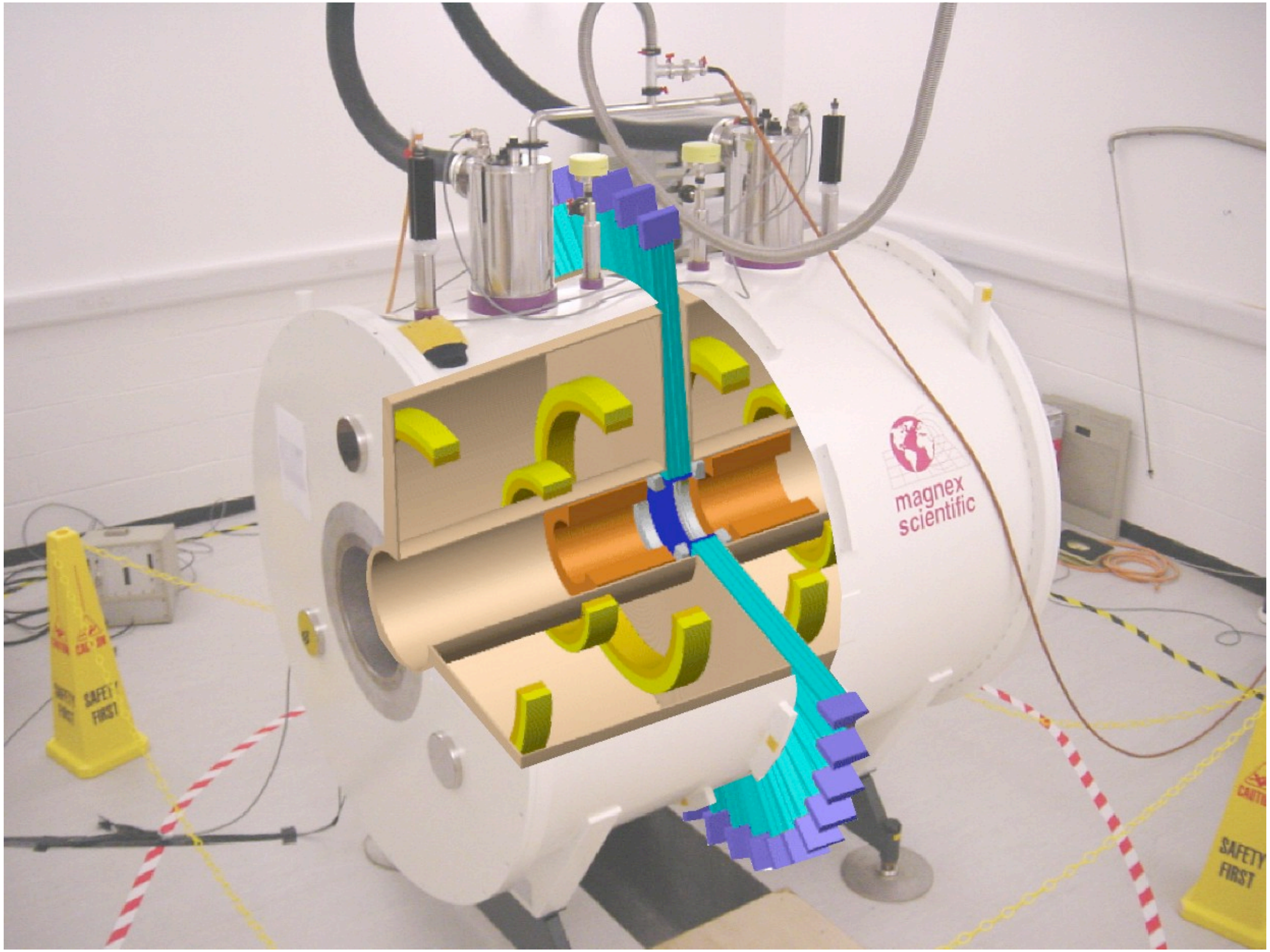

Technology for MR/PET (1)

- 1mT has minimal effect on PSPMT performance
- Long light guides reduce energy resolution from 17 -> 27%, but this shouldn't have too big an impact upon performance
- Can perform simultaneous and isocentric MR/PET measurements
- However, small axial FOV

Technology for MR/PET (2)

- Solid state devices
  - Avalanche Photodiodes (gain ~ 150)
  - Silicon Photomultiplier (gain ~ 10^6)
  - Less well established as PET detectors
- Can operate in high static field > 7T
- Need to shield devices from both gradients and RF

MR/PET Head Insert

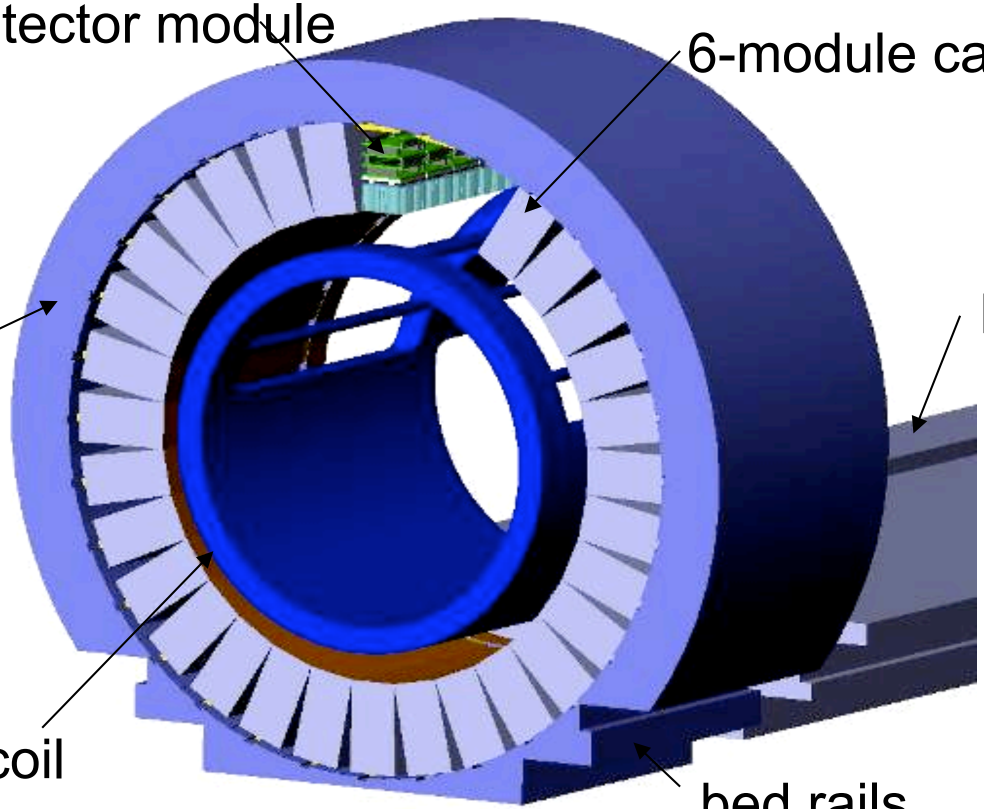

Scanner size: 36cm dia. x 20cm FOV

Courtesy of Berndt Pichler, University of Tubingen

Brain PET/MRI

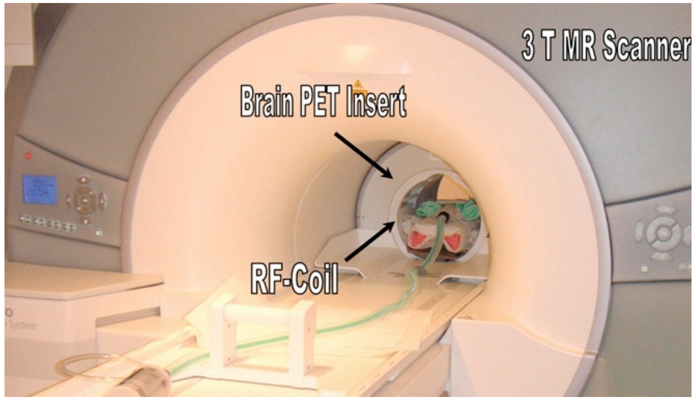

PET Insert

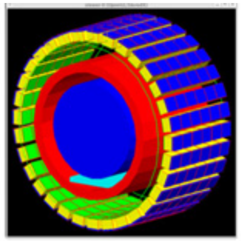

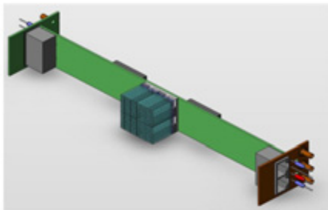

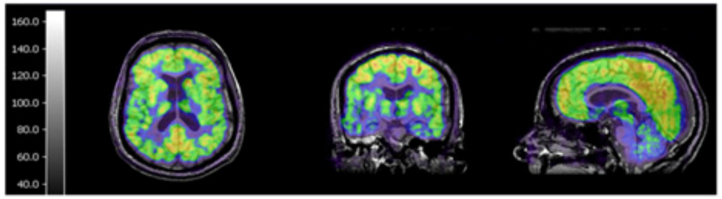

Patient study

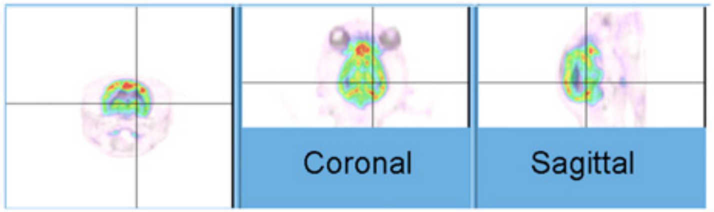

Dog study

- **Ring of LSO detectors inserted in a 3T MR tomograph**
- **Simultaneous PET and MR data acquisition**

- Six 12 x 12 arrays of 2.5 x 2.5 x 20 mm^3
- LSO blocks read out by 3 x 3 APD array
- Total of 192 LSO APD block detectors
- FOV: 35.5 cm x 19.25 cm axial
- Siemens 3T TRIO MR scanner

Courtesy of Berndt Pichler, University of Tubingen

The SiPM solution?

SOLID STATE PHOTODETECTOR→ SiPM: Multicell Avalanche Photodiode working in limited Geiger mode

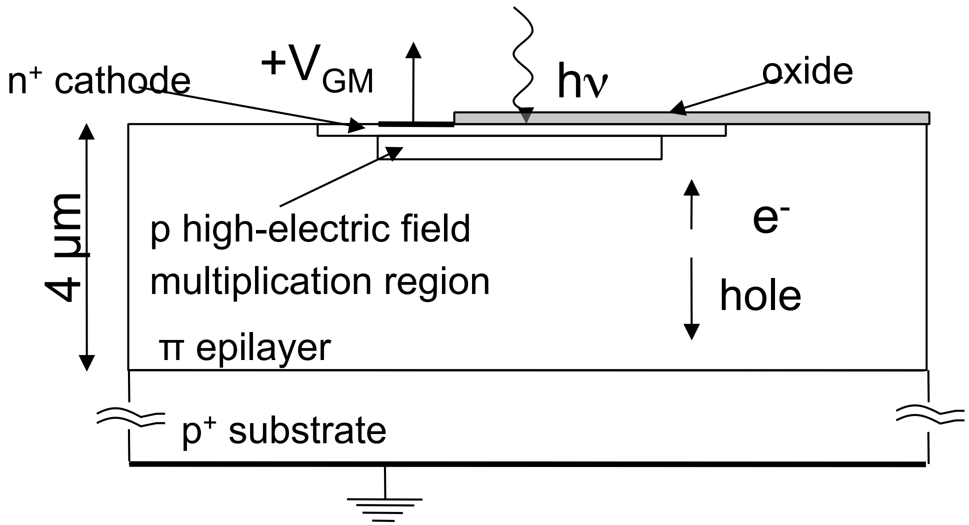

- 2D array of microcells: structures in a common bulk.

- Vbias > Vbreakdown: high field in multiplication region

- Microcells work in Geiger mode: the signal is independent of the particle energy

- The SiPM output is the sum of the signals produced in all microcells fired.

-The photon is absorbed and generates an electron/hole pair

-The electron/hole diffuses or drifts to the high-electric field multiplication region

-The drifted charge undergoes impact ionization and causes an avalanche breakdown.

-Resistor in series to quench the avalanche (limited Geiger mode).

As produced at FBK-irst,Trento, Italy→

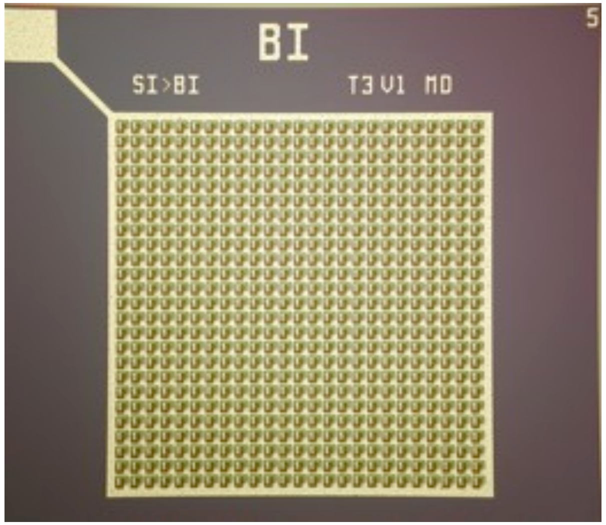

→High gain →Low noise → Good proportionality if $N_{photons} << N_{cells}$

Characterization

- Collaboration with FBK- irst (Trento, been developing SiPMs since 2005:
  - First detectors - Single SiPMs (2006)
  - First matrices 2x2 (2007)
  - First matrices 4x4 (2008)
  - First matrices 8x8 (2009)
- Breakdown voltage VB ~ 30V, very
- Gain: ~10^6
  - Linear for a few volts over VBD.
  - Related to the recharge of the diode capacitance CD the avalanche quenching. G=(VBIAS-VB) x CD/q
- Dark rate:
  - 1-3 MHz at 1-2 photoelectron (p.e.) level, ~kHz at 3-4 p
  - Not a concern for PET applications.

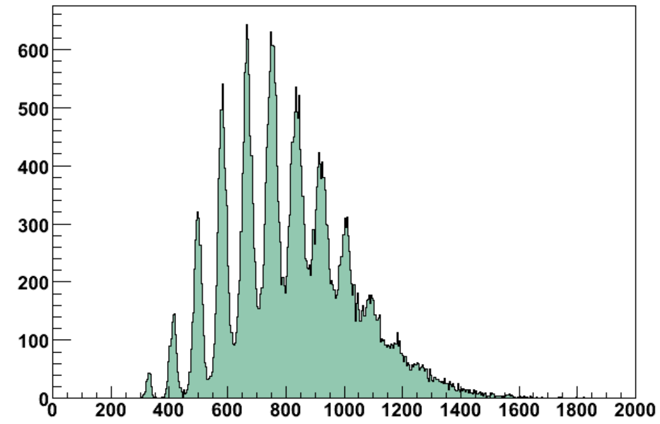

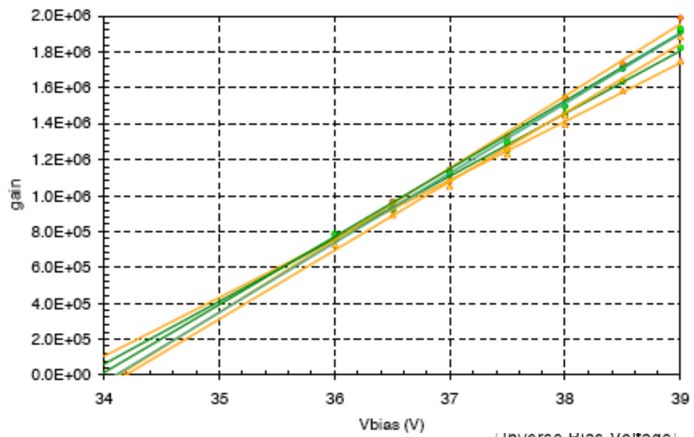

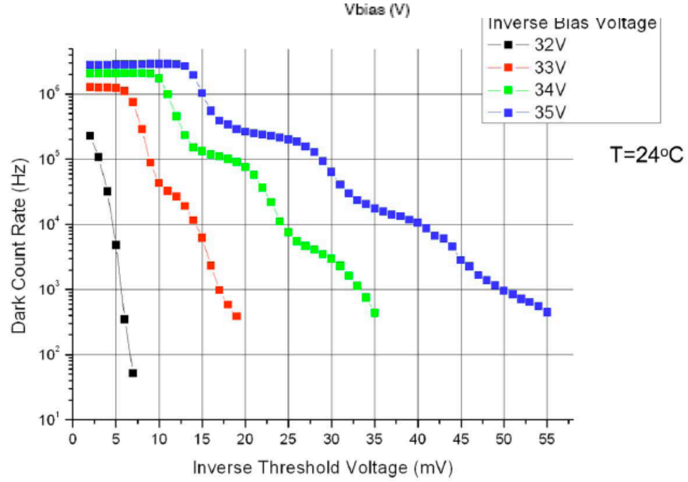

Results: New detectors (May 2007)

Different geometry,size,microcell size and GF.

40x40μm^2 => GF 44%
50x50μm^2 => GF 50%
100x100μm^2 => GF 76%

circular

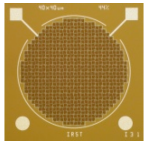

1mm ϕ

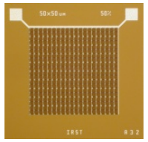

1x1mm^2

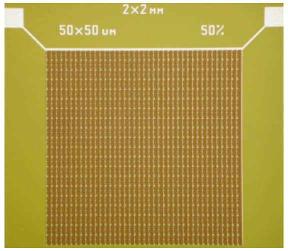

2x2mm^2

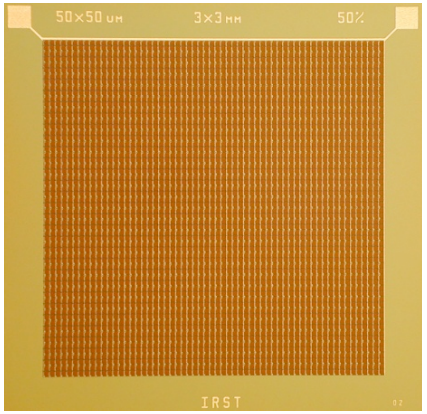

3x3mm^2 (3600 cells)

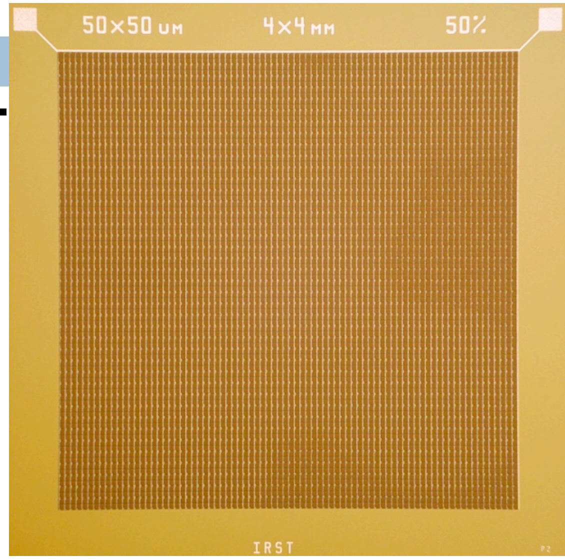

4x4mm^2 (6400 cells)

- Matrices 16 elements (4x4)

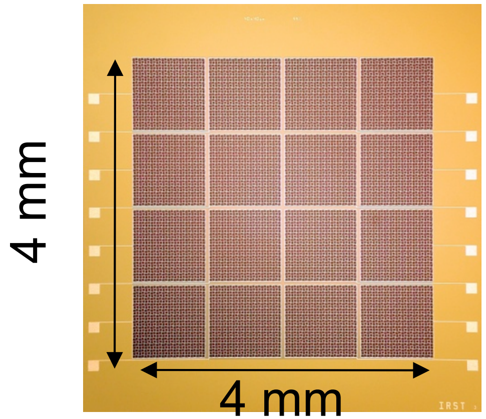

IV CURVES OF 9 MATRICES.

VERY UNIFORM BREAKDOWN POINT

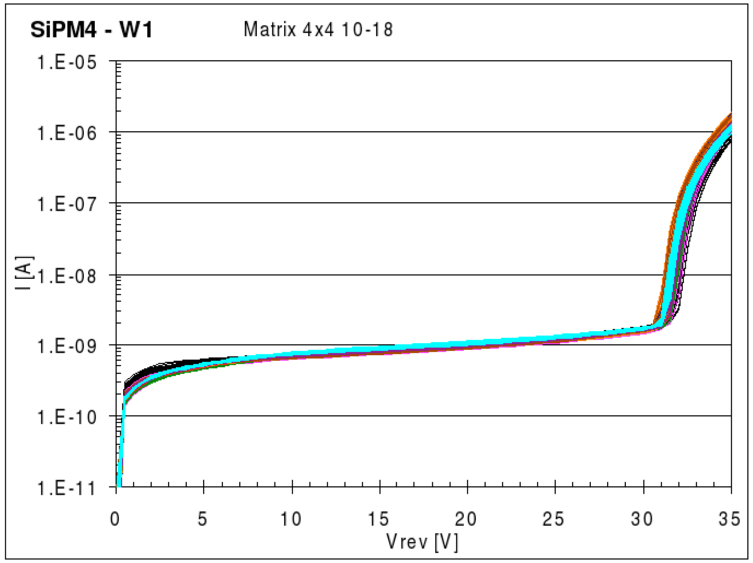

[C.Piemonte et al, Il Nuovo Cimento C, 2007,30(5),473-482]

Silicon Drift Detector

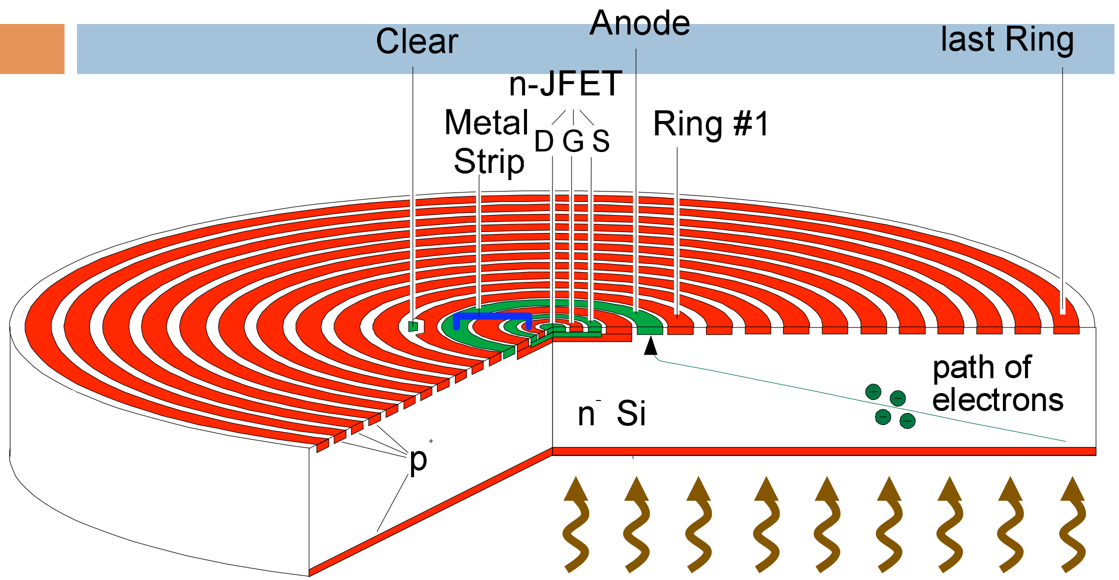

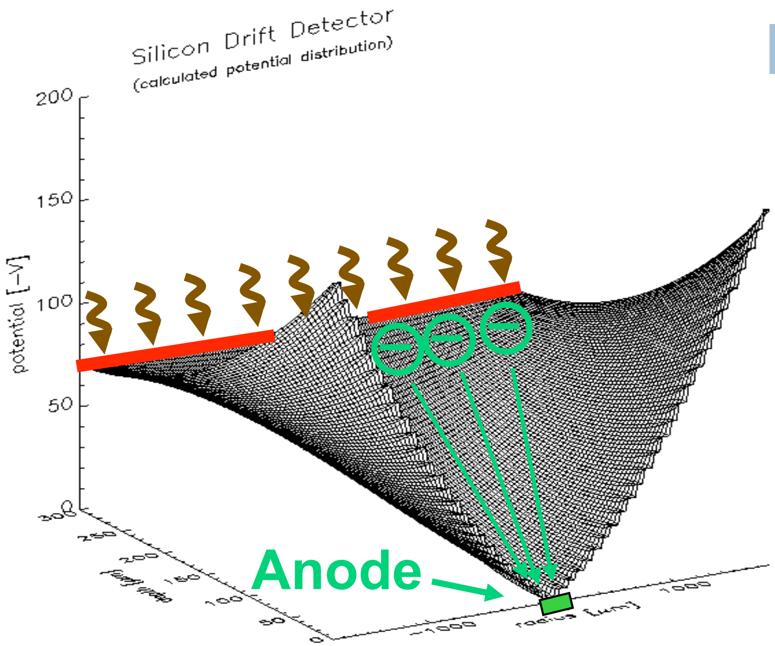

- ❑ low detector capacitance ⇒ low electronics noise
- ❑ JFET integrated on the detector chip
- ❑ homogeneous entrance window, with ARC for scintillation detection
- ❑ low leakage current necessary (~ 300pA/cm^2 @RT available at MPI-HLL)
- ❑ availability of monolithic arrays of SDDs

Summary of accelerators running in the world

CATEGORY OF ACCELERATORS	NUMBER IN USE (*)
High Energy acc. (E >1GeV)	~120
Synchrotron radiation sources	>100
Medical radioisotope production	~200 } 9000
Radiotherapy accelerators	> 7500 } 9000
Research acc. included biomedical research	~1000 } 9000
Acc. for industrial processing and research	~1500
Ion implanters, surface modification	>7000
TOTAL	> 17500

(*) W. Maciszewski and W. Scharf: Int. J. of Radiation Oncology, 2004

High-current cyclotrons used in medicine

Baby Cyclotrons (below 18 MeV)

In-house facility

Mainly used for production of short-lived positron emitters like ^{18}F, ^{11}C, ^{13}N, ^{15}O.

Medium Energy Cyclotrons (below 40 MeV)

Centralised facility

Majority of the cyclotron produced isotopes are produced using such machine viz, ^{123}I, ^{201}Tl, ^{67}Ga, ^{68}Ga, ^{103}Pd etc.

High Energy Cyclotrons (above 40 MeV)

Centralised facilities and research institutions

Used for production of few radioisotope requiring high energy for production viz, ^{67}Cu, ^{82}Sr, ^{211}At…..

Baby cyclotrons

Accelereted particles: H^-

TERA

Medium energy cyclotrons

High-energy cyclotrons

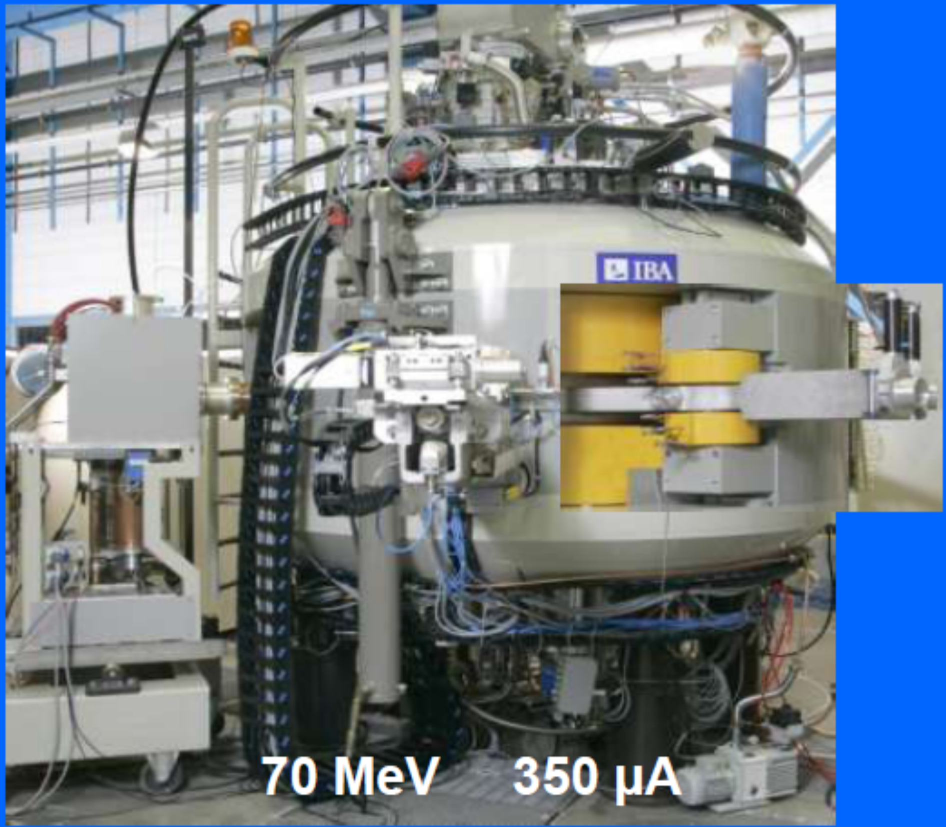

IBA's ARRONAX in Nantes

4 Particles: H^- / D^- / He^{2+}/ HH^+

Variable energy: 15 MeV → 70 MeV

Performances:

- 750 µA H^-
- 35 µA He^{2+}

ACCELERATORS

IN CANCER THERAPY

'Conventional' radiotherapy: linear accelerators dominate

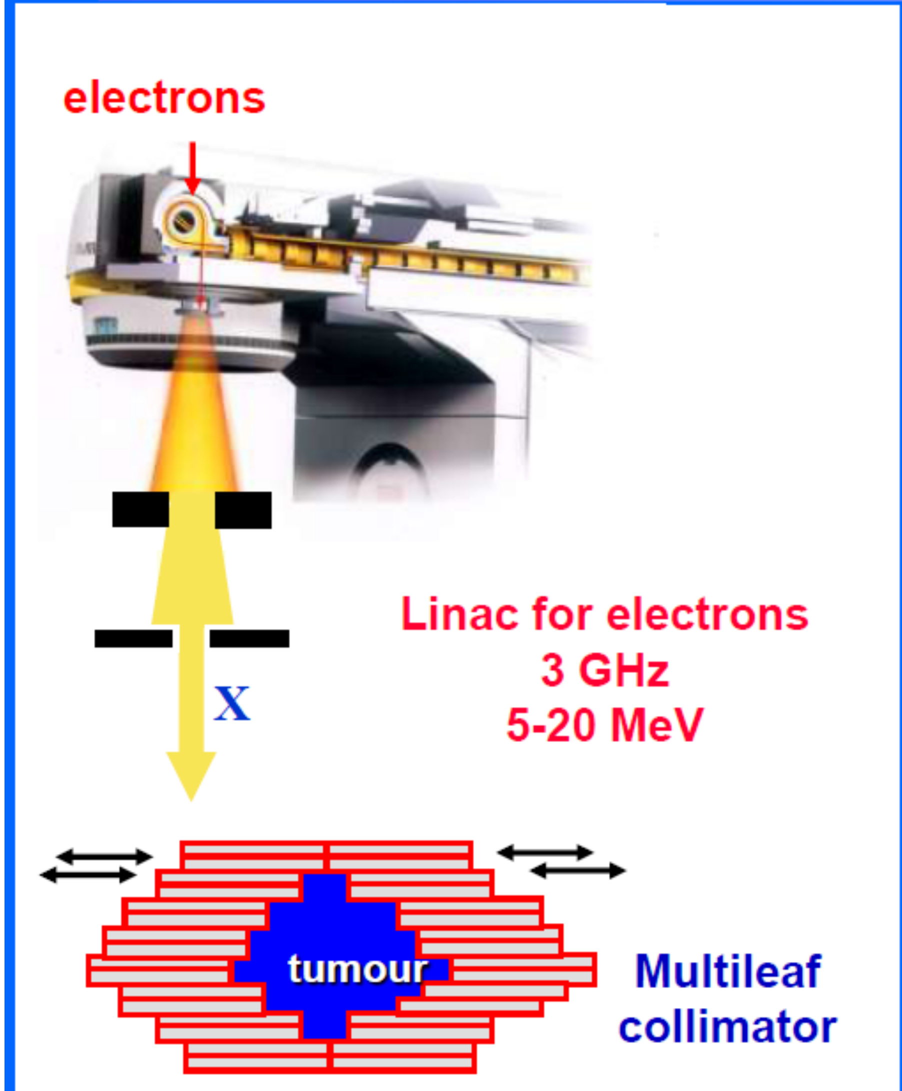

In the world radiation oncologists

use 15 000 electron linacs

40% of all the existing accelerators

Medical accelerators: electron linac

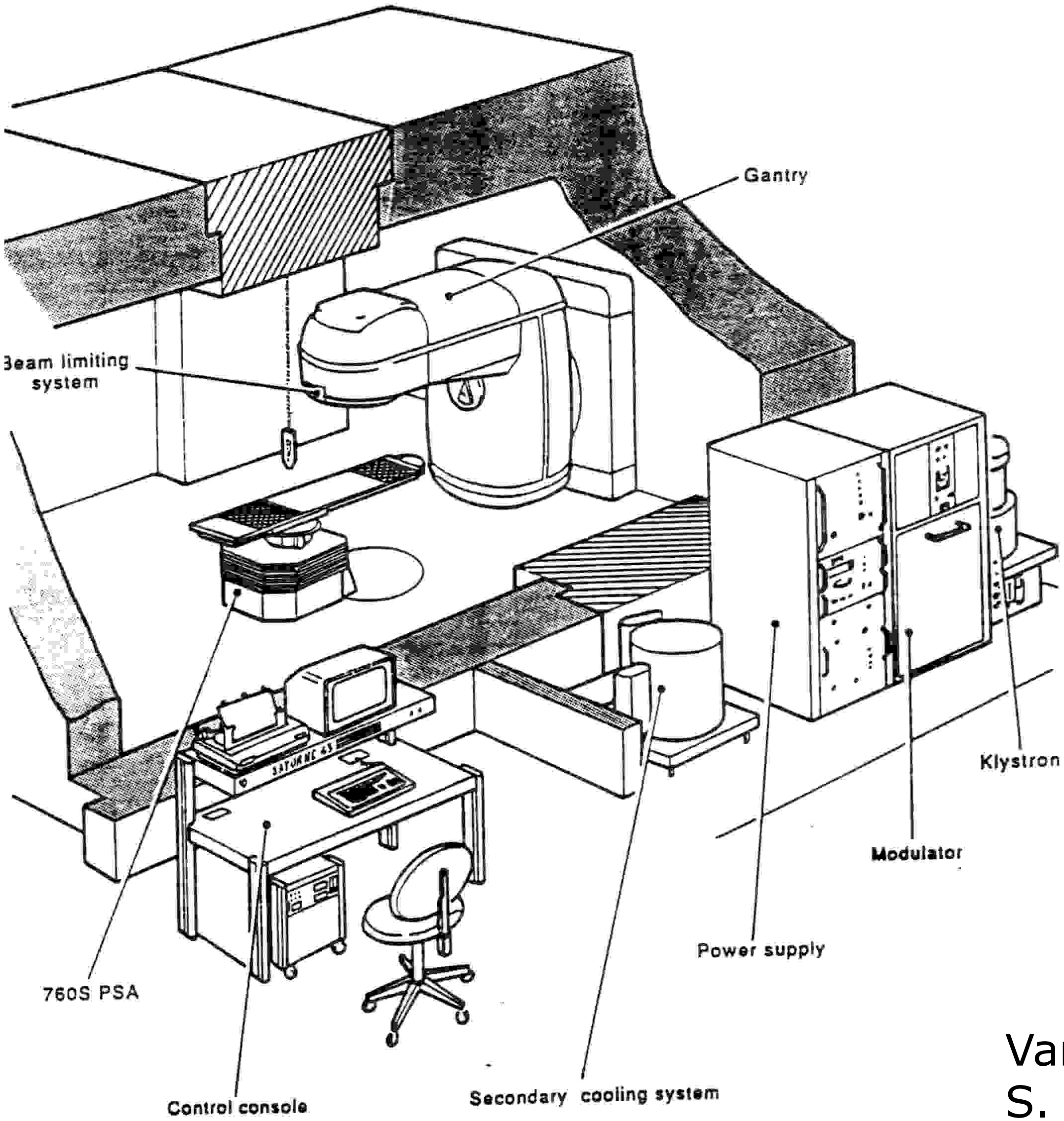

Varian Clinac 1800 installed in the S. Anna Hospital in Como (Italy)

X rays have a poor energy deposition

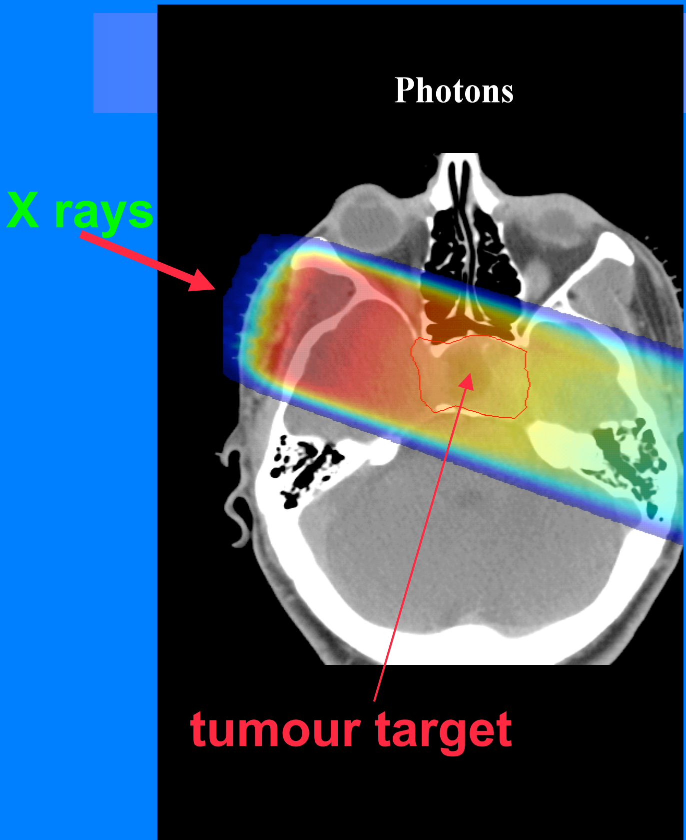

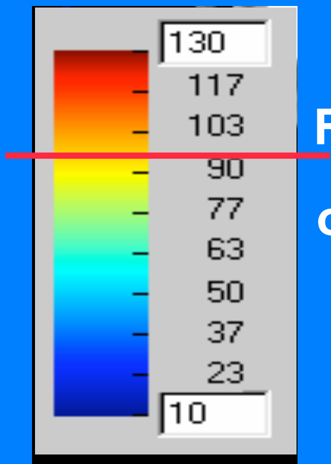

Fraction of dose

IMRT (Intensity Modulated Radiation Therapy)

with 9 crossed beams

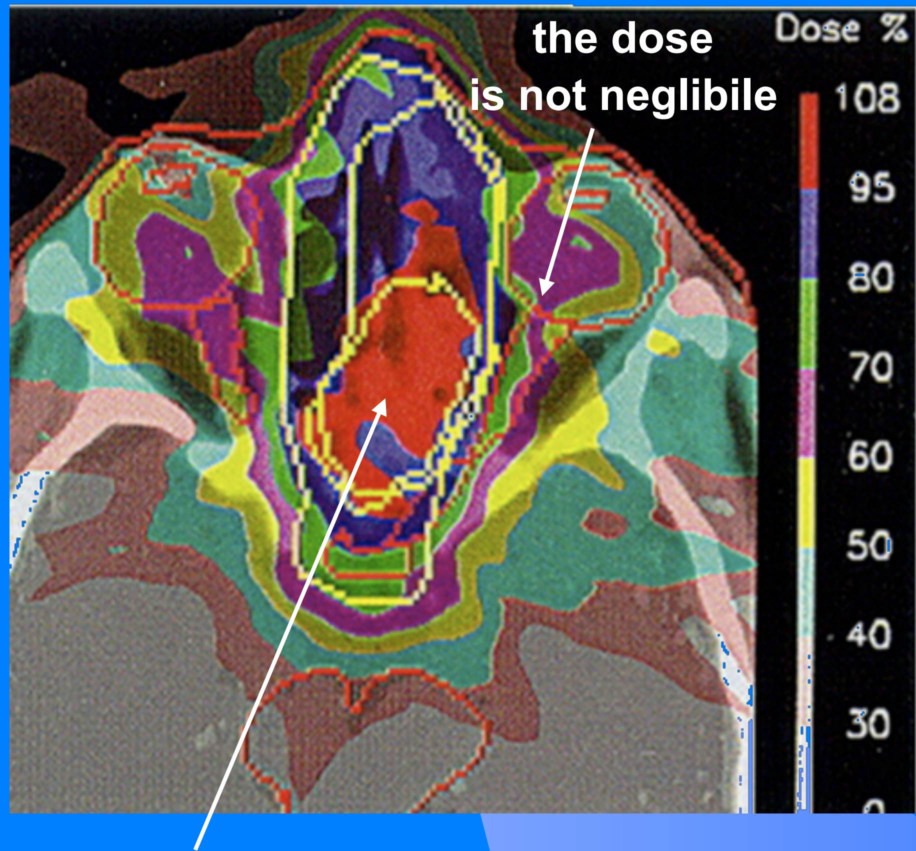

Tumour between the eyes

“Hadrontherapy” uses n, p and C-ion beams

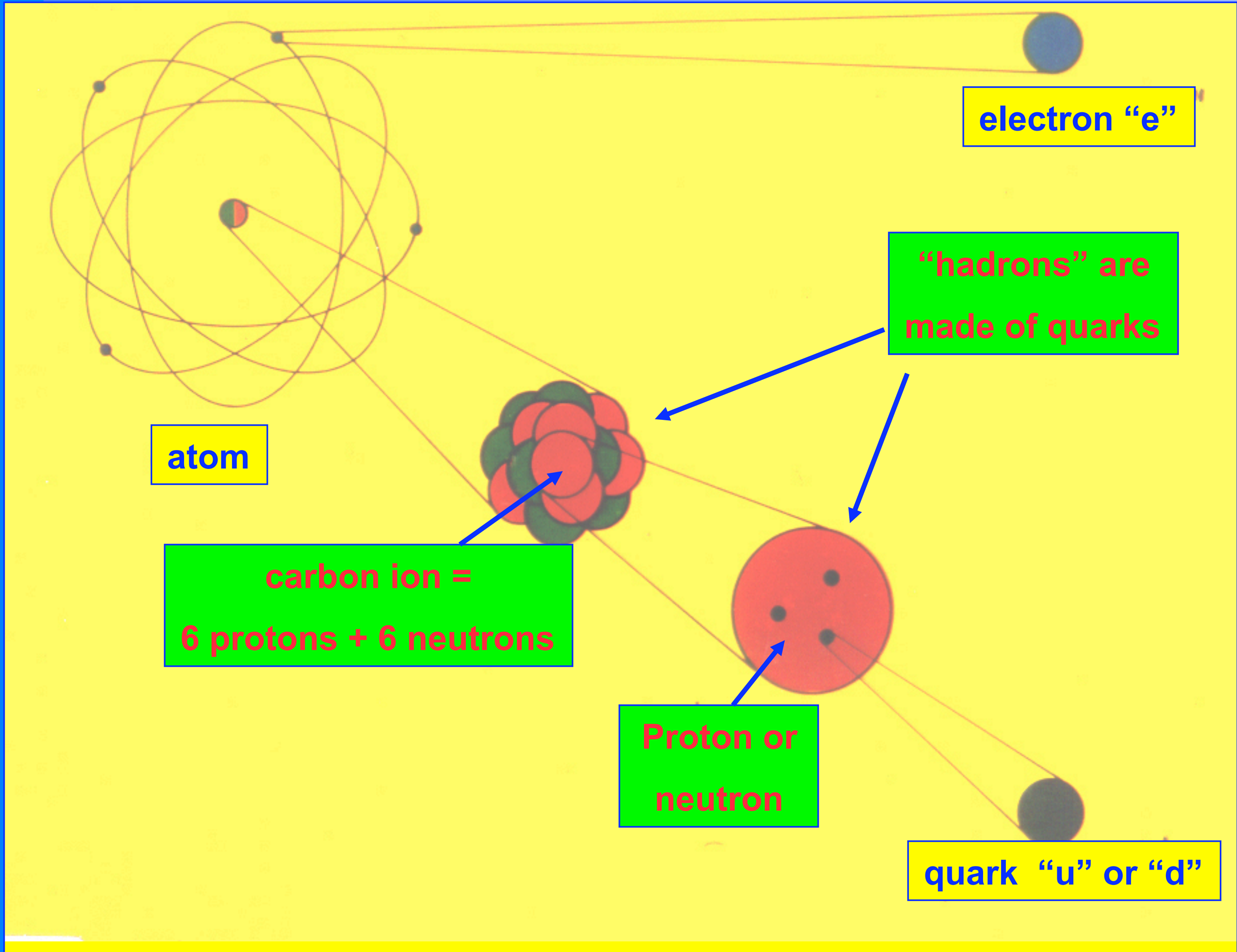

Ionization: the Bethe-Bloch formula

$$\left\langle \frac{dE}{dx} \right\rangle = -4\pi N_A r_e^2 m_e c^2 z^2 \frac{Z}{A} \frac{1}{\beta^2} \left[\frac{1}{2} \ln \frac{2 m_e c^2 \gamma^2 \beta^2}{I^2} T^{max} - \beta^2 - \frac{\delta}{2} \right]$$

$$T_{max} \approx 2 m_e c^2 \beta^2 \gamma^2$$

$$-\frac{dE}{dx} \approx K q^2 \frac{Z}{A\beta^2} \left[\ln \frac{2 m_e c^2 \beta^2 \gamma^2}{I^2} - \beta^2 \right]$$

Charaterized by:

- a fall off at low energy ~$1/\beta^2$
- a relativistic rise ~ $\ln \beta\gamma$
- a minimum at $\beta\gamma \approx 3$
- depends only on $\beta\gamma$ not on m

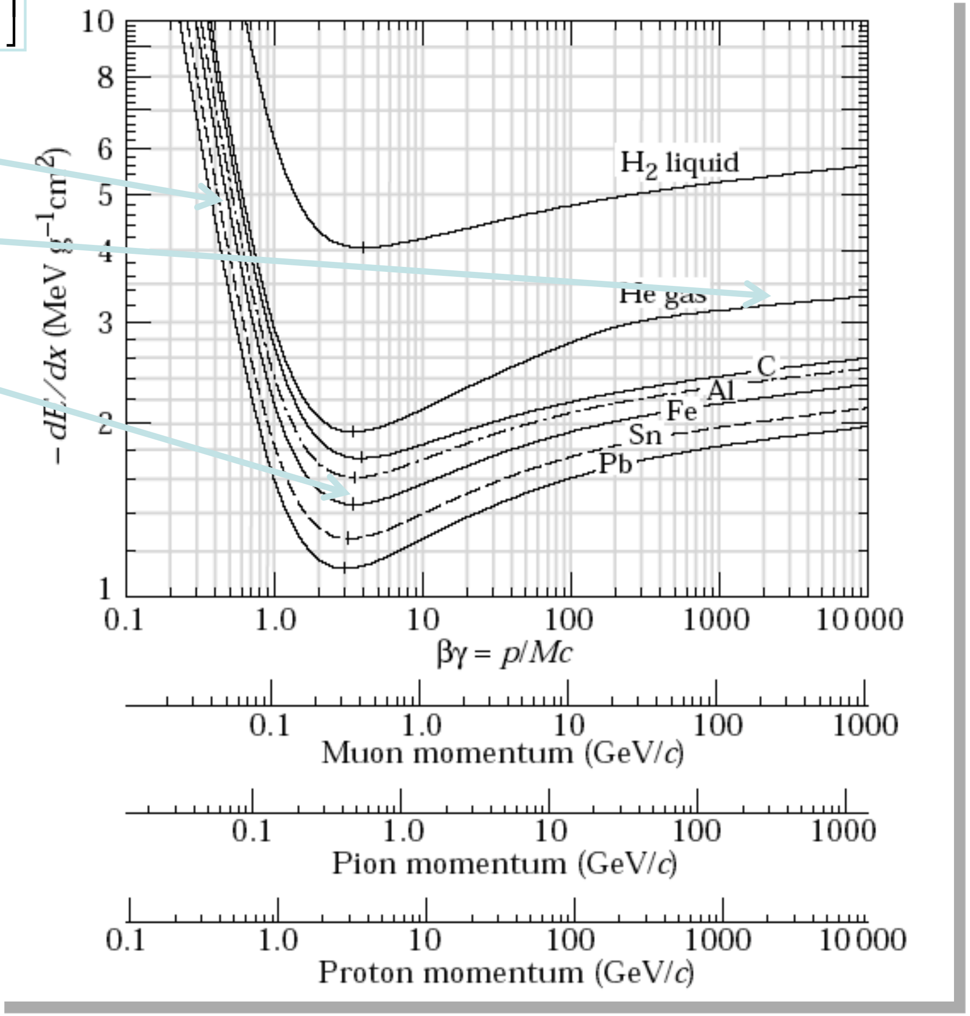

High energy charged particles lose energy **slowly** in material due to ionization leaving tracks as they pass (For $Z \approx 0.5A$ at $\beta\gamma \approx 3$ $1/\rho \; dE/dx \approx 1.4$ MeV cm ^{2}/g)

➔ many kinds of tracking detectors can be done !

Depth Dose Profile

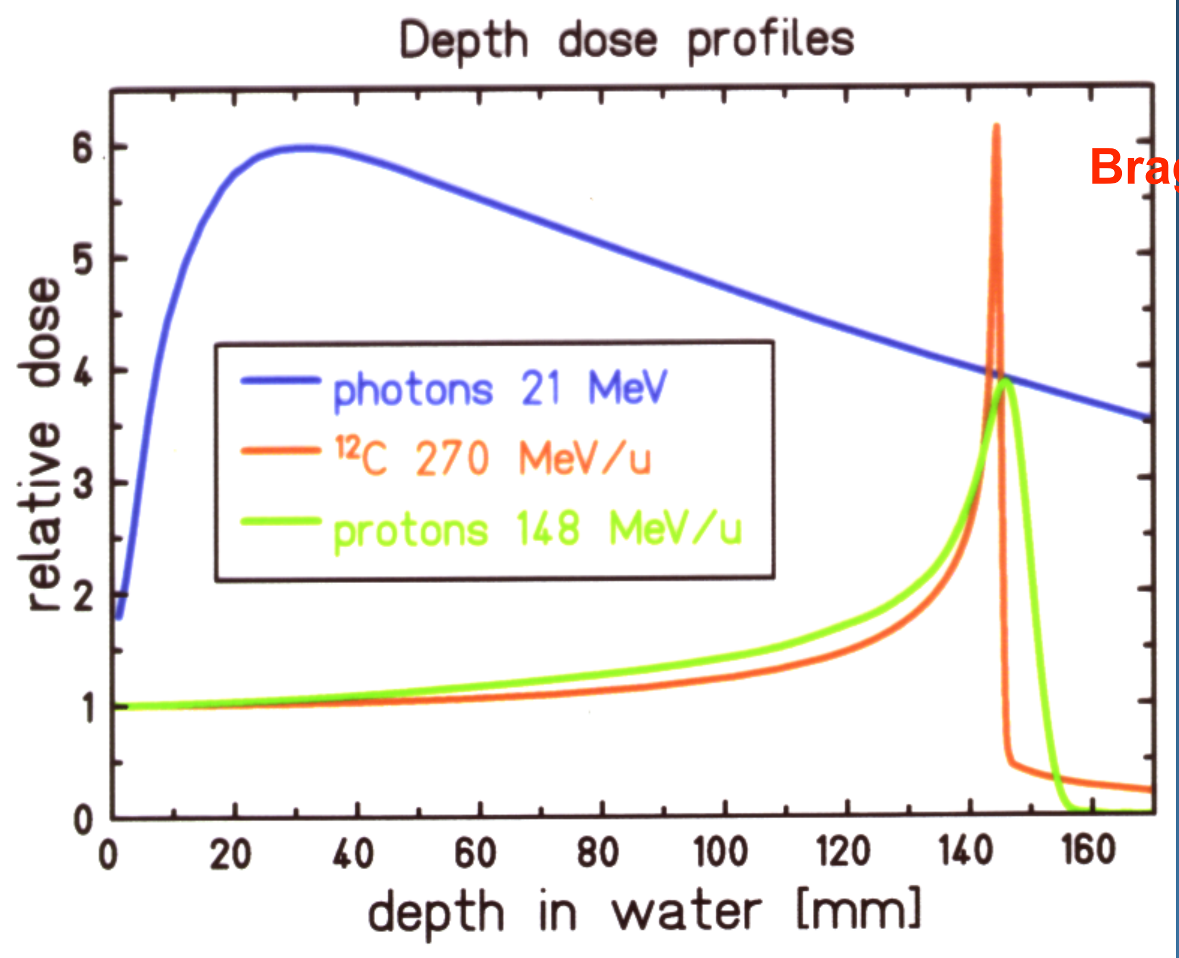

Bragg Peak

Charged hadrons have a much better energy deposition

200 MeV protons

4800 MeV carbon ions

which control radioresistant tumours

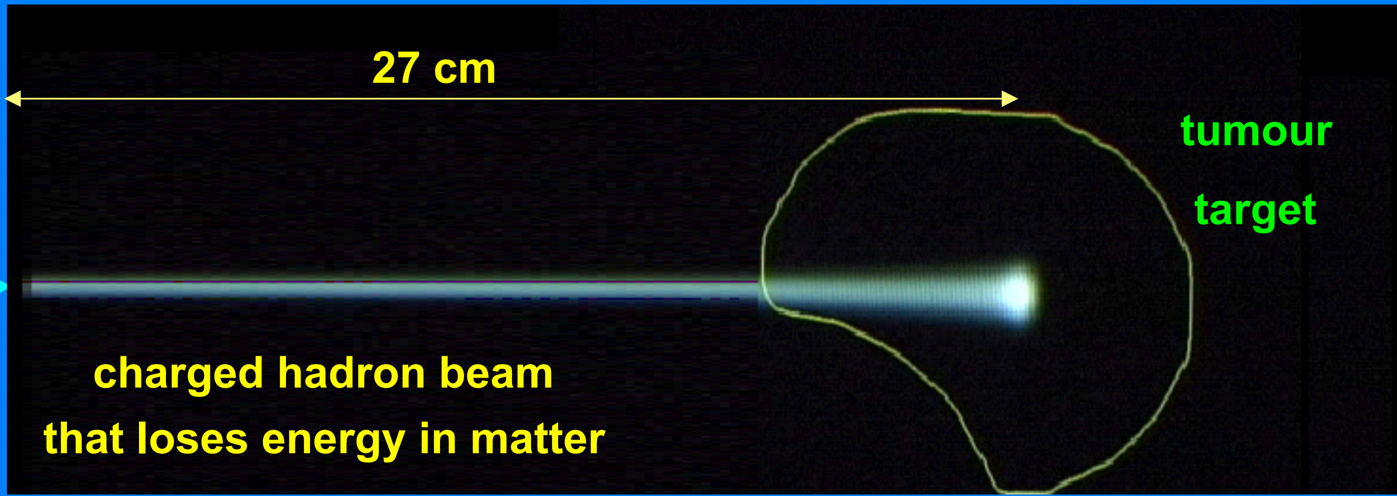

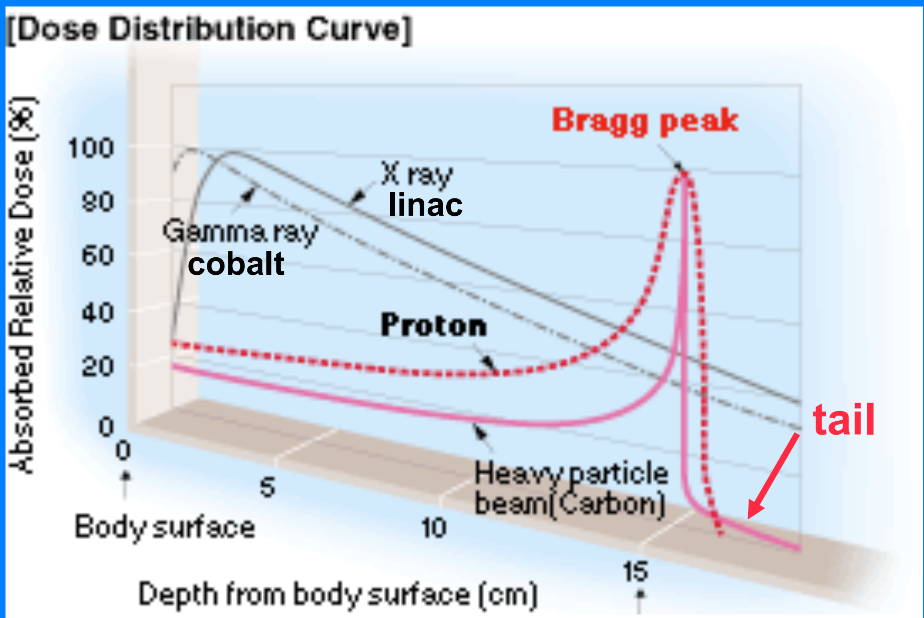

httt://global.mitsubishielectric.com/bu/particlebeam/index_b.html

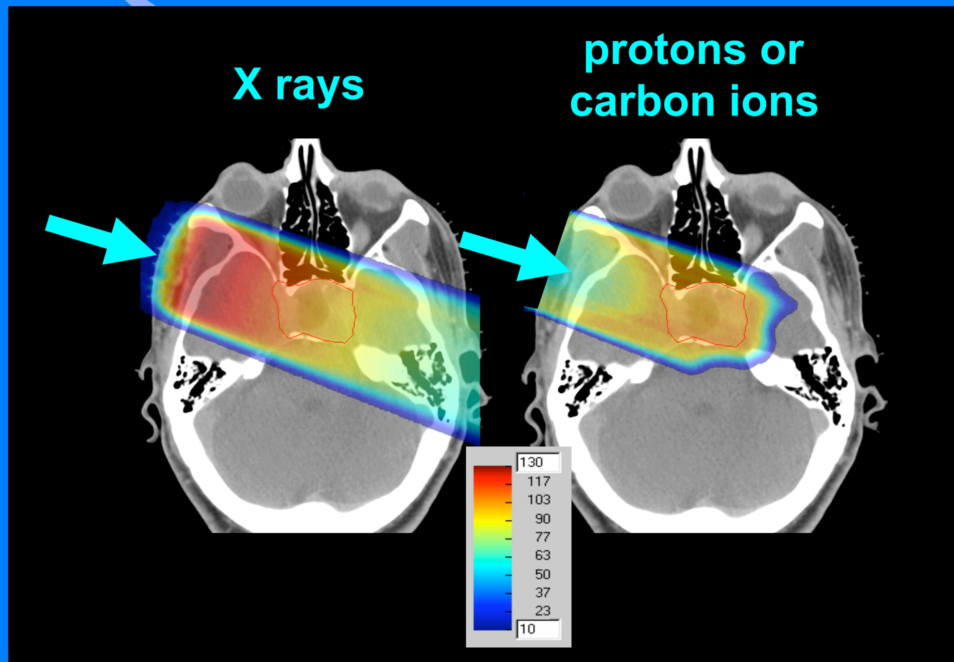

Charged hadrons can deliver the dose in three dimensions

Longitudinal mouvement by varying the energy of the beam

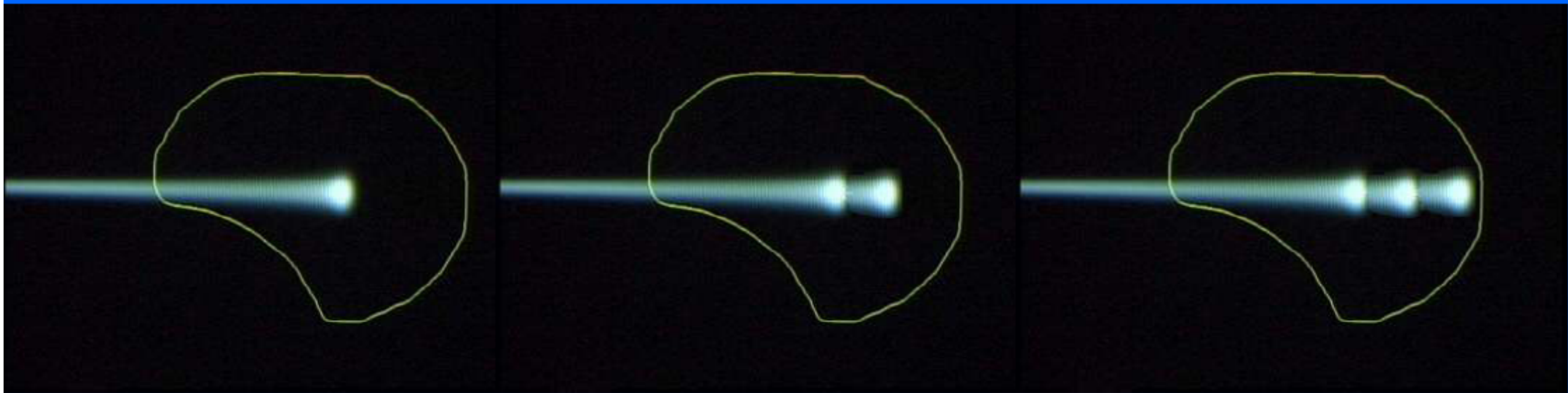

Charged hadrons can deliver the dose in three dimensions

Lateral movement with a transverse magnetic field

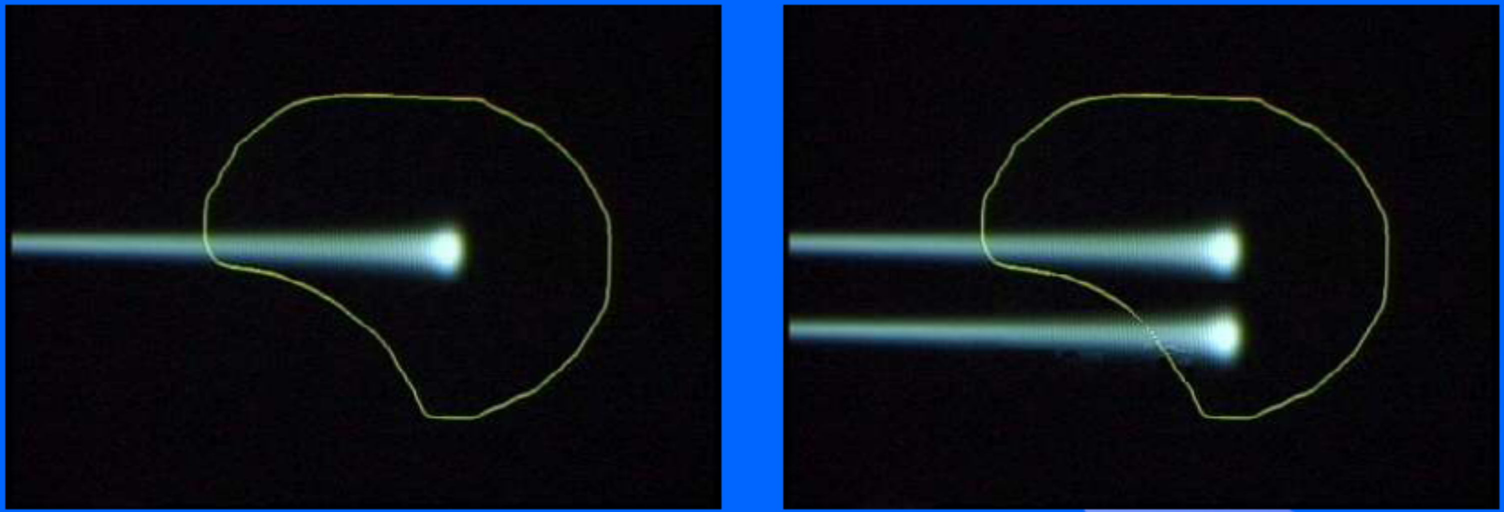

Magnetic scanning with pencil beam

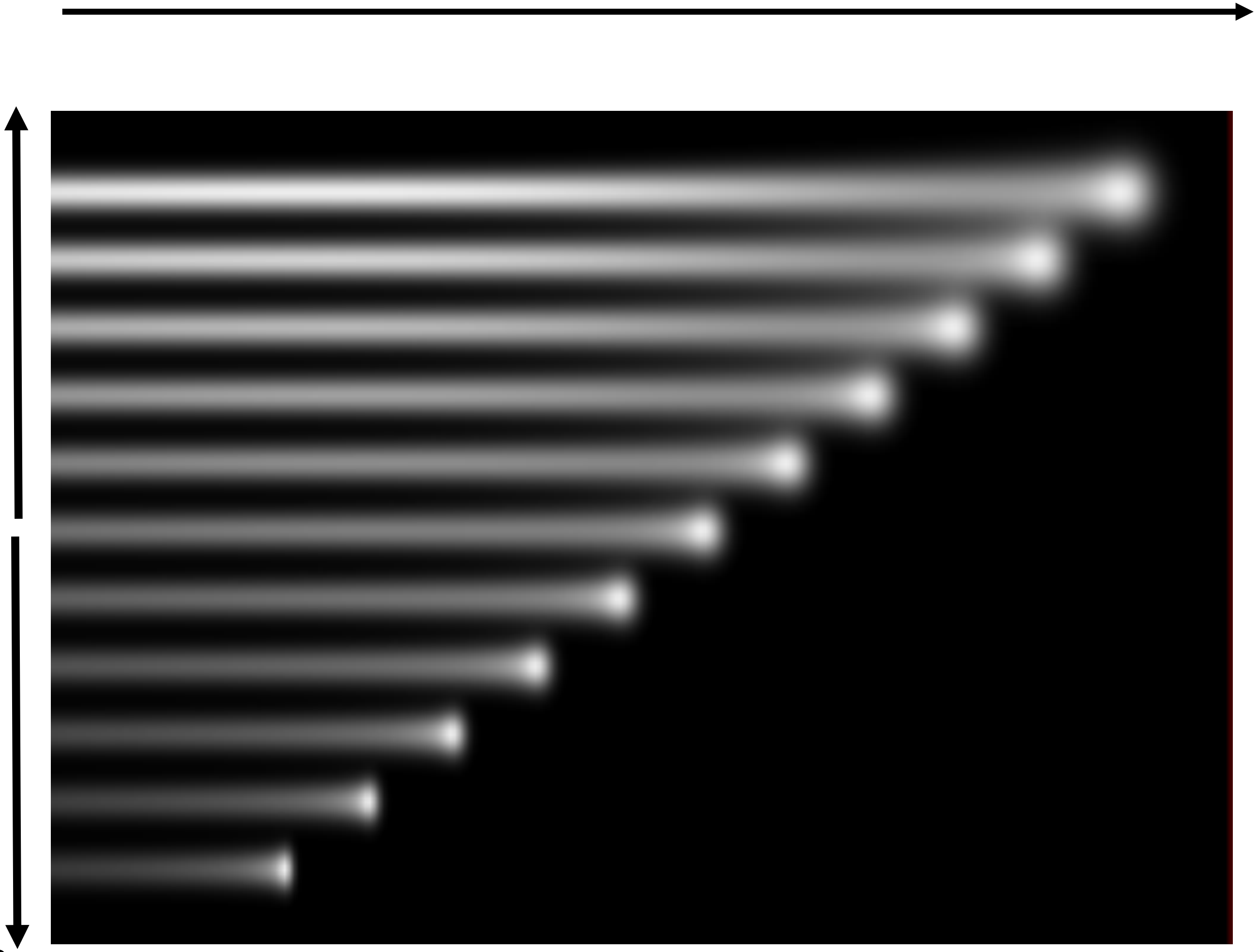

Monte Carlo simulation:

200 MeV protons in water

- Fully 3d conformal (fixed range modulation)
- Fully automated (no specific hardware needed)

Protons are <u>qualitatively</u> different from X-rays

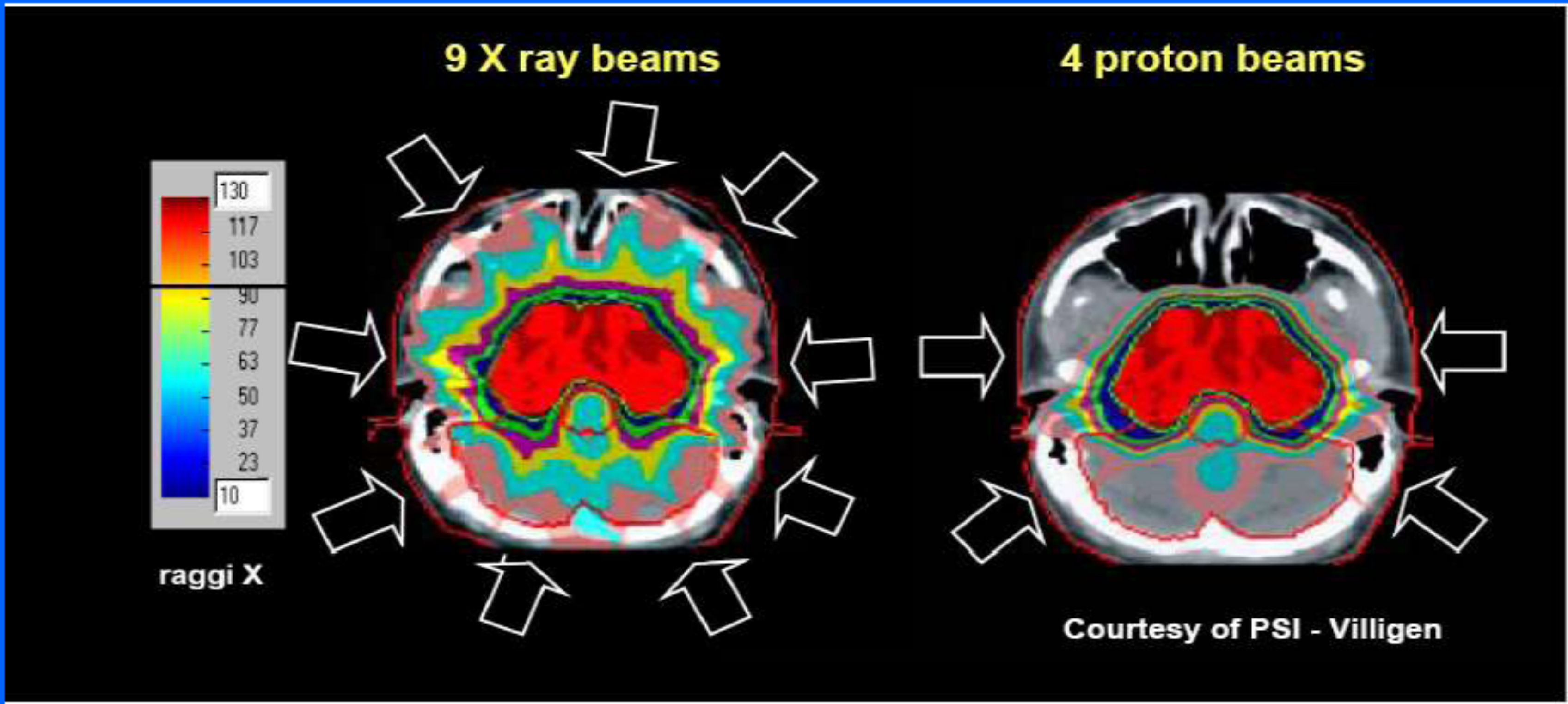

Carbon ions deposit in a cell 24 times more energy than a proton producing not reparable <u>multiple close-by double strand breaks</u>

Carbon ions can control radio-resistant tumours

Trasferimento tecnologico

Particle physics software aids space and medicine

"Geant4 is a showcase example of technology transfer from particle physics to other fields such as space and medical science [...]".

CERN Courier, June 2002

Software di Simulazione

E' stato sviluppato un sistema dosimetrico, basato su simulazione Montecarlo, con lo scopo di ricavare sia la distribuzione di dose in tre dimensioni, sia le relative curve di isodose nei tessuti.

Geant 4 (1)

- software basato su un'architettura ed una programmazione orientata agli oggetti
- processo di sviluppo rigoroso basato sul metodo iterativo incrementale
- interfaccia astratta utilizzo versatile per l'utente

Contemporaneamente si rende necessario uno strumento per il confronto statistico (Goodness of Fit) delle curve/distribuzioni simulate con i dati sperimentali .

(1) http://www.ge.infn.it/geant4

Adroterapia

Fa uso di fasci di protoni che depositano dosi terapeutiche di radiazione vicino al tumore, utilizzando tecniche di precisione balistica.

Adroterapia con protoni

Melanoma oculare

CATANA

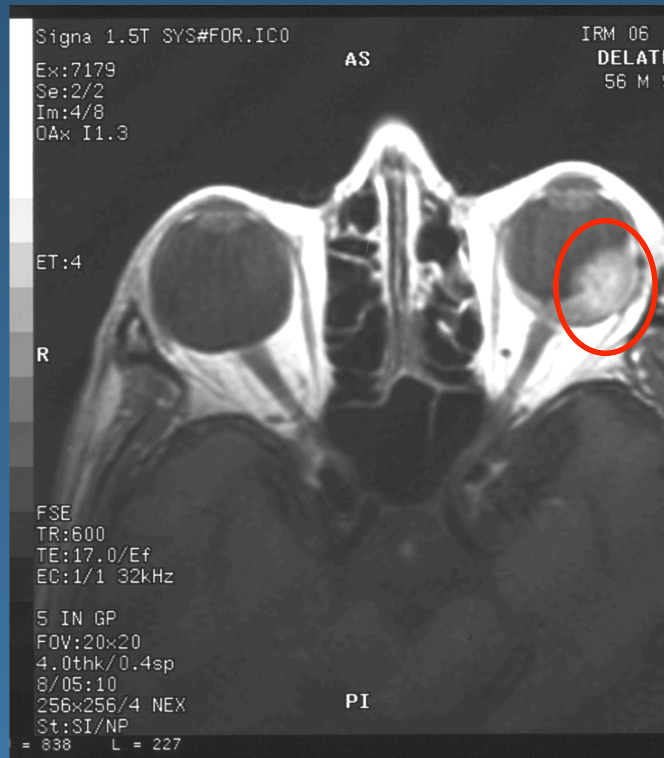

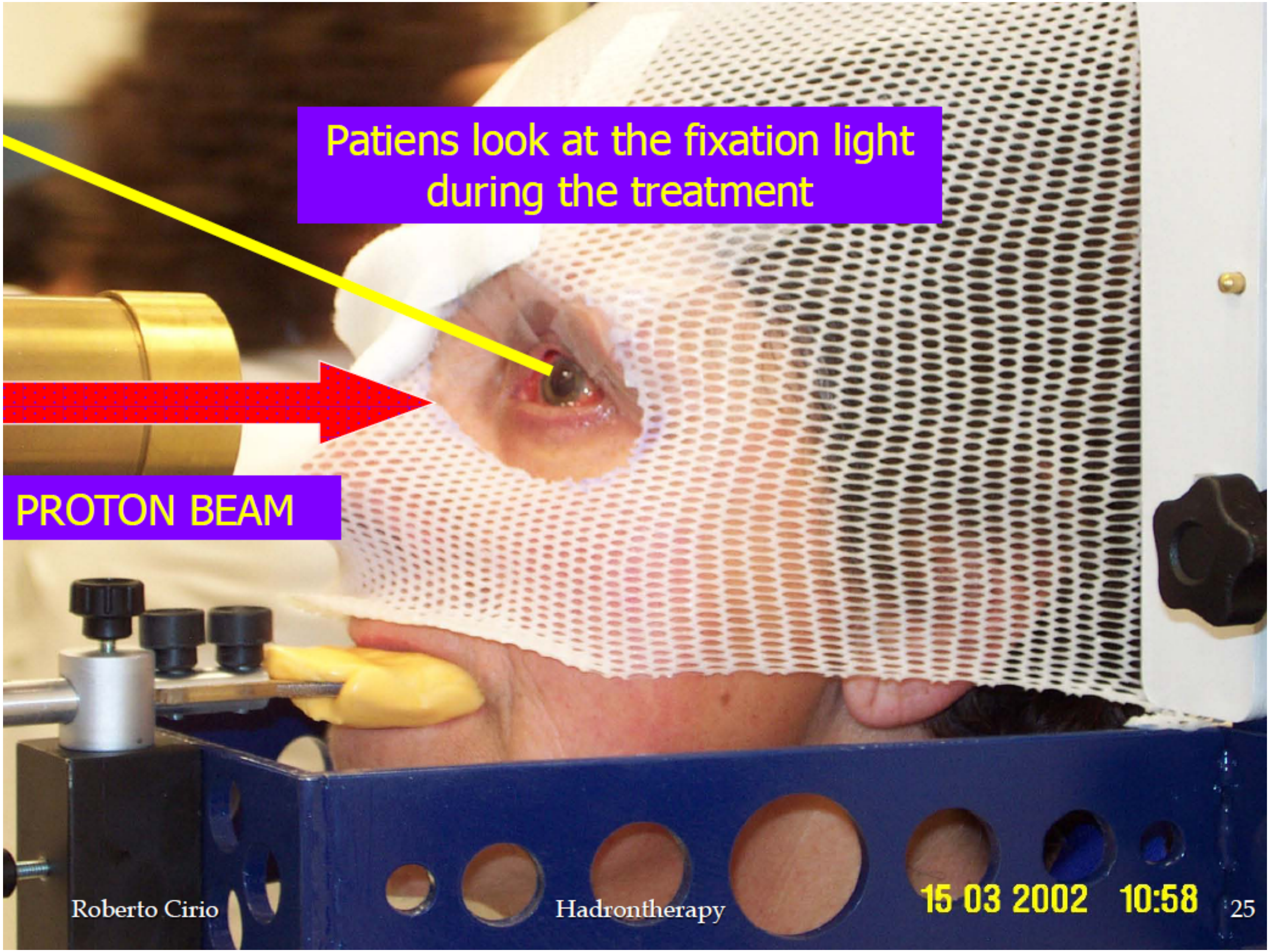
Patiens look at the fixation light
during the treatment
PROTON BEAM
15 03 2002 10:58

Protoni – picco di Bragg - Acqua

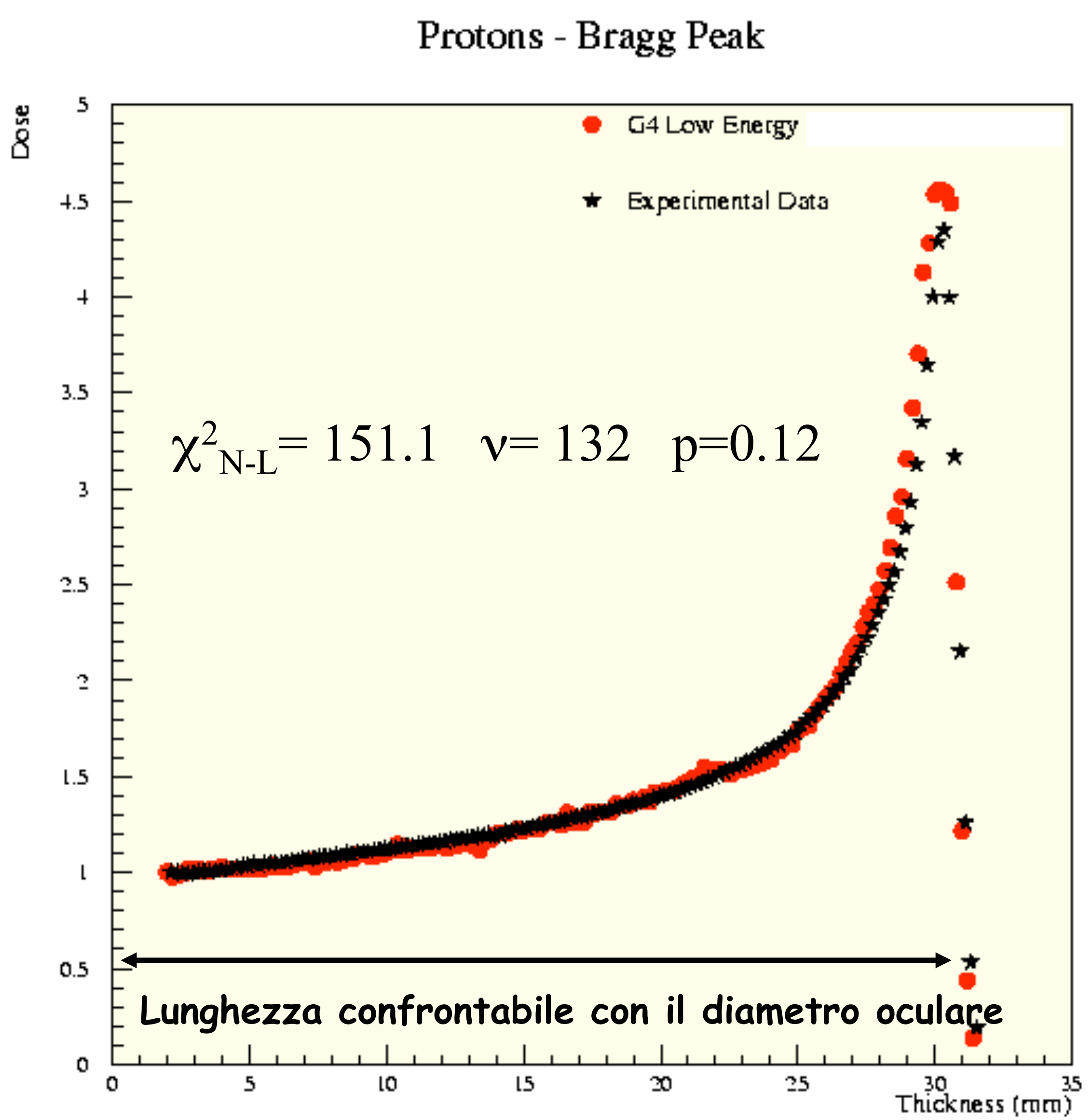

Dati sperimentali acquisiti presso ESPERIMENTO CATANA (INFN, LNS Catania)

Le simulazioni del picco di Bragg basate sul toolkit Geant4 (LowE) rappresentano uno strumento valido per la simulazione dei piani di trattamento negli studi di adroterapia applicati di melanoma oculare.

http://www.lns.infn.it/catanaweb

Particelle e grandezze fisiche studiate

Elettroni CSDA Range, Potere frenante, Coefficienti di trasmissione, Coefficienti di backscattering.

Fotoni Coefficienti di assorbimento e di trasmissione, sezioni d'urto.

Le grandezze fisiche sono state simulate per TUTTI gli elementi della tavola periodica (circa 100)

Positroni Coefficienti di trasmissione e di backscattering

Protoni CSDA Range, Potere frenante, picco di Bragg

PRESENT TREATMENT ROOM

- 0 ° respect the switching magnet
- 80 meter after extraction
- 3 m proton beam line

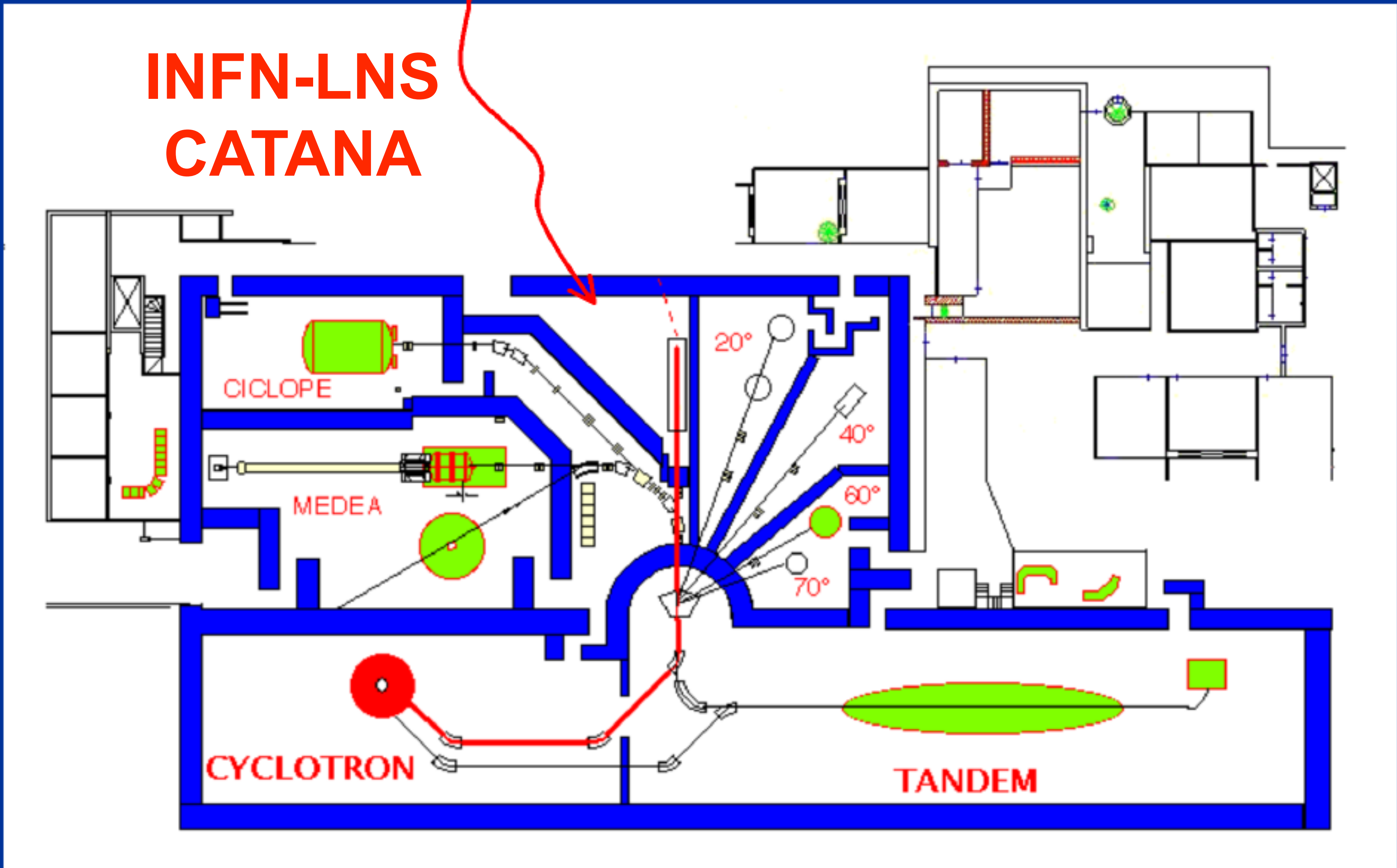

Loma Linda Medical University Centre: first patient 1992

- **First hospital-based proton-therapy centre**

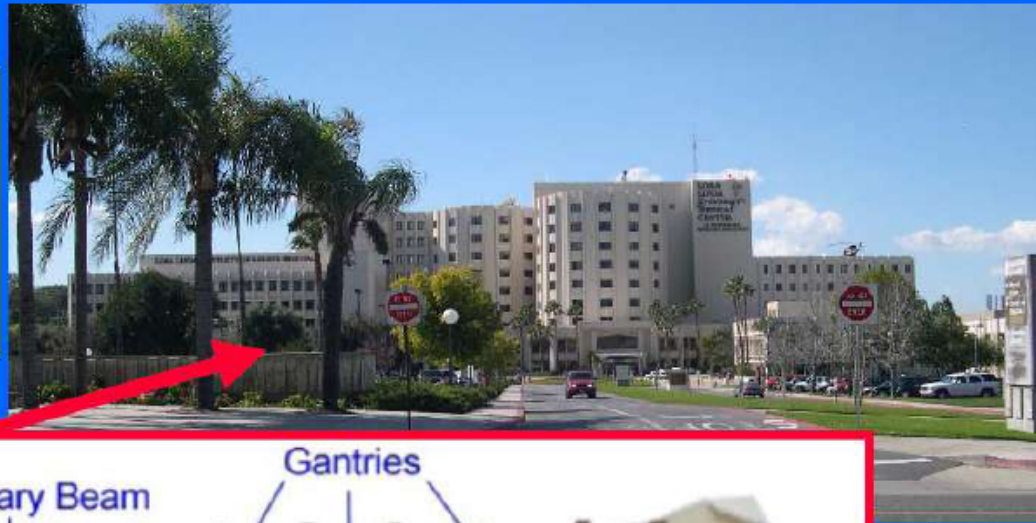

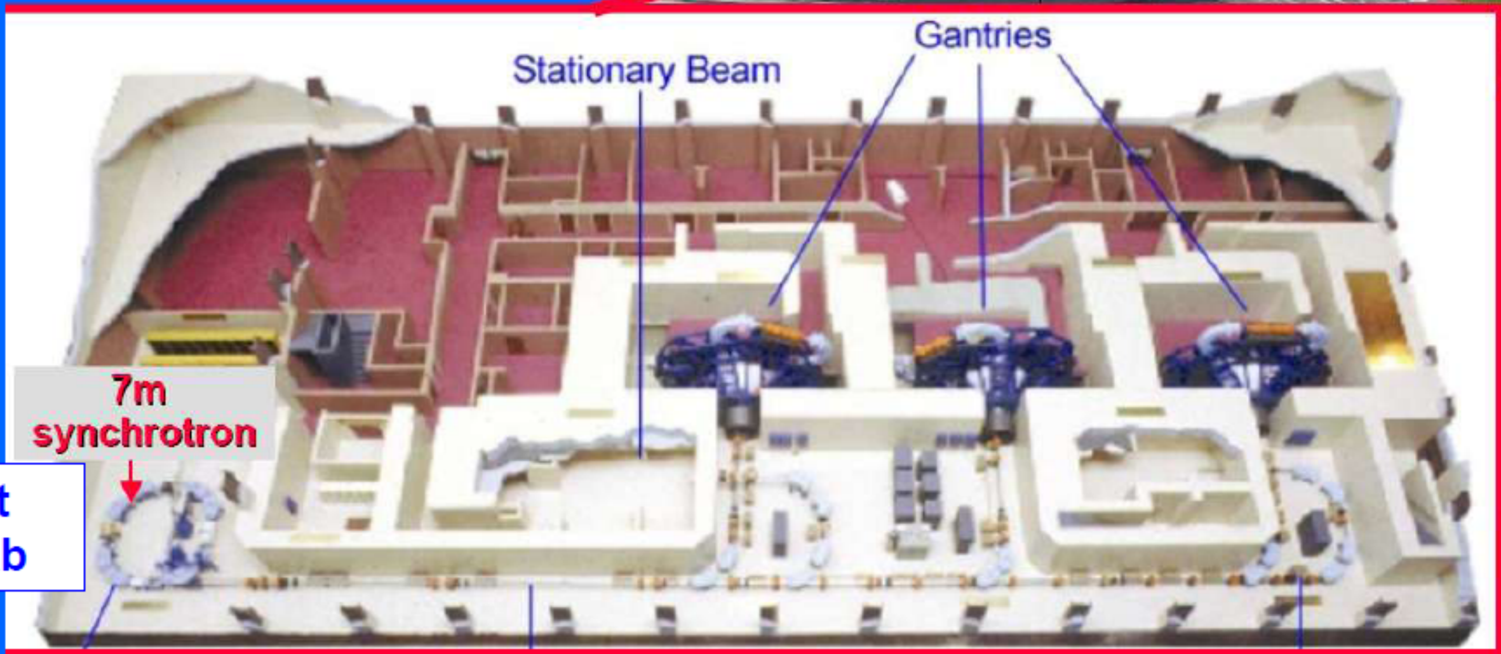

Built at Fermilab

Hospital centres for deep protontherapy (>500 pts/year)

5 in USA, 4 in Japan, 2 in China, 1 in Switzerland, 1 in Germany,
1 in Korea, 1 in Italy

(running or financed)

Five companies offer turn-key centres

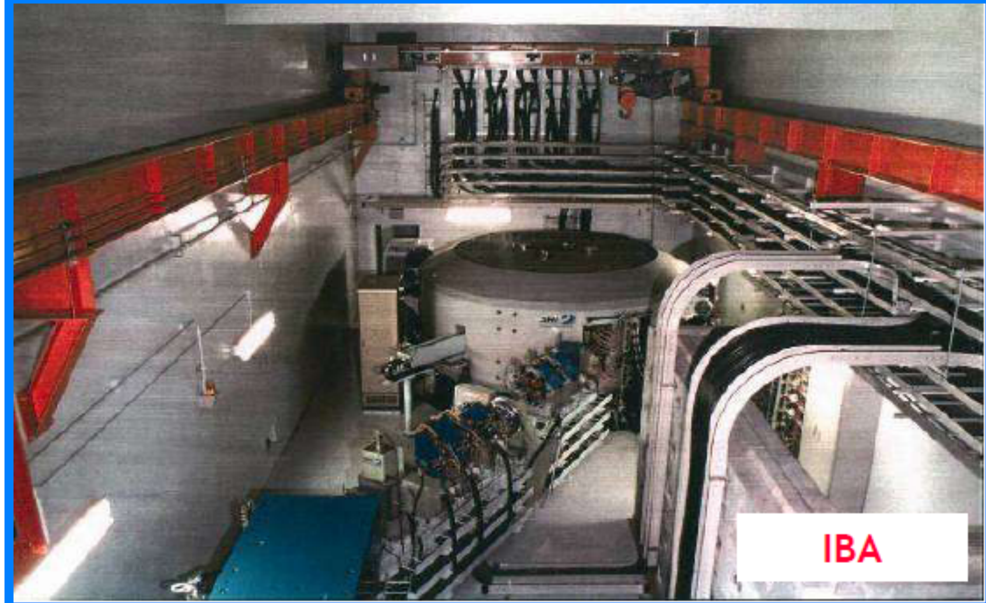

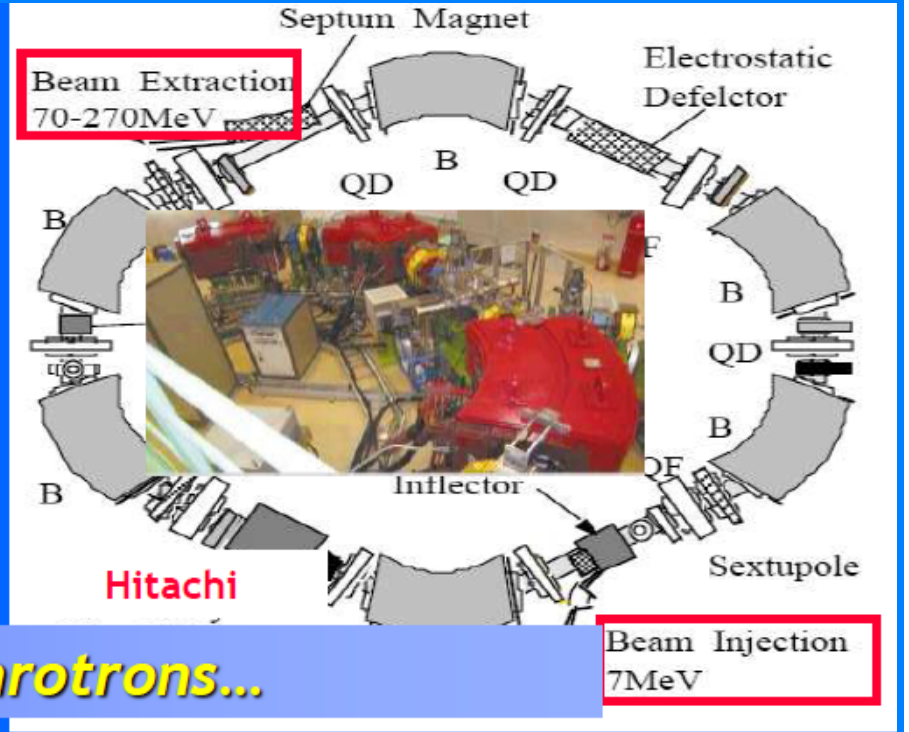

Protontherapy: cyclotrons and synchrotrons…

HIMAC in Chiba is the pioner of carbon therapy (Prof H. Tsujii)

Yasuo Hirao

15 Hirao, Y. et al, "Heavy Ion Synchrotron for Medical Use: HIMAC Project at NIRS Japan" Nucl. Phys. A538, 541c (1992)

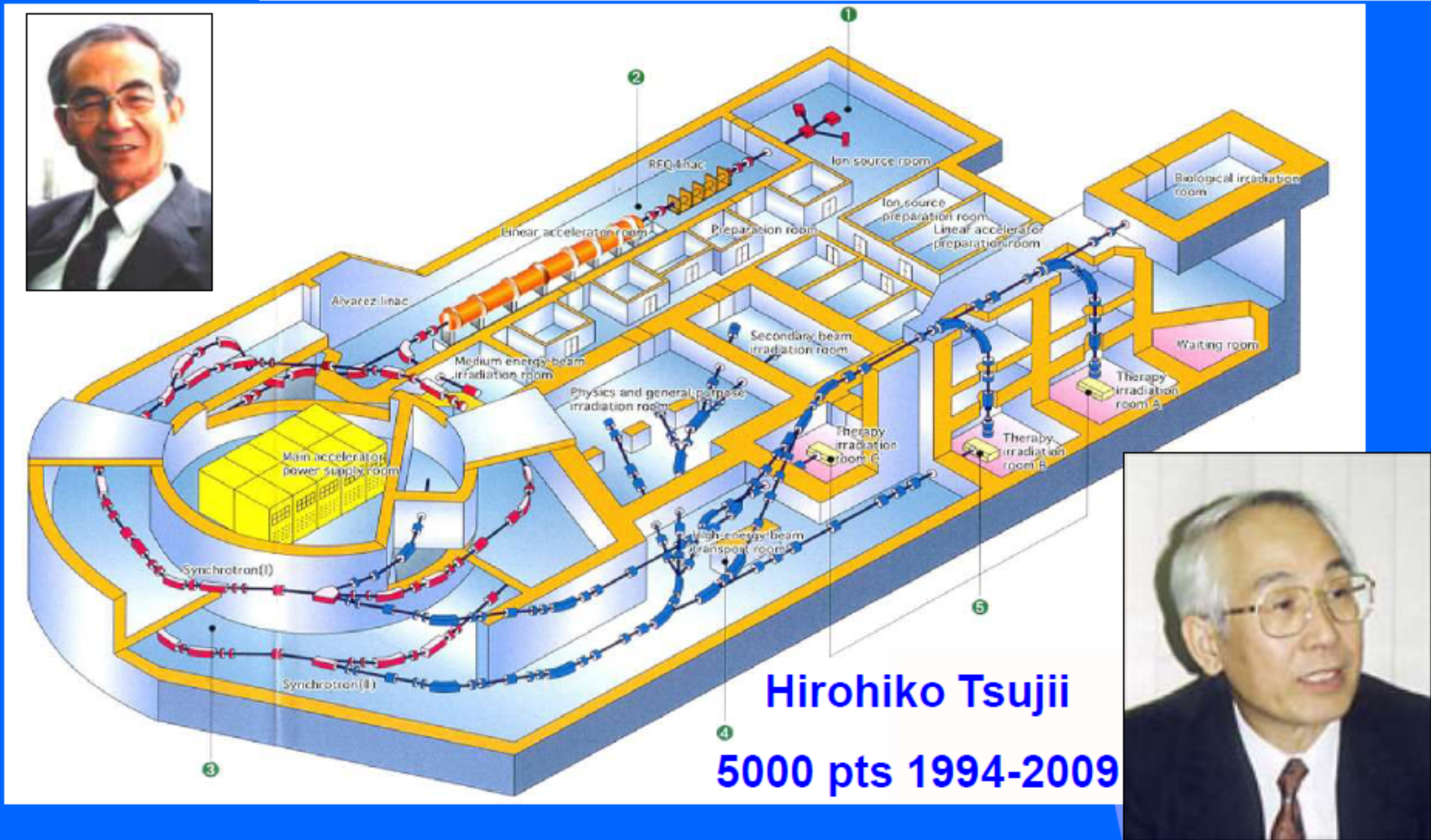

Hirohiko Tsujii

5000 pts 1994-2009

The Hyogo 'dual' Centre

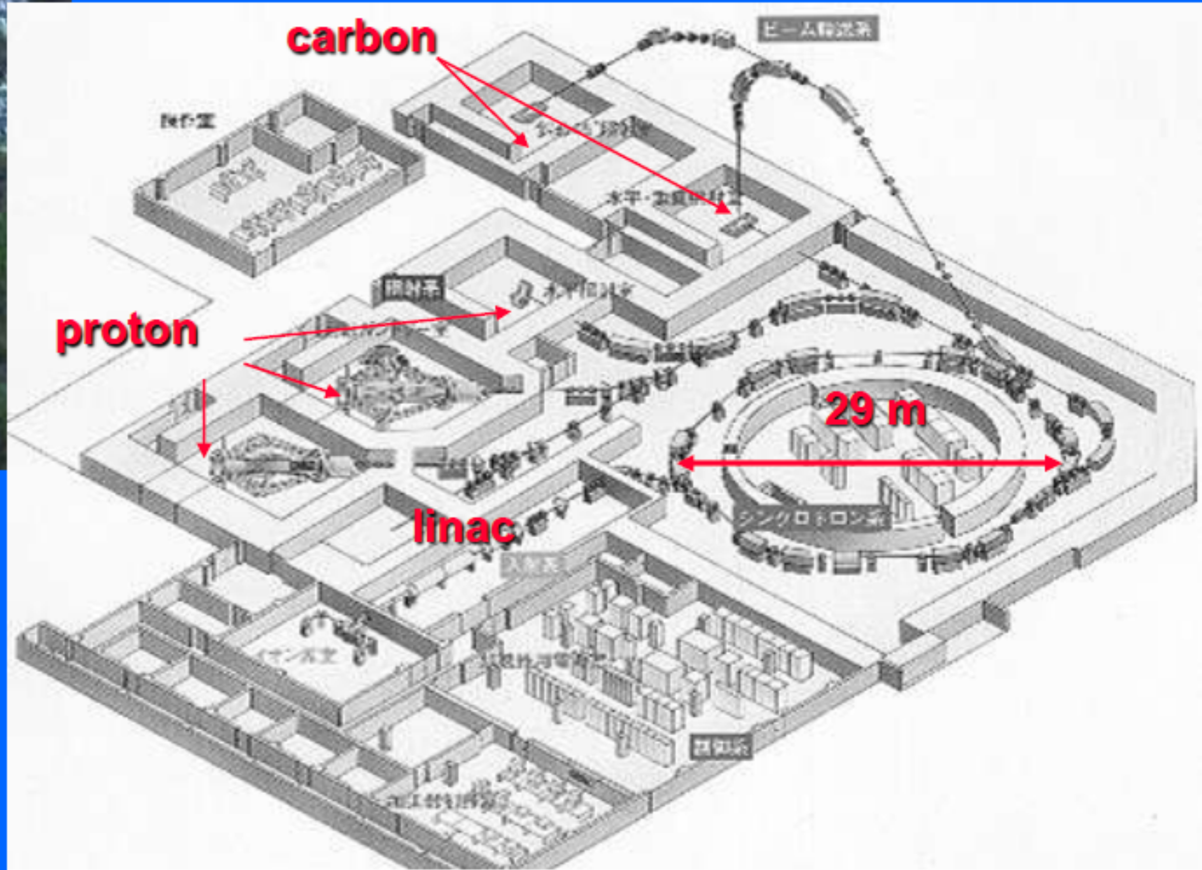

Mitsubishi: turn-key system

End of 2008

protons: 2000 patients

carbon ions: 500 patients

Japan: 4 proton Centres and 2 carbon ion centres

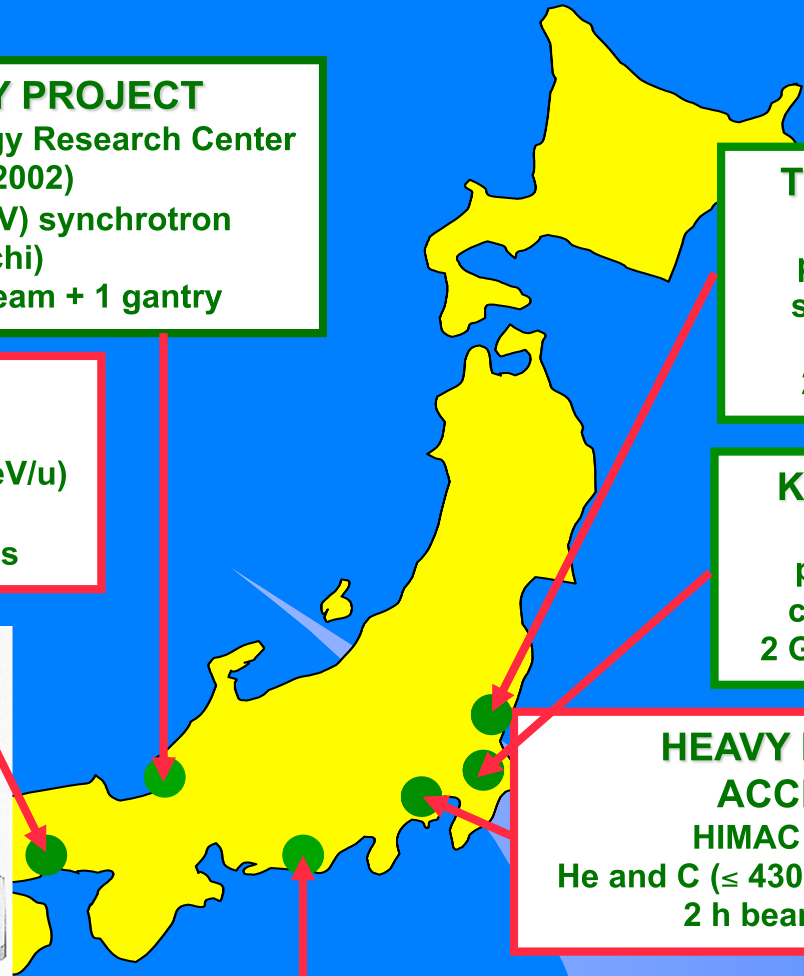

WAKASA BAY PROJECT
by Wakasa-Bay Energy Research Center
Fukui (2002)
protons (≤ 200 MeV) synchrotron
(Hitachi)
1 h beam + 1 v beam + 1 gantry

TSUKUBA CENTRE
Ibaraki (2001)
protons (≤ 270 MeV)
synchrotron (Hitachi)
2 gantries
2 beam for research

HYOGO MED CENTRE
Hyogo (2001)
protons (≤ 230 MeV) - He and C ions (≤ 320 MeV/u)
Mitsubishi synchrotron
2 p gantries + 2 fixed p beam + 2 ion rooms

KASHIWA CENTER
Chiba (1998)
protons (≤ 235 MeV)
cyclotron (IBA – SHI)
2 Gantries + 1 hor. beam

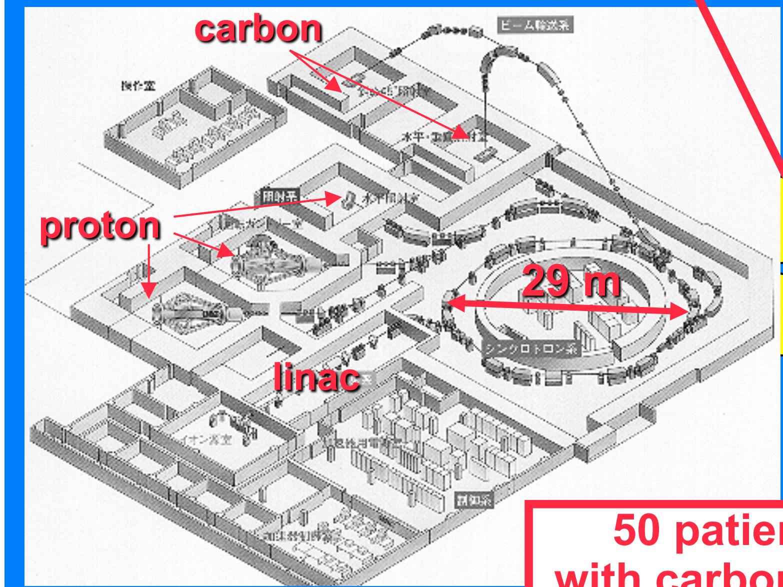

HEAVY ION MEDICAL ACCELERATOR
HIMAC of NIRS (1995)
He and C (≤ 430 MeV/u) 2 synchrotrons
2 h beams + 2 v beams

2000 patients with carbon ions

SHIZUOKA FACILITY
Shizuoka (2002)
Proton synchrotron
2 gantries + 1 h beam

50 patients with carbon ions

Germany: the GSI pilot project

J. Debus

1998-2009
500 patients treated
with carbon ions

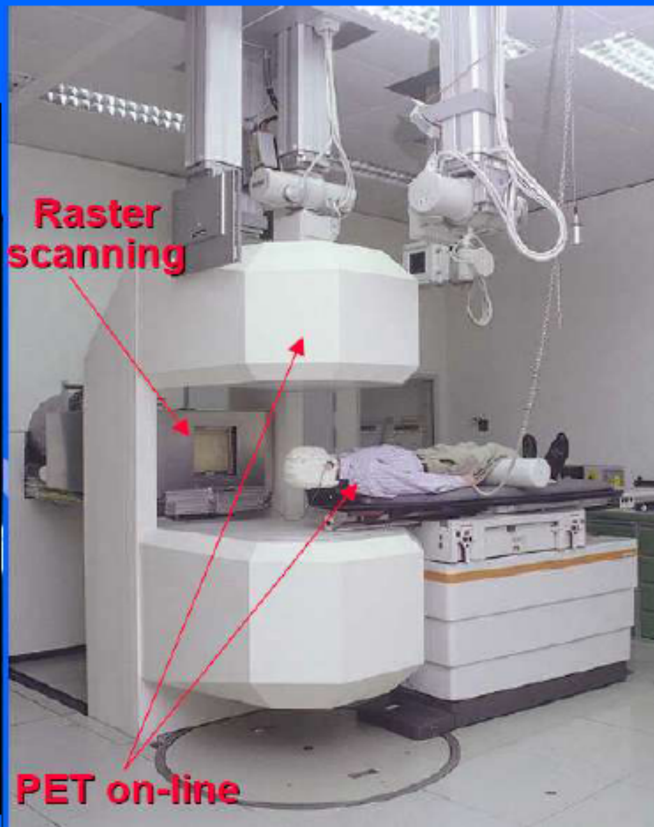

Patients of hadrontherapy

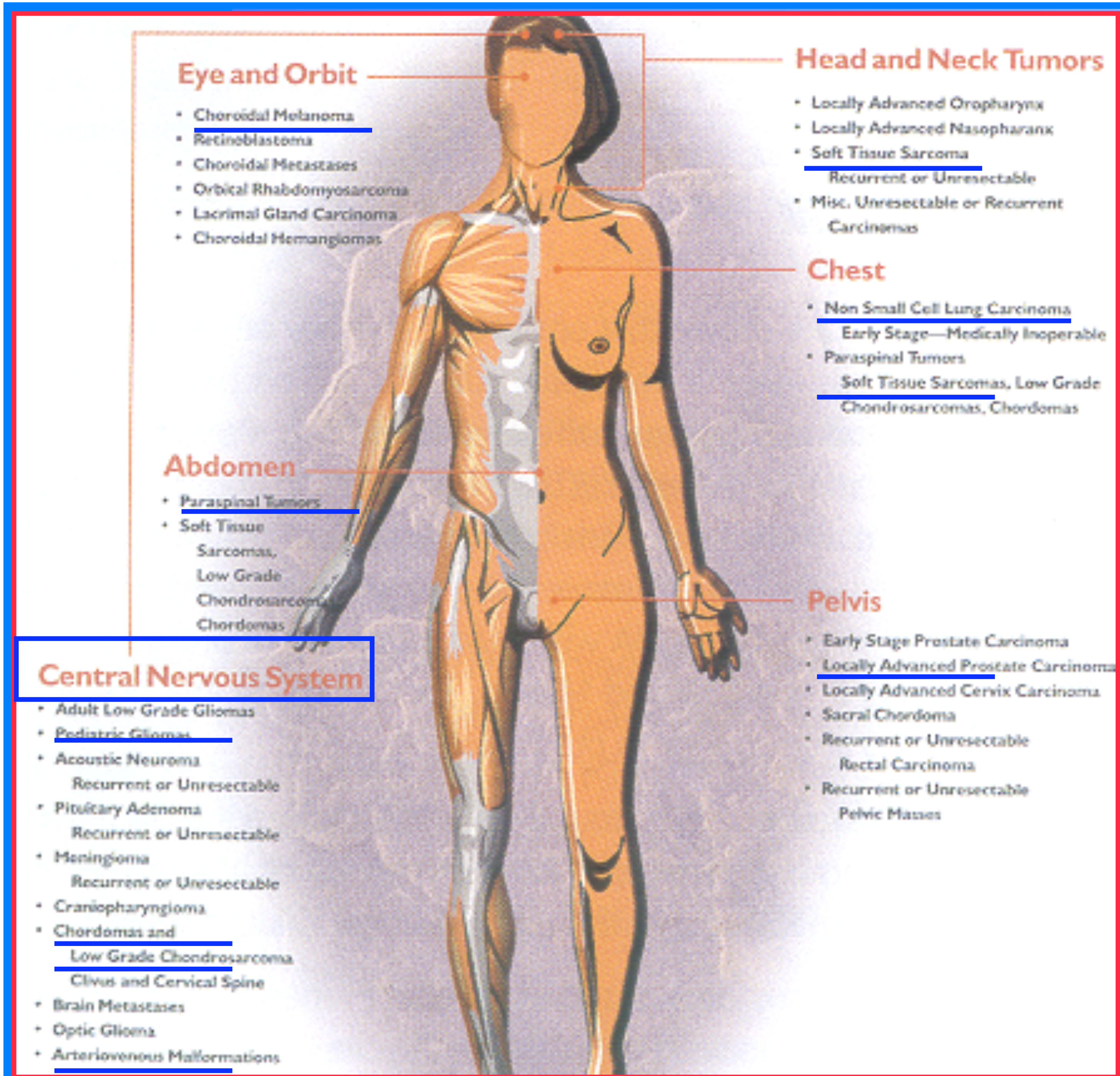

Protontherapy:
60'000 patients
Carbon ion therapy
5 000 patients
mainly at HIMAC

Cost about 20'000 Euro
2-3 x X-rays
If cost would be the same as for X-rays
90% of the treatments would be with protons !

Numbers of potential patients (*)

X-ray therapy

every 10 million inhabitants: 20'000 pts/year

Protontherapy

12% of X-ray patients 2'400 pts/year

Therapy with Carbon ions for radio-resistant tumour

3% of X-ray patients 600 pts/year

TOTAL every 10 M about 3'000 pts/year

(*) Combining studies made in Austria, Germany, France, Italy and Sweden - ENLIGHT

New Center

Courtesy H. Tsujii

HIMAC new facility

Completion: end 2010

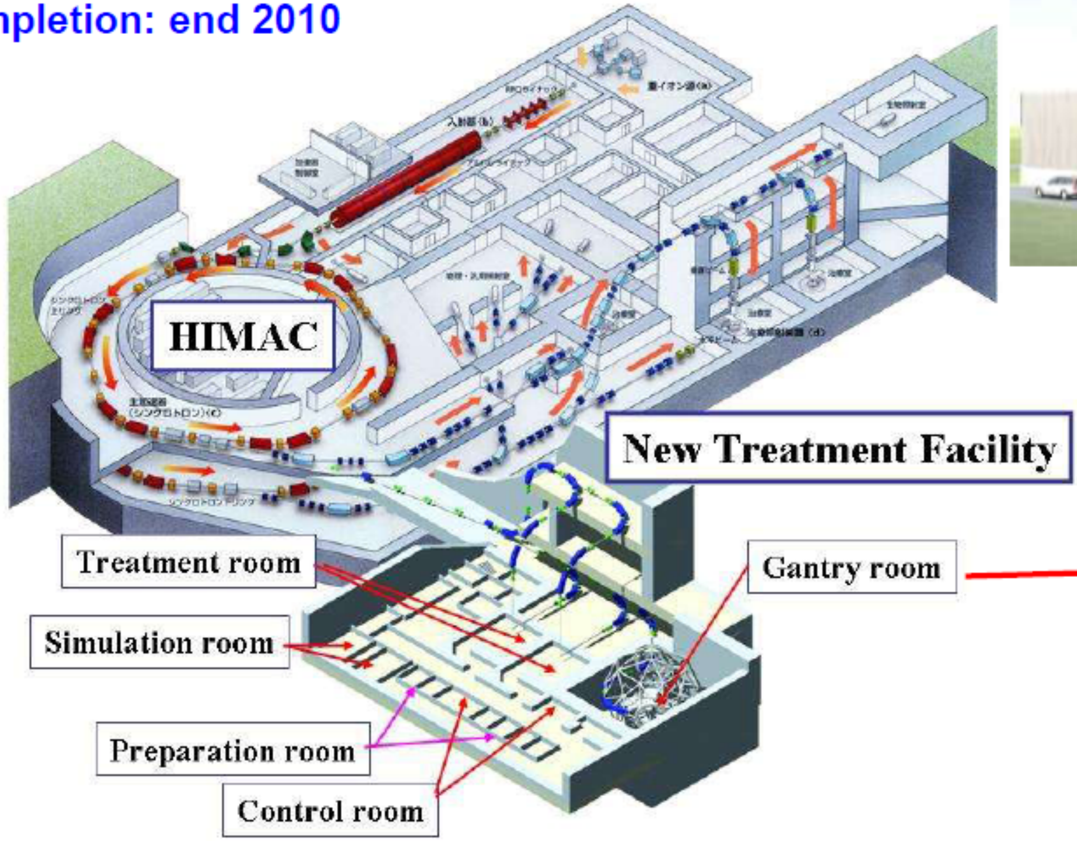

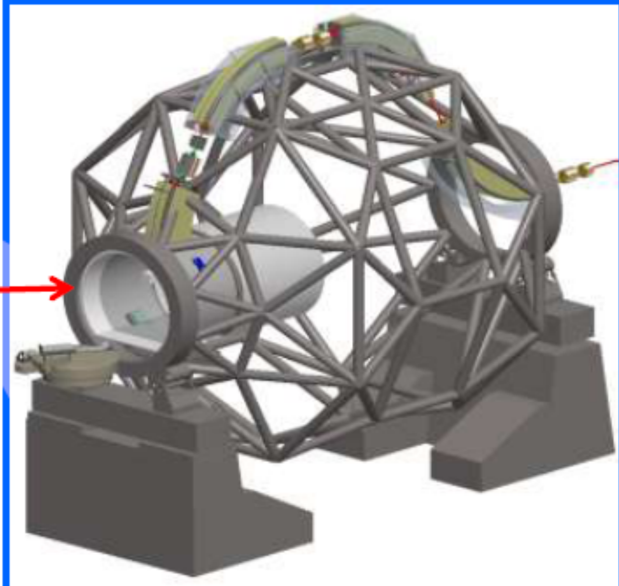

HIT at Heidelberg

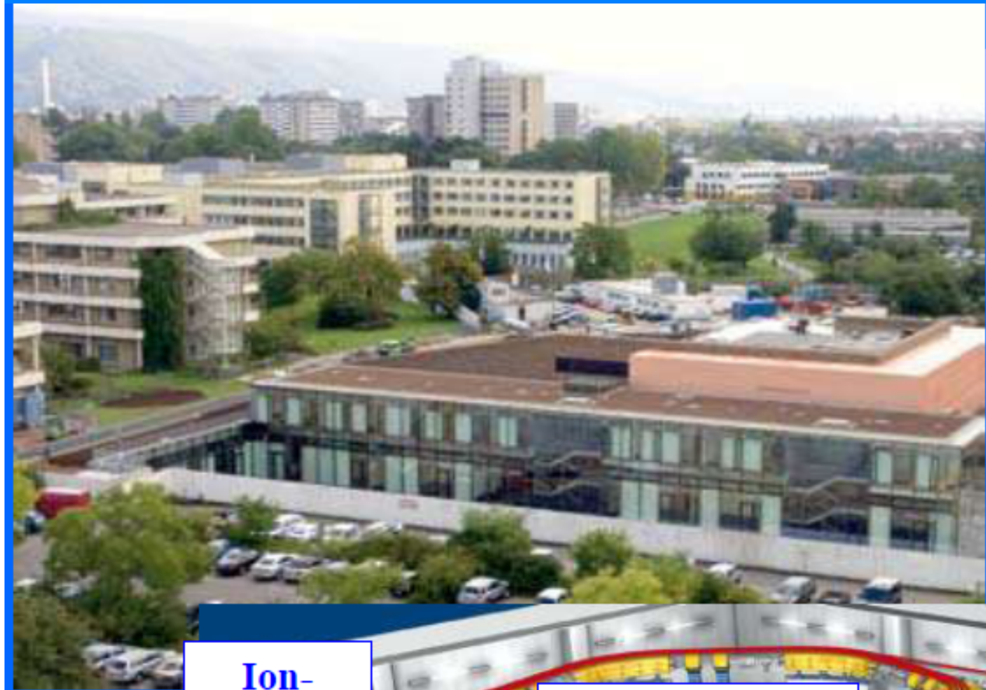

First beam extracted in 2007

First patient: summer 2009

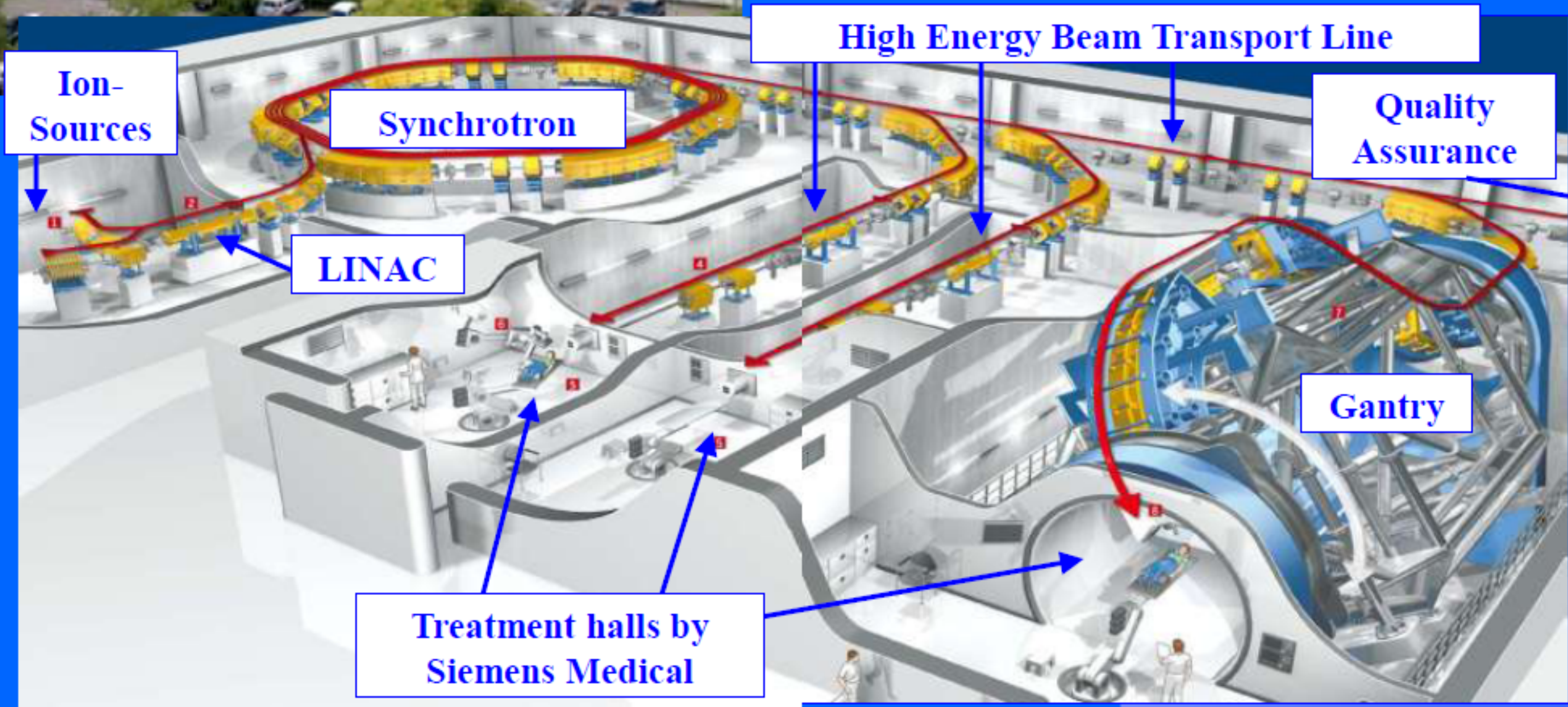

Courtesy H. Haberer

Heidelberg ion gantry: patient room

Patient Gantry Room November 2007

Tilt floor, pending on Gantry position

Nozzle

Bumber mats

Patienttable, Roboter

TERA programmes since 1992

TERA has proposed and designed the 'dual' National Centre for carbon ions and protons

1. CNAO is being built in Pavia

TERA has introduced and developed a novel type of accelerator:

the "cyclinac"

2. "cyclinacs for protons and carbon ions

CNAO = Centro Nazionale di Adroterapia

CNAO Foundation was created by the Italian Government in 2001
to realize CNAO: 4 Hospitals in Milan, 1 Hospital in Pavia and TERA
Since 2003 INFN is Institutional Participant

In September 2003 TERA has completed and passed to CNAO
the design of the high-tech part of CNAO and 25 people

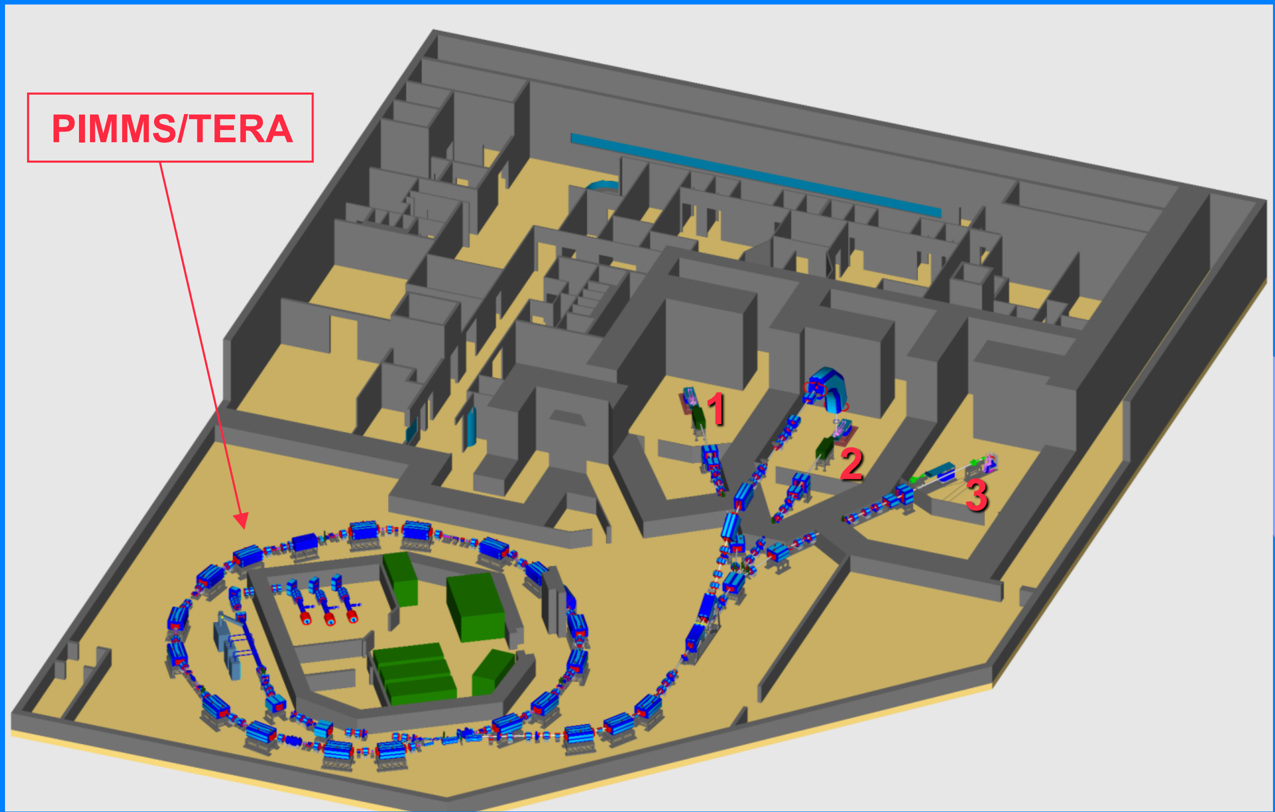

President: E. Borloni

Med. Dir.: R. Orecchia
Tech. Dir: S. Rossi

CNAO = Centro Nazionale di Adroterapia at Pavia

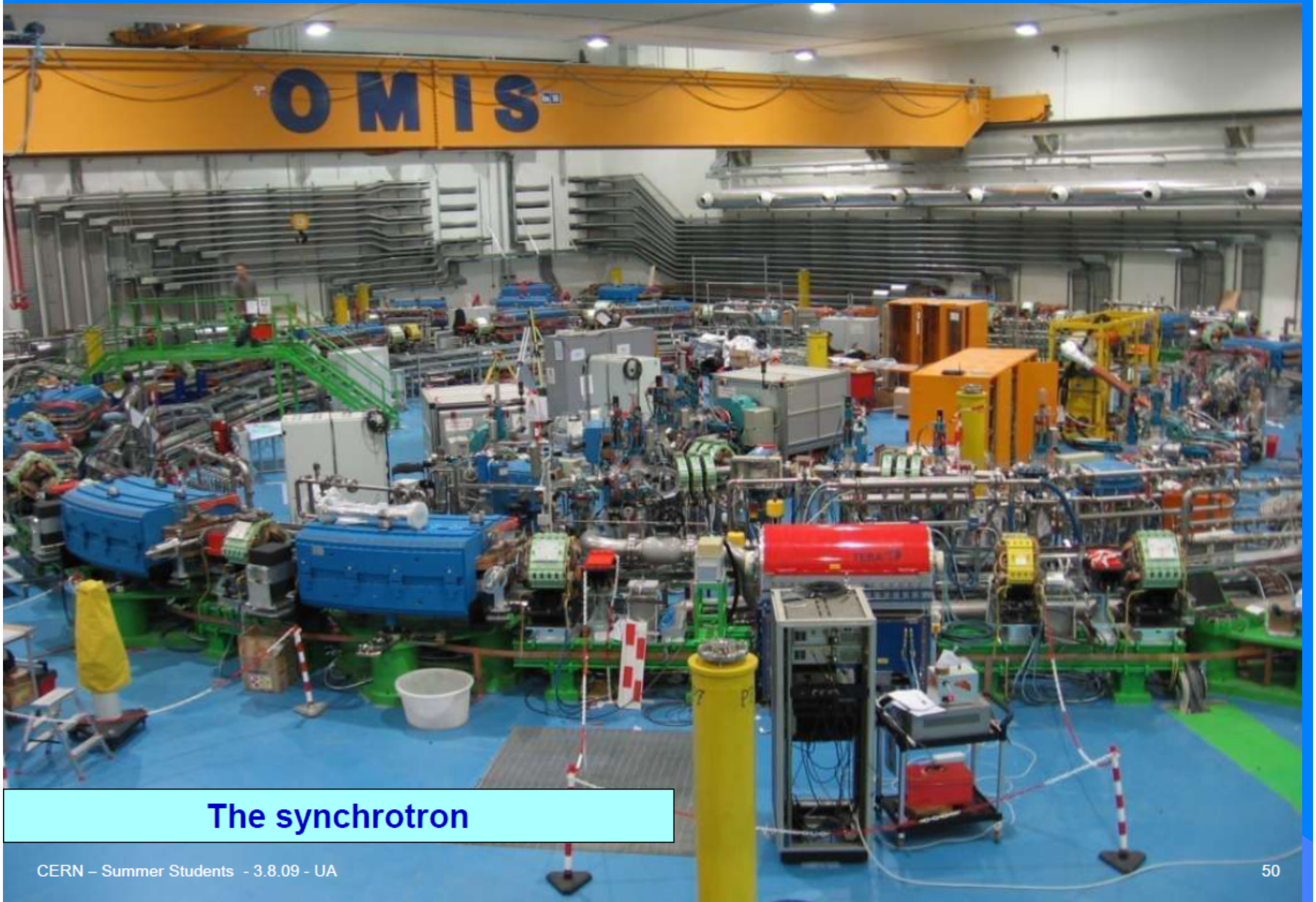

The synchrotron

ENLIGHT and the European projects

European Network for LIGht-ion Hadron Therapy – 2002 - 2005

- GSI project for the University of Heidelberg Clinics (ready to treat)
- TERA project for CNAO in Pavia (completing construction)
- Marburg and Kiel centres (in construction by Siemens Medical)
- Med-Austron for Wiener Neustadt (approved)
- ETOILE in Lyon (approved)
  Competitive tendering

SINCE 2002 THESE GROUPS + CERN + GSI AND MANY OTHERS ARE PART OF THE

ENLIGHT PLATFORM co-ordinated by Dr. Manjit Dosanjh

Programs approved in FP7 : PARTNER , ULICE , ENVISION

for a total of 20 MEuro

Protontherapy is booming

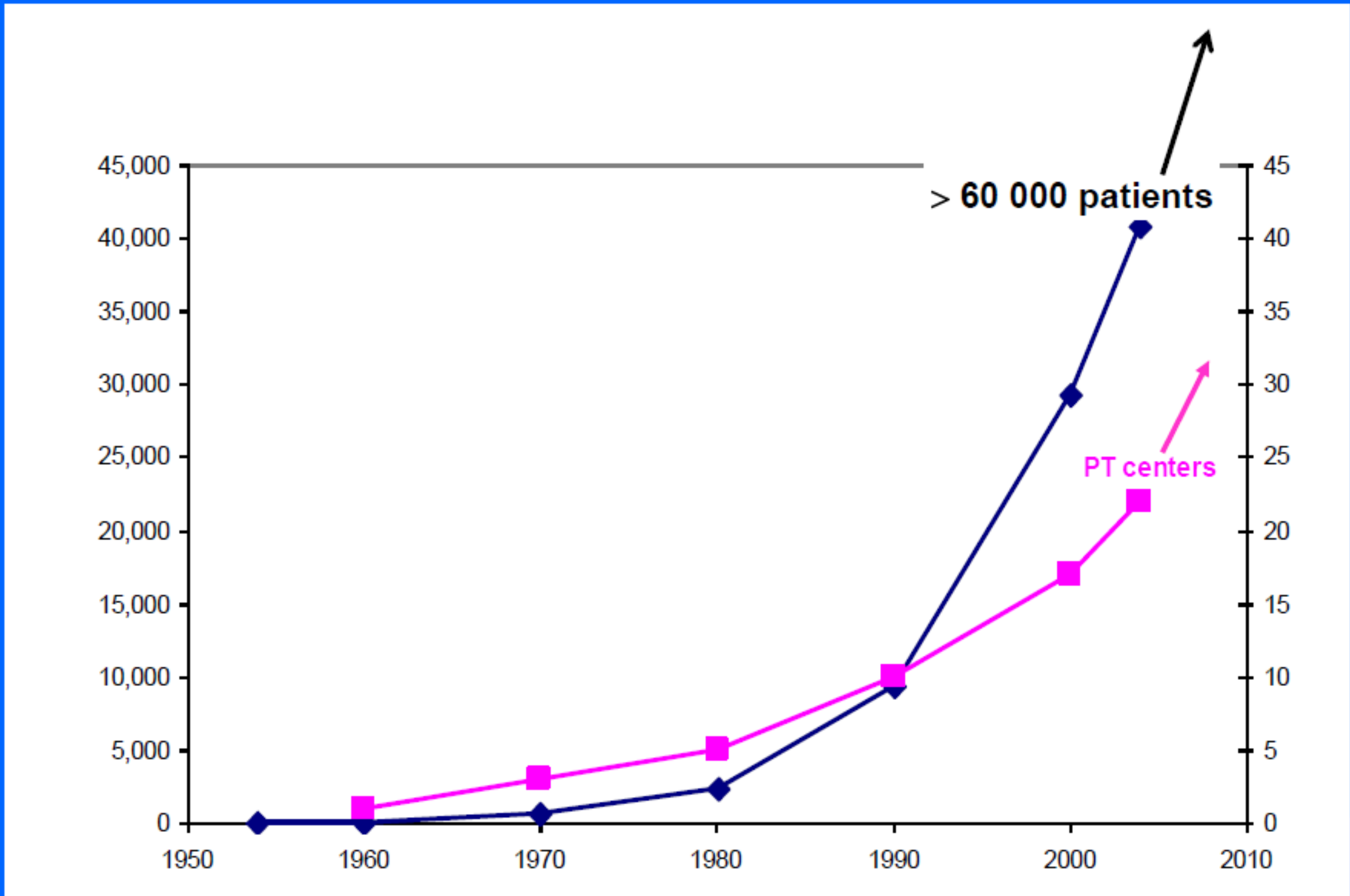

Tumours of the central nervous system

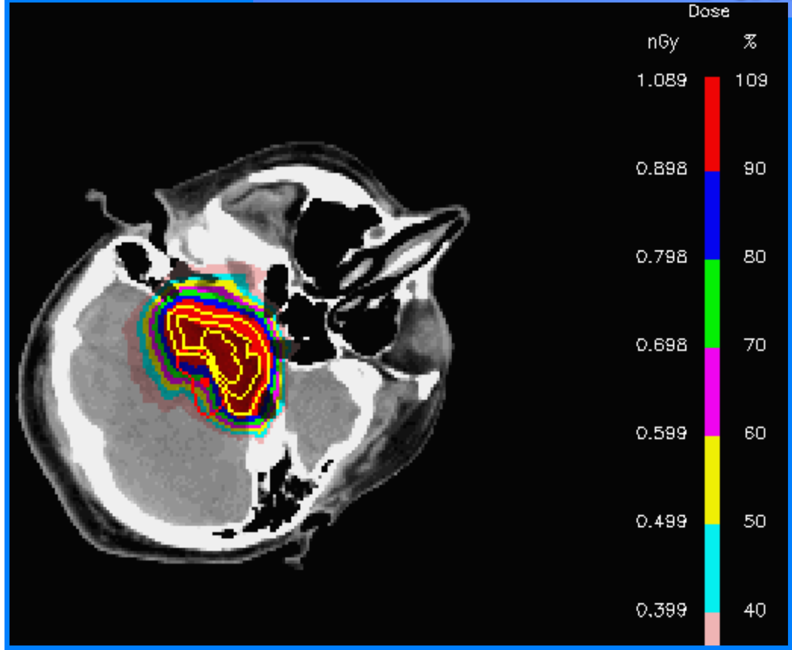

	Control at 5 years	
	RT	Protoni
Chordomas	17-50%	73-83%
Chondrosarcomas	50-60%	90-98%

The percentages are larger with carbon ions

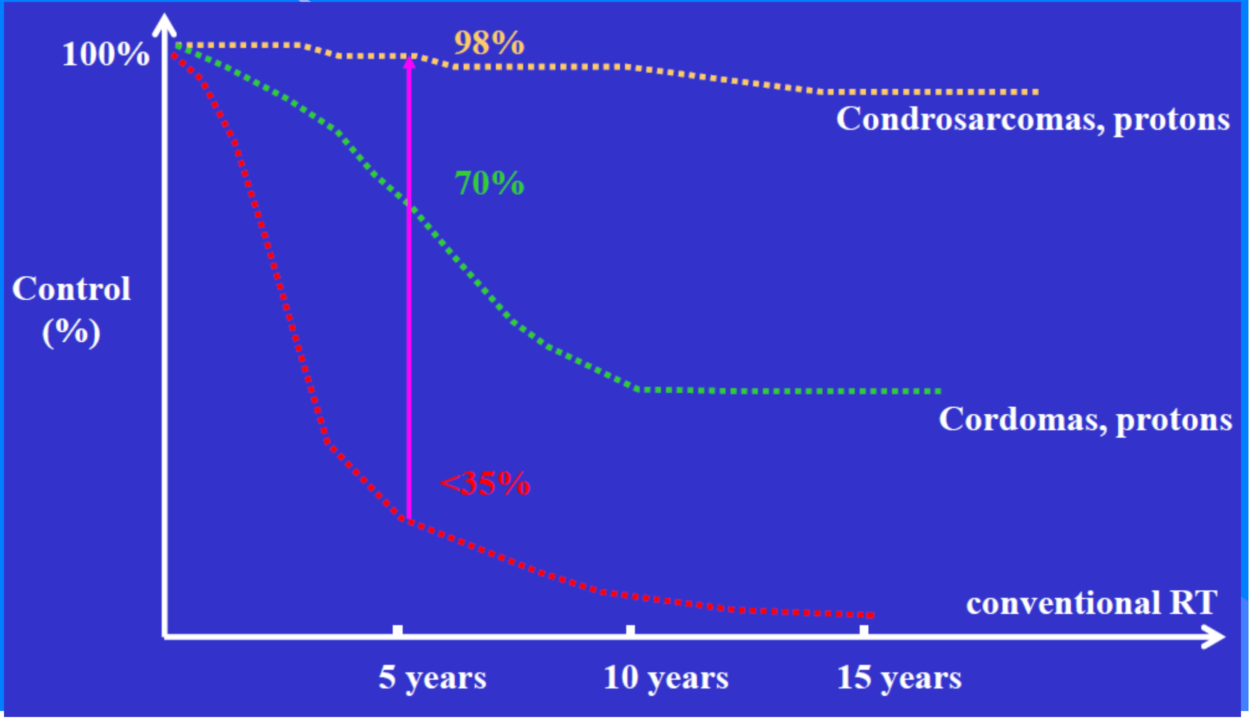

MORE

SLIDES

VOLUMETRIC CT

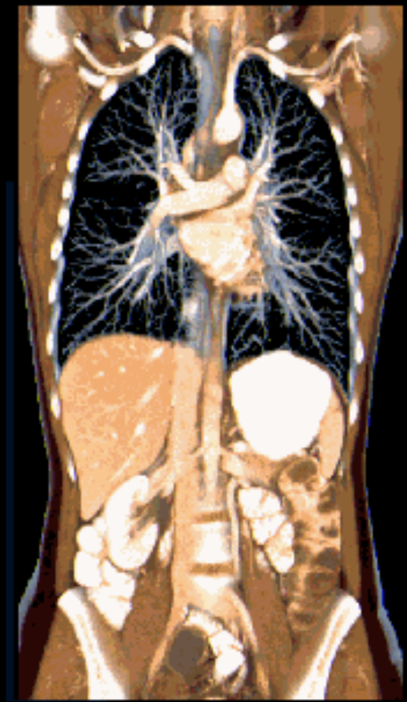
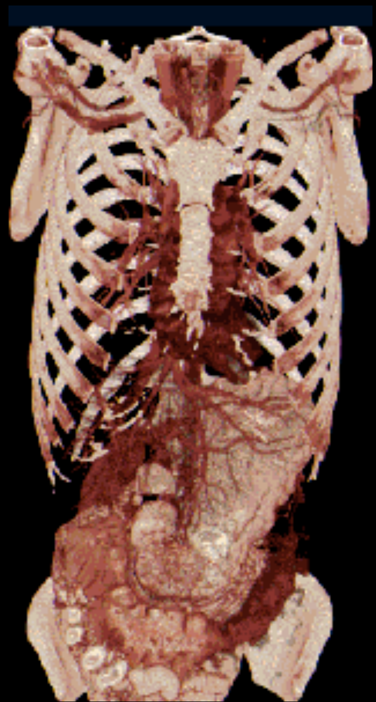


< 0,4 sec/ rotation
Organ in a sec (17 cm/sec)
Whole body < 10 sec


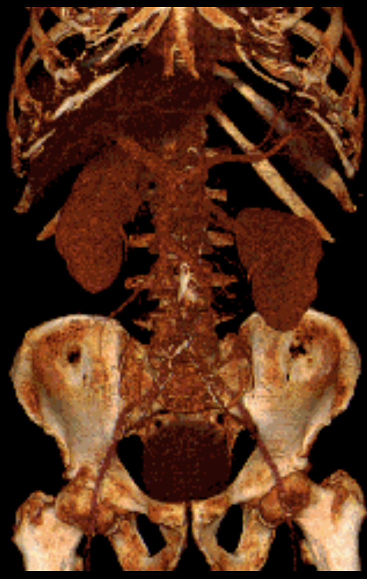

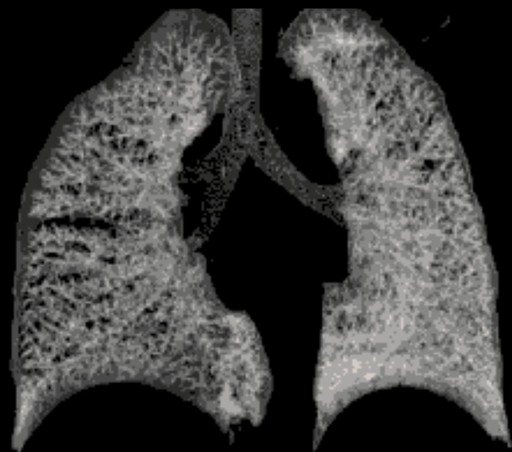

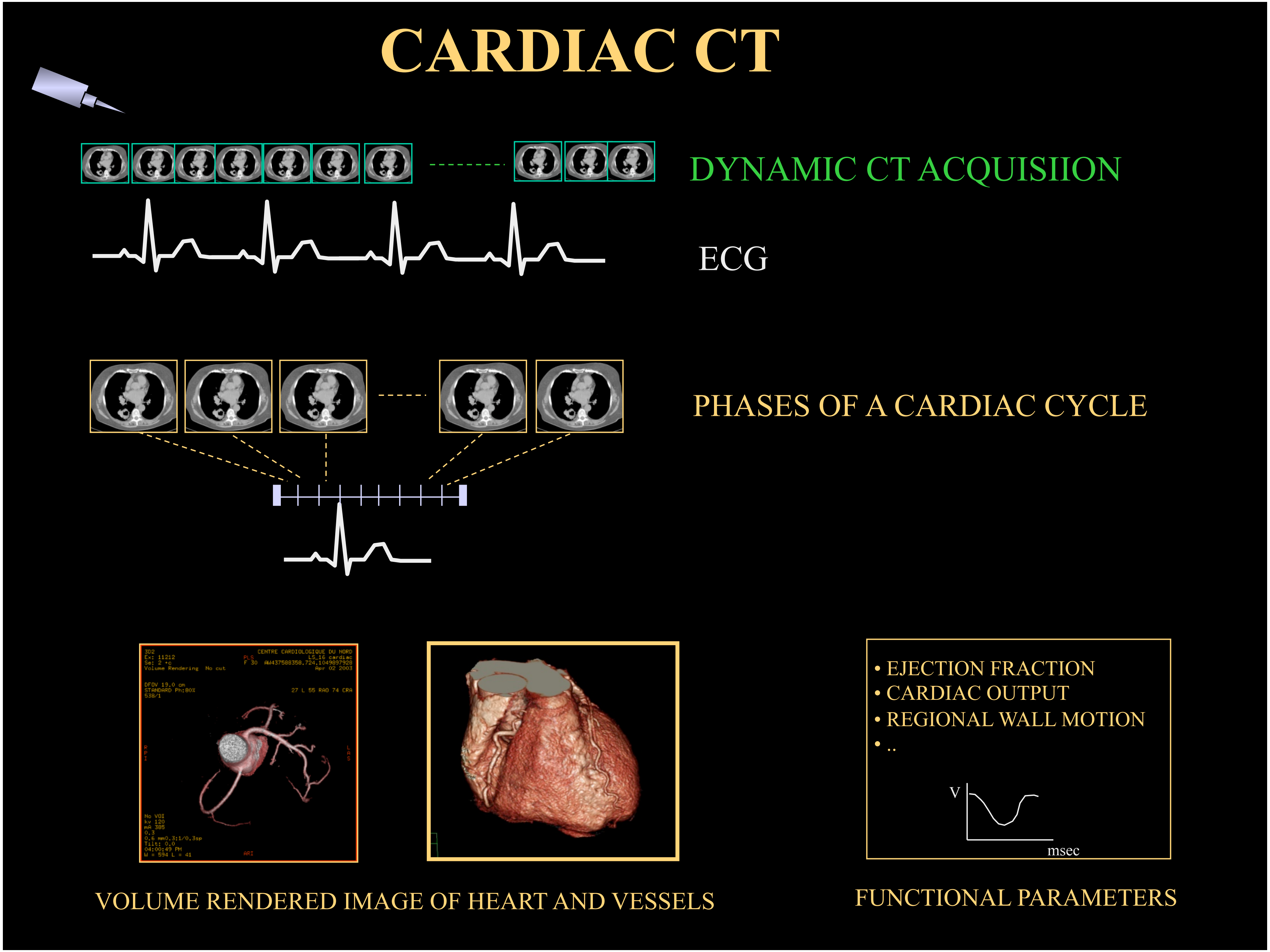
CARDIAC CT
DYNAMIC CT ACQUISIION
ECG
PHASES OF A CARDIAC CYCLE
• EJECTION FRACTION
• CARDIAC OUTPUT
• REGIONAL WALL MOTION
• ..
V
msec
VOLUME RENDERED IMAGE OF HEART AND VESSELS
FUNCTIONAL PARAMETERS

PET FUNCTIONAL RECEPTOR IMAGING

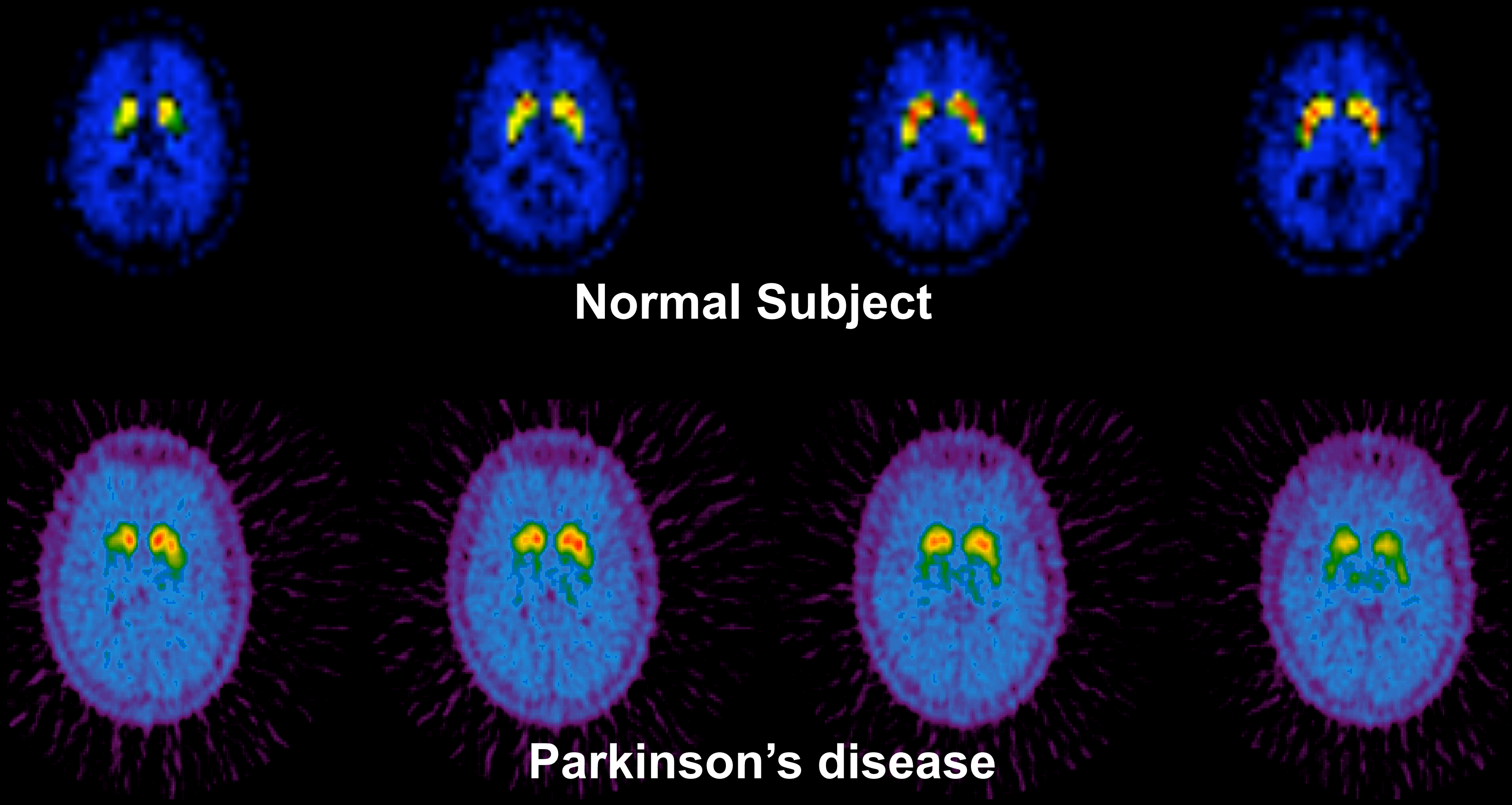

$[^{11}C]$ FE-CIT

^{18}F-FDG PET/CT

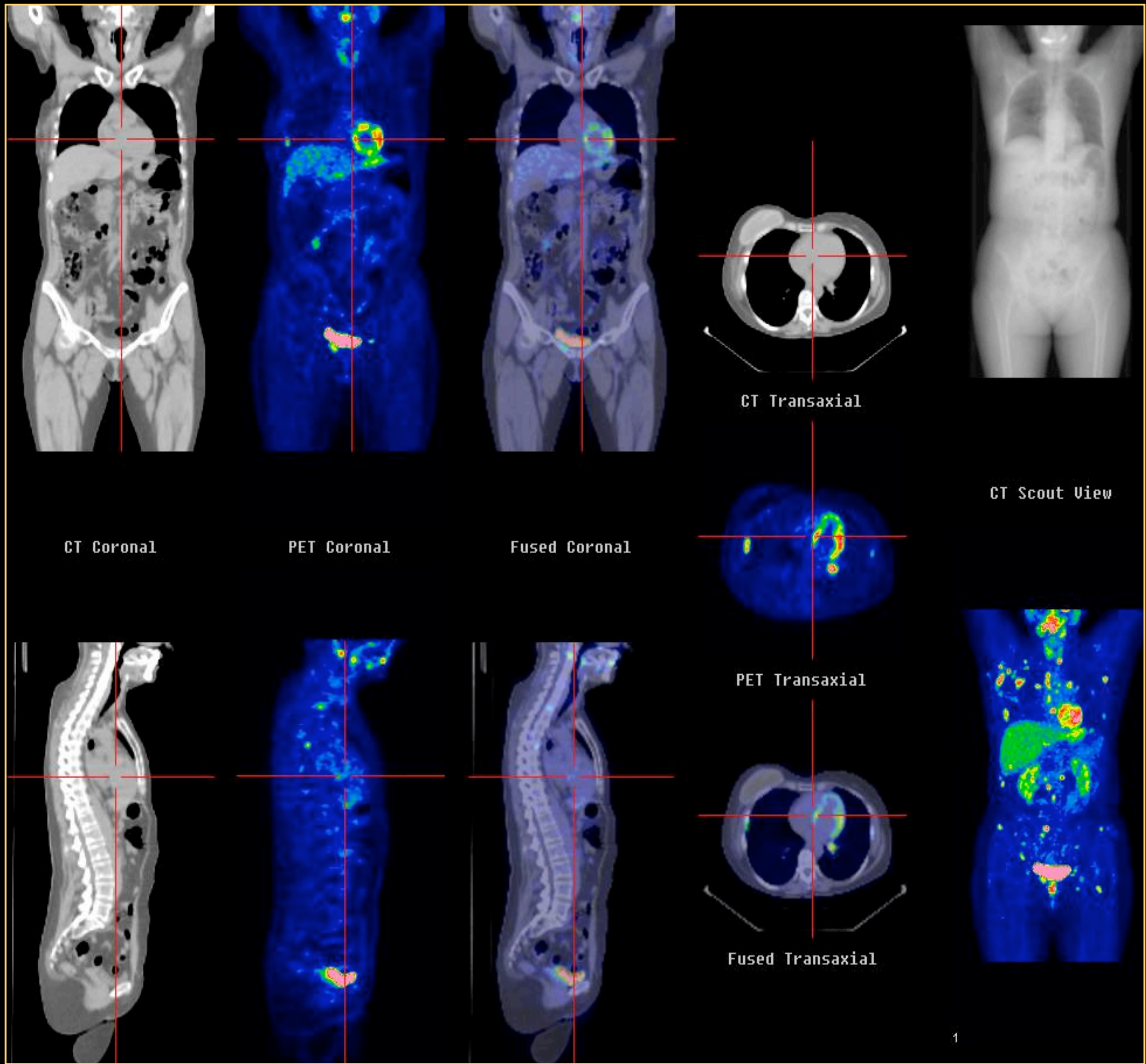

HSR MILANO

CT/PET UNAMBIGUOUS TISSUE LOCALIZATION

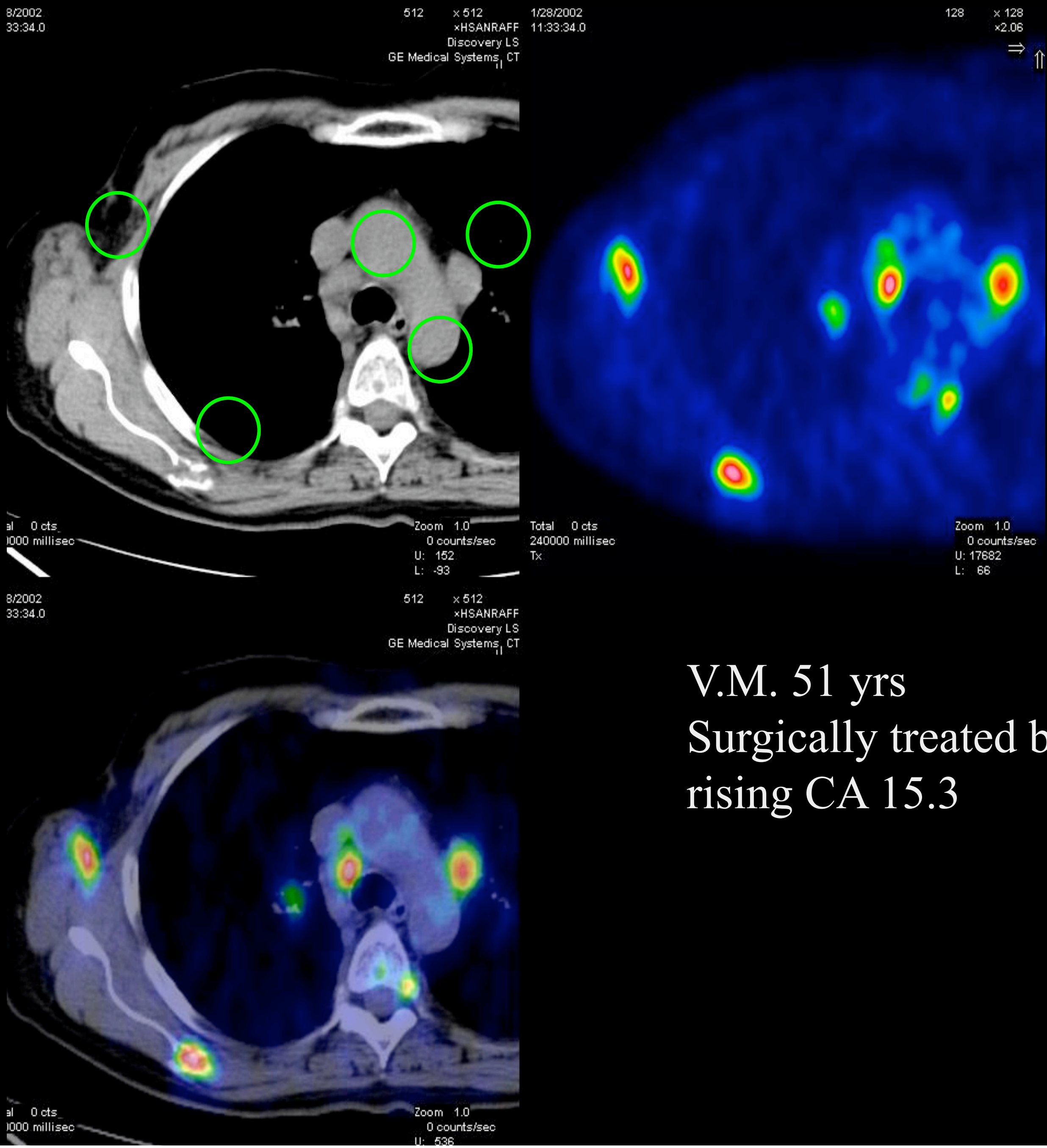

V.M. 51 yrs
Surgically treated breast cancer
rising CA 15.3

HSR Milan

First Clinical Positron Imaging Device

1952

This instrument followed the general concepts of the instrument build in 1950 but included many refinements. It produced both a coincidence scan as well as an unbalance scan. The unbalance of the two detectors was used to create an unbalance image using two symbols to record any unbalance in the single channel rates of the two detectors.

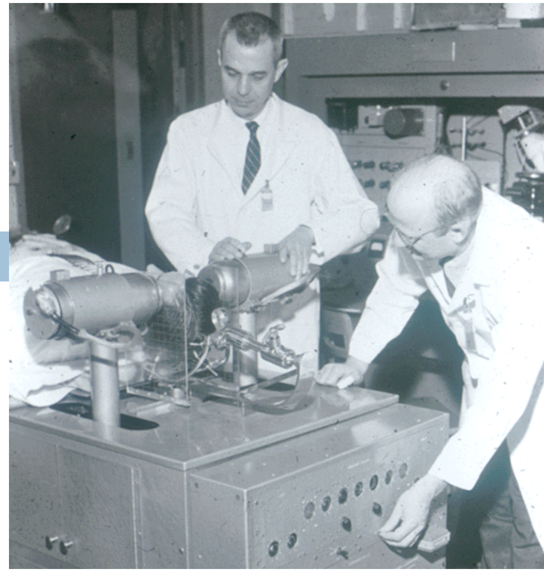

First clinical positron imaging device. Dr. Brownell (left) and Dr. Aronow are shown with the scanner (1953).

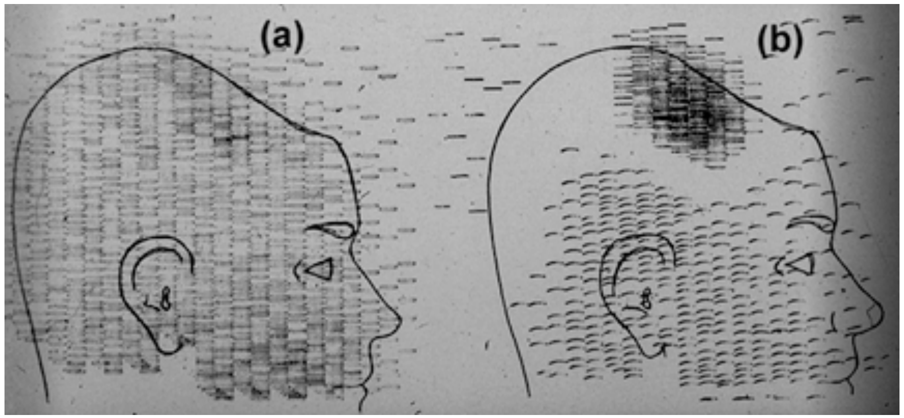

Coincidence and unbalance scans of patient with recurring brain tumor. Coincidence scan (a) of a patient showing recurrence of tumor under previous operation site, and unbalance scan (b) showing asymmetry to the left. (Reproduced from Brownell and Sweet 1953).

MEDICAL IMAGING

TECHNIQUE		YEAR	ENERGY	PHYSICAL PROPERTY	IMAGING
RADIOLOGY	X RAYS IMAGING	**1895**	X RAYS	ABSORPTION	
ECHOGRAPHY	ULTRASOUND IMAGING	1950	US	REFLECTION TRANSMISSION	
NUCLEAR MEDICINE	RADIOISOTOPE IMAGING	1950	γ RAYS	RADIATION EMISSION	

COMPUTERIZED TOMOGRAPHY

TECHNIQUE		YEAR	ENERGY	PHYSICAL PROPERTY	IMAGING	
X RAYS COMPUTERIZED TOMOGRAPHY	**CT**	**1971**	X RAYS	ABSORPTION		MORPHOLOGY
MAGNETIC RESONANCE IMAGING	MRI	1980	RADIO WAVES	MAGNETIC RESONANCE	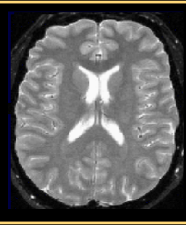	MORPHOLOGY /FUNCTION
POSITRON EMISSION TOMOGRAPHY	PET	1973	γ RAYS	RADIATION EMISSION	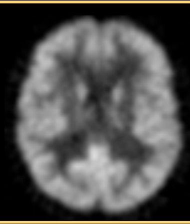	FUNCTION

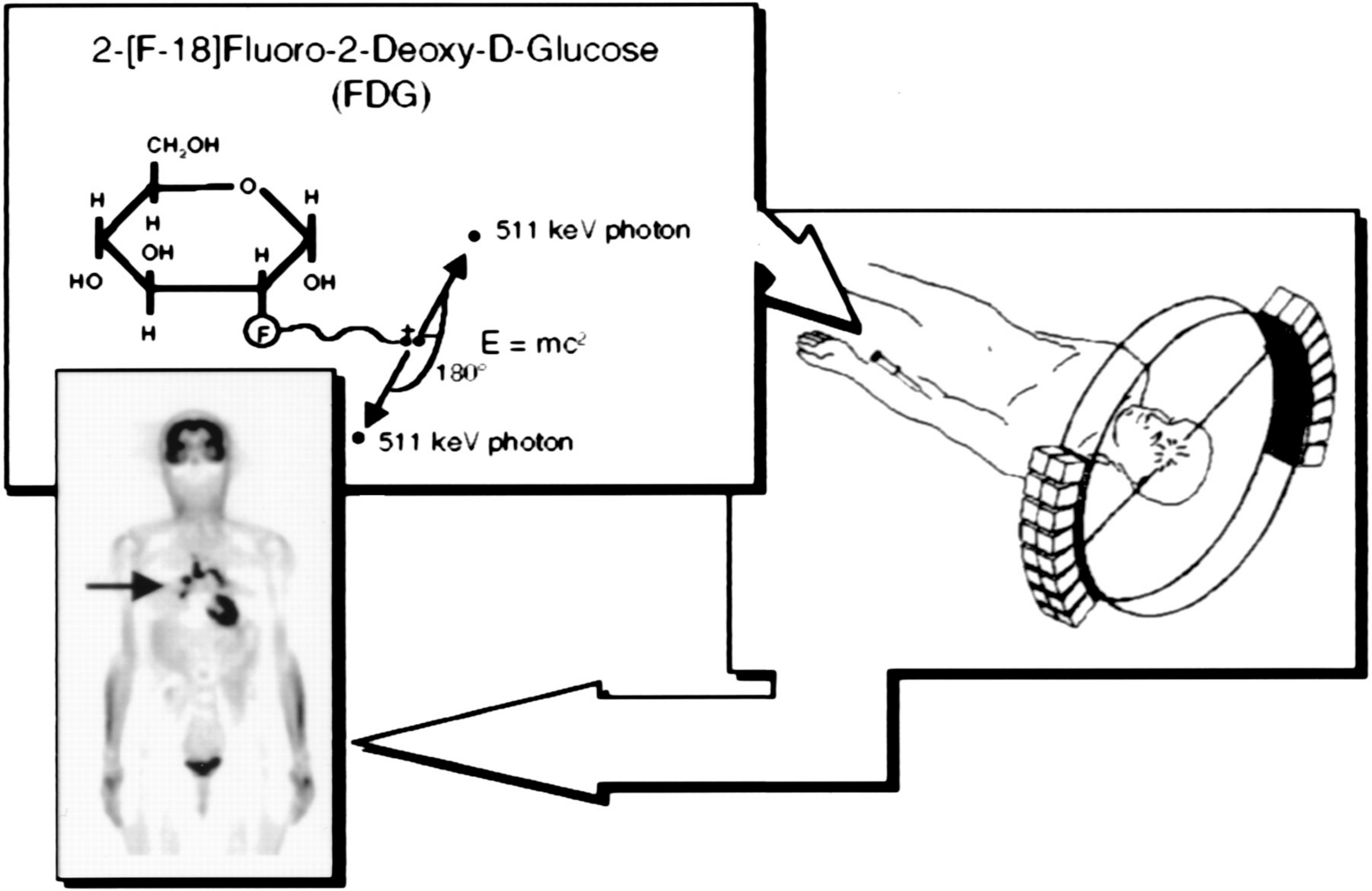

2-[F-18]Fluoro-2-Deoxy-D-Glucose
(FDG)
CH2OH
O
H
H
H
OH
H
HO
OH
H
F
511 keV photon
E = mc2
180°
511 keV photon